Illinois U Library

The American Mineralogist

Journal of the Mineralogical Society of America

Vol. 39 MAY-JUNE, 1954 Nos. 5 and 6

Contents

Contributions to Canadian Mineralogy

Volume 5, Part 6

Sponsored by the Walker Mineralogical Club

Edited by L. G. Berry, *Kingston*

Studies of mineral sulpho-salts: XVIII—Pavonite, a new mineral. . E. W. Nuffield 409
The structures of the minerals of the descloizite and adelite groups: I—Descloizite and conichalcite (part 1). . . . . M. M. Qurashi and W. H. Barnes 416
Determination of columbium in ores by *x*-ray fluorescence. . John S. Stevenson 436
Studies of radioactive compounds: VII—Phosphuranylite and dewindtite . . . . D. D. Hogarth and E. W. Nuffield 444
Studies of uranium minerals (XIV): Renardite . . . . Clifford Frondel and Frank Cuttitta 448
An association of trace elements and mineralization at Sudbury. . H. Stonehouse 452
X-ray measurements on argentopyrite. . . . . J. Murdoch and L. G. Berry 475
The distribution of major and minor elements among some co-existing ferromagnesian silicates. . . . . E. H. Nickel 486
The distribution of iron, manganese, nickel and cobalt between co-existing pyrite and biotite in wallrock alteration . . . . E. H. Nickel 494
The crystal structure of covellite, CuSe and klockmannite, CuSe. . L. G. Berry 504
Germanium and other trace elements in some western Canadian coals. . . . . John A. C. Fortescue 510
Notes and News: Brannerite from Ontario, Canada. . . . . E. W. Nuffield 520
A magnesium borate from Isère, France and Swift River, Yukon Territory, with *x*-ray powder data for some anhydrous borates . . . . R. M. Thompson and J. A. Gower 522
Naumannite from Republic, Washington. . . . . R. M. Thompson 525
Mineral occurrences in Western Canada. . . . . R. M. Thompson 525
Native tin associated with pitchblende at Nesbitt LaBine Uranium Mines . . . . Jack F. B. Silman 529
On the occurrence and origin of xonotlite. . . . . Charles H. Smith 531
Walker Mineralogical Club. 533
Annual meeting. 535
Nomination of officers for 1955. 535

EDITOR: WALTER F. HUNT
ASSISTANT EDITOR: LEWIS S. RAMSDELL

BOARD OF ASSOCIATE EDITORS:
MICHAEL FLEISCHER GEORGE TUNELL (1954)
ELBURT F. OSBORN ADOLF PABST (1954–55)
IAN CAMPBELL BRIAN MASON (1954–56)

Published bi-monthly by the Society

Mineralogical Society of America

ASSOCIATED WITH THE GEOLOGICAL SOCIETY OF AMERICA

President: **Sterling B. Hendricks**, U. S. Department of Agriculture, Beltsville, Maryland.

Vice-President: **Harry H. Hess**, Princeton University, Princeton, New Jersey.

Secretary: **C. S. Hurlbut, Jr.**, Harvard University, Cambridge, Massachusetts.

Treasurer: **Earl Ingerson**, U. S. Geological Survey, Washington 25, D. C.

Editor: **Walter F. Hunt**, University of Michigan, Ann Arbor, Michigan.

Councillors: **George T. Faust**, U. S. Geological Survey, Washington 25, D. C.
Victor T. Allen, Institute of Geophysical Technology, St. Louis, Missouri.
C. Osborne Hutton, Stanford University, Palo Alto, California.
Felix Chayes, Geophysical Laboratory, Washington, D. C.
J. D. H. Donnay, The Johns Hopkins University, Baltimore, Maryland.

The enlarged issues of this journal for 1954 are made possible by a grant from the Penrose Fund of the Geological Society of America.

The American Mineralogist—Journal of the Mineralogical Society of America

A journal containing articles on mineralogy, crystallography, petrography, and allied sciences, is issued every two months. Contributions are invited from everyone.

Office of Publication, Mineralogical Laboratory, Ann Arbor, Mich.

The general conduct of the journal is in the hands of the editor, **Walter F. Hunt**, Ann Arbor, Michigan, to whom all manuscripts should be submitted. To assist the editor the council of the Mineralogical Society has appointed **Lewis S. Ramsdell**, Ann Arbor, Michigan, assistant editor, and the following board of associate editors:

Ian Campbell, California Institute of Technology, Pasadena 4, California.
Michael Fleischer, U. S. Geological Survey, Washington, D. C.
Brian H. Mason, American Museum of Natural History, New York, N. Y.
Elburt F. Osborn, Pennsylvania State College, State College, Pa.
Adolf Pabst, University of California, Berkeley 4, California.
George Tunell, University of California at Los Angeles, California.

It will expedite publication if two copies of each manuscript are submitted to the editor.

Contributors of leading articles are given without charge 100 reprints (without covers) of their article. If additional reprints are desired these can be purchased at the following rates:

Pages	*1–4*	*5–8*	*9–12*	*13–16*	*17–20*	*21–24*	*25–28*	*29–32*	*Covers*
Copies									
25	$3.50	$5.00	$ 8.00	$ 9.50	$11.00	$13.00	$15.00	$16.00	$4.90
50	3.80	5.55	8.80	10.40	12.10	14.20	16.40	17.50	5.50
75	4.10	6.10	9.60	11.30	13.20	15.40	17.80	19.00	6.10
100	4.40	6.65	10.40	12.20	14.30	16.60	19.20	20.50	6.70
Addl. C's	1.20	2.20	3.20	3.60	4.40	4.80	5.60	6.00	2.40

Cover Composition $1.55.

Sent to all members and fellows of the Mineralogical Society of America. Subscription price, $4.00 per year (single copies of normal issues, $1.00 plus postage).

Entered as second class matter at the post office at Menasha, Wis., under Act of March 3, 1879. Acceptance for mailing at the special rate of postage provided for in section 1103, Act of Oct. 3, 1917, paragraph 4 section 429 P. L. & R. authorized March 13, 1922.

Notice of change of address, orders, and remittances should be sent to Dr. Earl Ingerson, U. S. Geological Survey, Washington 25, D. C.

Printed by the George Banta Publishing Company, Menasha, Wisconsin
Printed in the United States of America

THE AMERICAN MINERALOGIST

JOURNAL OF THE MINERALOGICAL SOCIETY OF AMERICA

Vol. 39 MAY-JUNE, 1954 Nos. 5 and 6

STUDIES OF MINERAL SULPHO-SALTS: XVIII—PAVONITE, A NEW MINERAL

E. W. NUFFIELD, *University of Toronto, Toronto, Canada.*

ABSTRACT

Alaskaite (benjaminite) from Cerro Bonete, Sur-Lipez province, Bolivia has been found to be a new mineral: $C2/m$; a 13.35, b 4.03, c 16.34 Å, β 94½°; probable composition and cell contents 4[$AgBi_3S_5$].

The species has been named pavonite from the Latin pavo, peacock in honour of the late Professor M. A. Peacock.

Alaskaite was the name proposed by Koenig (1881) for a supposedly new species from the Alaska mine in Colorado. The species was founded on a number of chemical analyses, some partial, which showed considerable variation. In Dana (1944), the formula $Pb(Ag,Cu)_2Bi_4S_8$ is given as best representing the uncertain results of most of Koenig's analyses. Ahlfeld (1926) announced the discovery of a second occurrence of alaskaite near Cerro Bonete in Sur-Lipez province, Bolivia associated with chalcopyrite and bismuthinite. The identification was based on a chemical analysis by Herzenberg.

Thompson (1950) examined specimens from the two localities both in polished sections and by means of x-ray powder patterns. He identified aikinite ($PbCuBiS_3$), matildite ($AgBiS_2$) as well as sphalerite, tetrahedrite and galena in the Colorado material. Koenig was not aware of the presence of aikinite and matildite, and it is therefore reasonable to conclude with Thompson that the analyses were made on mixtures and that alaskaite from the type locality must be discredited as a species. On a typical specimen of the Cerro Bonete material Thompson identified benjaminite. Since the composition of benjaminite is given in Dana (1944) as $Pb(Cu,Ag)Bi_2S_4$(?), he surmised that this was the mineral, at least in large part, which had been analyzed by Herzenberg.

THE BOLIVIAN "BENJAMINITE"

During a recent study of type benjaminite (Nuffield, 1953) from Nye County, Nevada the present writer examined the "alaskaite" from Cerro

Bonete which had been reported as benjaminite by Thompson. The *x*-ray powder patterns obtained by Thompson were available for this purpose. A comparison of the patterns of Bolivian material with those obtained from type Nevada benjaminite did indeed show a close similarity. The main difference appeared to be in the quality of the pattern. Several of the diffraction arcs of the type benjaminite are characteristically diffuse while patterns of the Bolivian mineral are sharp suggesting that the latter mineral is more perfectly crystalline.

Specimens of the Bolivian mineral favourable for single crystal studies were now sought in order to explain, if possible, the slight differences in the powder patterns. A Harvard specimen obtained through the kindness of Professor Frondel, labelled "No. 2, benjaminite, pure mass with bismuthinite and ankerite, Porvenir mine, Cerro Bonete (Aceroduyok), Province Sur-Lipez, Bolivia" offered crystals suitable for single crystal *x*-ray studies, and gave powder patterns identical in every detail with Thompson's pattern of the Bolivian mineral. The Weissenberg films which were subsequently obtained proved however, to be different from those obtained on type benjaminite. Measurement of the films indicated that two lattice constants are very similar and this probably accounts for the resemblance between the powder patterns (see Figs. 1 & 2):

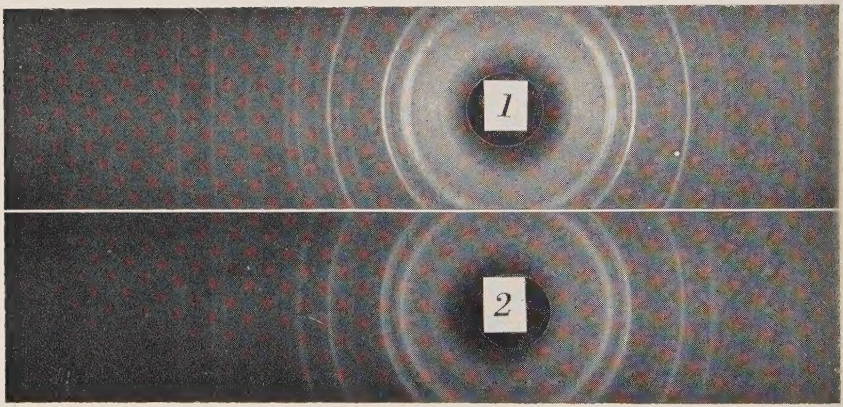

FIGS. 1 and 2. *X*-ray powder patterns; Cu/Ni radiation; camera diameter 57.3 mm.; full size contact prints. 1—Pavonite, Cerro Bonete, Bolivia; 2—Benjaminite, Outlaw Mine, Nye County, Nevada (U.S.N.M. 95058).

Benjaminite, Nevada a' 13.34, b' 4.06, c' 20.25 Å; β 104°
"Benjaminite," Bolivia a 13.35, b 4.03, c 16.34 Å; β $94\frac{1}{2}$°

The new cell, like the strong pseudo-cell of benjaminite is monoclinic, $C2/m$.

The Bolivian mineral is therefore not benjaminite. Its cell constants and powder pattern cannot be matched with the published data of known sulpho-salt minerals. Consequently a detailed study of the probably new species was undertaken.

Physical properties

The new mineral occurs abundantly on the Harvard specimen both massive and as tiny bladed crystals elongated parallel *b*[010], which display a highly-reflecting surface. In colour, lustre and hardness it closely resembles bismuthinite with which it is intimately associated. Chalcopyrite and aikinite were also identified.

A polished section of the specimen showed that the bismuthinite, aikinite and non-metallic gangue are so intimately intergrown that it would be impossible to thoroughly clean a large quantity of the mineral. Specific gravity determinations using a Berman balance were made on a number of grains which were subsequently crushed, examined under the binocular microscope and finally used for the preparation of *x*-ray powder patterns to ensure a high degree of purity. Three values (6.54, 6.47, and 6.39) measured on three grains weighing between 2.5 and 4.0 mgrs. were obtained in this way. The grains were too small to guarantee high accuracy and from the invariable presence of tiny cavities it might be inferred that the values would tend to be low. A 200 mgr. sample was chosen in much the same way for chemical tests, although with less care since it was obviously impossible to test each grain with an *x*-ray powder pattern.

Chemical properties

A portion of the cleaned material was submitted to Mr. D. A. Moddle of the Ontario Department of Mines for a semi-quantitative spectrographic analysis of the metallic components and the remainder to Mr. E. J. Brooker of the Geological Survey of Canada for an *x*-ray fluorescence analysis. Table 1 shows that the results agree within acceptable limits. The table also presents the chemical analysis of Herzenberg for comparison.

The *x*-ray fluorescence (IIA) and chemical (III) data cannot be compared directly since elements of atomic number below 22 (S, Si, O, etc.) could not be determined with the fluorescence equipment. However the values for bismuth, silver, lead and copper are compatible. The chief difference lies in the lead content which in the chemical data is proportionately much higher. This difference can safely be attributed to aikinite which had not been recognized by Ahlfeld and was therefore not removed before the analysis. The present polished section study having shown the intimate association of the various minerals in our specimen,

TABLE 1. COMPARISON OF CHEMICAL DATA FOR PAVONITE

	I *Spectrographic Analysis*	II *X-Ray Fluorescence* A Wt. % ratios	 B Atomic ratios	III *Chemical Analysis* Herzenberg
Bi	10–100%	53.8%	0.258	56.11%
Ag	5–15	7.8	0.072	9.07
Pb	0.5–5	5.1	0.025	14.41
Cu	1–10	2.8	0.044	2.68
Fe	0.1–1	1.1	0.020	—
Zn	trace	0.3	0.005	—
As	trace	0.2	0.003	—
Sb, Cd	trace	—	—	—

I. Spectrographic analysis by D. A. Moddle & W. Taylor, Ontario Dept. Mines. II. *X*-ray fluorescence analysis by E. J. Brooker, Radioactivity Lab., Geo. Surv. Canada: A. Weight percentage ratios (limit of accuracy: Bi ±5% of amount present, Ag, Pb, Cu ±10%, Fe, Zn, As ±30%). B. Atomic ratios. III. Chemical analysis by Herzenberg (in Ahlfeld, 1926) recalculated to 100%, S omitted.

suggested that at least a portion of the lead found by the spectrographic and fluorescence analysis was also due to aikinite. Consequently the copper content of a number of grains was next studied in some detail by spectrographic methods. This showed a variation from grain to grain and again suggested that our 200 mgr. sample was contaminated by aikinite.

As a first approximation it was assumed that all of the lead (0.025 of Table 1, column IIB) together with an equal portion of copper and bismuth of the fluorescence analysis was due to aikinite and that the remainder of the copper (0.019) which just matched the iron content(0.020) was due to chalcopyrite. This left 0.233 parts of bismuth and 0.072 parts of silver, giving the ratio Bi/Ag = 0.233/0.072 or 3.24/1. A Bi/Ag ratio of 3/1 seemed more probable and consequently sufficient bismuth (0.017) to reduce the Bi/Ag ratio to 0.216/0.072 or 3/1, was relegated to bismuthinite, another probable component in the sample. Thus the formula $AgBi_3S_5$ or $Ag_2S \cdot 3Bi_2S_3$ was derived as representing the ideal composition of the new mineral. The apportioning of the elements as described above is presented in Table 2.

Fusion experiments were now made to test the validity of the above assumptions. Two separate charges were prepared of the elements in the stoichiometrical proportions Ag:Bi:S = 1:3:5. The charges were

TABLE 2. PROBABLE COMPONENTS IN SAMPLE USED FOR X-RAY FLUORESCENCE ANALYSIS

	Bi	Ag	Pb	Cu	Fe
aikinite ($PbCuBiS_3$)	0.025		0.025	0.025	
chalcopyrite ($CuFeS_2$)				0.019	0.020
bismuthinite (Bi_2S_3)	0.017				
$AgBi_3S_5$	0.216	0.072			
	0.258	0.072	0.025	0.044	0.020

inserted in silica glass tubes, the air removed and the tubes sealed off. They were next heated until the constituents melted, held at this temperature for about an hour and then allowed to cool slowly. Polished sections were prepared of various portions of the products and a number of x-ray powder patterns made. The polished sections showed that a perfectly homogeneous product had been formed; the x-ray powder patterns agreed to the last detail with powder patterns of the natural mineral from Bolivia. It is reasonable to assume therefore that the formula $AgBi_3S_5$ represents the ideal composition of the mineral. The calculated specific gravity 6.79, for $4[AgBi_3S_5]$ is in satisfactory agreement with the highest measured value, 6.54, considering the weight and condition of the grains measured. Unfortunately, the fusion products were quite porous and therefore unsuitable for gravity determinations.

The composition of the new mineral is unusual. Although silver is an essential element in many sulpho-salt minerals, hitherto only one mineral, matildite, was known to be composed of only silver, bismuth and sulphur. Furthermore the semi-metal to metal ratio (3/1) is remarkably high. In this respect it is surpassed by only livingstonite ($HgSb_4S_7$) and equalled by only vrbaite ($TlAs_2SbS_5$).

Since the type alaskaite has been discredited and its name and supposed composition are not applicable to the Bolivian mineral, it is desirable to give the species a new name. The name pavonite (pa/von/īt) from the Latin Pavo, peacock, has been selected to honour the memory of the late Professor M. A. Peacock (1898–1950). Professor Peacock devoted himself from 1937 when he joined the Toronto staff until his untimely death, to studies of the mineral sulpho-salts, producing well over a score of published papers. The full scope of his contributions will only be realized when his "Atlas of X-Ray Data for the Ore Minerals" appears as a posthumous work.

Pavonite is almost unique among the new sulpho-salts recently described in that it is probably not a rarity in existing collections. Several typical specimens were located in the Royal Ontario Museum and it is likely that numerous specimens are housed in Museum and University collections throughout the world under the label of either alaskaite or benjaminite.

Polished section studies

Pavonite is white, much like jamesonite, in polished section. It is strongly anisotropic with polarization colours that are pale to intense blue, and light tan to brown. Standard reagents gave the following tests:

40% KOH, 5% $HgCl_2$, 20% KCN—negative
20% $FeCl_3$—stains light brown but does not etch; easily rubbed off.
1:1 HCl—negative or faint gray stain
1:1 HNO_3—slowly stains grayish-brown without effervescence; fumes stain

The artificial mineral gives similar reactions.

It is interesting to note that the optical behaviour and etch tests given by Short (1940) for an alaskaite from Silverton, Colorado are almost identical with those he observed on schapbachite (matildite) from Schapbach, Baden. This substantiates Thompson's work which showed that alaskaite from Colorado is a mixture of aikinite and matildite.

X-ray powder pattern

The new mineral gives a well-defined powder pattern with numerous diffraction lines. The usual powder data are presented in Table 3, partially indexed to show that the cell constants derived by the Weissenberg study, are compatible with the *x*-ray powder spacings.

TABLE 3. *X*-RAY POWDER DATA FOR PAVONITE
Monoclinic *C2/m*; *a* 13.35, *b* 4.03, *c* 16.34; $\beta=94\frac{1}{2}°$

I	*d*(meas.)	*d*(calc.)	*hkl*	*I*	*d*(meas.)	*I*	*d*(meas.)	*I*	*d*(meas.)
2	5.36	5.36	$(\bar{2}02)$	½	2.58	½	1.457	1	0.967
1	4.03	4.07	(004)	3	2.25	2	1.423	2	0.949
½	3.85	3.86	(110)	2	2.19	½	1.315	½	0.919
6	3.58	3.60	$(\bar{2}04)$	3	2.10	3	1.272	2	0.901
6	3.44	3.46	(112)	7	2.01	½	1.201	2	0.860
6	3.33	3.36 3.33 3.31	(204) (400) $(\bar{4}01)$	½	1.963	3	1.162	1	0.790
				2	1.893	½	1.126		
				1	1.753	½	1.114		
3	2.96	2.96 2.94	$(\bar{3}11)$ $(\bar{4}03)$	3	1.721	½	1.100		
				3	1.637	1	1.009		
10	2.84	2.85	$(\bar{3}12)$	½	1.484	1	0.987		

Ni filtered Cu radiation; $\lambda=1.5418$ Å.

ACKNOWLEDGMENT

I am indebted to the Ontario Research Council for a Fund in Aid of Research.

REFERENCES

AHLFELD, FRIEDRICH (1926): Zinkteallit und Alaskait aus Bolivien, *Cbl. Min.*, A, 388–391.

DANA, J. D. & E. S. (1944): *System of Mineralogy* **1**, ed. 7, by C. Palache, H. Berman and C. Frondel—New York.

KOENIG, G. A. (1881): On alaskaite, a new member from the series of bismuth sulphosalts, *Am. Phil. Soc.*, Proc., **19**, 472–477.

NUFFIELD, E. W. (1953): Benjaminite, *Am. Mineral.*, **38**, 550–551.

SHORT, M. N. (1940): Microscopic determination of the ore minerals—*U. S. Geol. Surv., Bull.* **914**.

THOMPSON, R. M. (1950): The probable non-existence of alaskaite, *Am. Mineral.*, **35**, 456–457.

THE STRUCTURES OF THE MINERALS OF THE DESCLOIZITE AND ADELITE GROUPS: I—DESCLOIZITE AND CONICHALCITE (PART 1)

M. M. Qurashi[1] and W. H. Barnes, *Division of Physics, National Research Council, Ottawa, Canada.*

Abstract

Descloizite, Pb(Zn, Cu)(VO_4)(OH), and conichalcite, CaCu(AsO_4)(OH), are typical members of the descloizite and adelite groups of minerals, respectively, and the determination of the structures of the individual members of both groups is dependent on the success with which that of descloizite can be established. The structure of descloizite has been found by a rigorously deductive and quantitative interpretation of Patterson maps. All important features have been brought out by preliminary Fourier syntheses; the atomic positions differ markedly from an arrangement recently proposed by Bachmann. The structure of conichalcite has been obtained by numerical comparison of Patterson maps with the corresponding ones for descloizite. Preliminary difference-syntheses have established the detailed similarity of the metal-atom positions in the two structures and have indicated some differences in the sites of the oxygen atoms. The oxygen coordination around the metalloid atoms (V, As) is approximately tetrahedral in both minerals.

Introduction

The minerals of the descloizite and adelite groups are very closely related in morphology and composition (Dana, 1951); they are orthorhombic with closely-similar axial lengths, and can theoretically be derived from one another by suitable substitution of appropriate metal atoms. The probable space group of descloizite, Pb(Zn, Cu)(VO_4)(OH), has been reported as *Pnma* (or *Pn2a*) (Bannister, 1933; Richmond, 1940; Barnes & Qurashi, 1952), while that of conichalcite, CaCu(AsO_4)(OH), is $P2_12_12_1$ (Dana, 1951; Qurashi, Barnes & Berry, 1953). Hägele (1939) has argued from the resemblance of Weissenberg photographs of adelite, CaMg(AsO_4)(OH), and descloizite that the space group of the latter is really $P2_12_12_1$, with the metal atoms in positions of *Pnma* symmetry, and that the effect of the deviations of the oxygen atoms from *Pnma* positions is masked by the heavy lead atoms. Conichalcite (Qurashi, Barnes & Berry, 1953) exhibits similar characteristics, viz., reflections contradicting the *n* and *a* glides of *Pnma* are all very weak, and some experimental evidence has also been obtained to support Hägele's contention regarding the space group of descloizite.

The present paper is the first of a series dealing with the structures of the descloizite and adelite groups of minerals. It is limited to one representative of each, namely, descloizite and conichalcite. The structures of pyrobelonite, $MnPb(VO_4)(OH)$, (Strunz, 1939; Richmond, 1940; Barnes & Qurashi, 1952), and of the closely-related monoclinic mineral, brackebuschite, $(Mn, Fe)Pb_2(VO_4)_2 \cdot H_2O$ (Berry & Graham, 1948; Barnes & Qurashi, 1952), will be described in subsequent papers. The structural interest of these four minerals is evident from the precession photographs of the principal zones of each reproduced in Fig. 1 A, B. For direct comparison purposes, a B-centered cell ($B2_1/m$, or $B2_1$) for brackebuschite has been chosen and the orientation of the orthorhombic cells has been selected so that b coincides with the unique (b) axis of brackebuschite; this has the additional advantage of placing descloizite and pyrobelonite in the standard orientation (*Pnma; International Tables*, 1952) for D_{2h}^{16}.

---

[1] National Research Laboratories Postdoctorate Fellow, now with the Department of Scientific and Industrial Research, Government of Pakistan, Karachi.

Since the present investigation was commenced (Barnes & Qurashi, 1952), a structure for descloizite has been proposed by Bachmann (1953), based on Weissenberg data ($CuK\alpha$ radiation), powder photographs ($CuK\alpha$ radiation) and spectrometer records ($FeK\alpha$, β and $CuK\alpha$ radiation). Although atomic scattering factors and Lorentz-polarization factors were used in the structure factor calculations, there is no reference to absorption corrections which are significantly large with Cu, and especially with Fe, radiation. For various reasons, atomic positions and parameters, together with the coordinations of the oxygen atoms around the metal atoms, had to be assumed; it was not feasible to perform Patterson or Fourier analyses (Bachmann, private communication, 1953).

The solution of the structures of all minerals of the descloizite and adelite groups must depend ultimately on that for descloizite. For this reason the approach to the problem in this laboratory from the beginning has been as rigorously deductive as possible, and the interpretation of the experimental data is given in some detail in the present paper. This is particularly necessary in view of certain fundamental differences between the present structure and that obtained by Bachmann (1953).

In order to avoid any possible confusion throughout the present paper among references to Patterson projections, Fourier projections and structure projections, the first two are designated "maps" (with the appropriate adjective, Patterson or Fourier) and the term "projection" refers specifically to the structure. It is also convenient to denote "the (x, z) peak" in an $(h0l)$ Patterson (or Fourier) map as "the $(x, -, z)$ peak," the dash (–) indicating the undetermined coordinate; this convention has been adopted for the three principal zonal maps of each type.

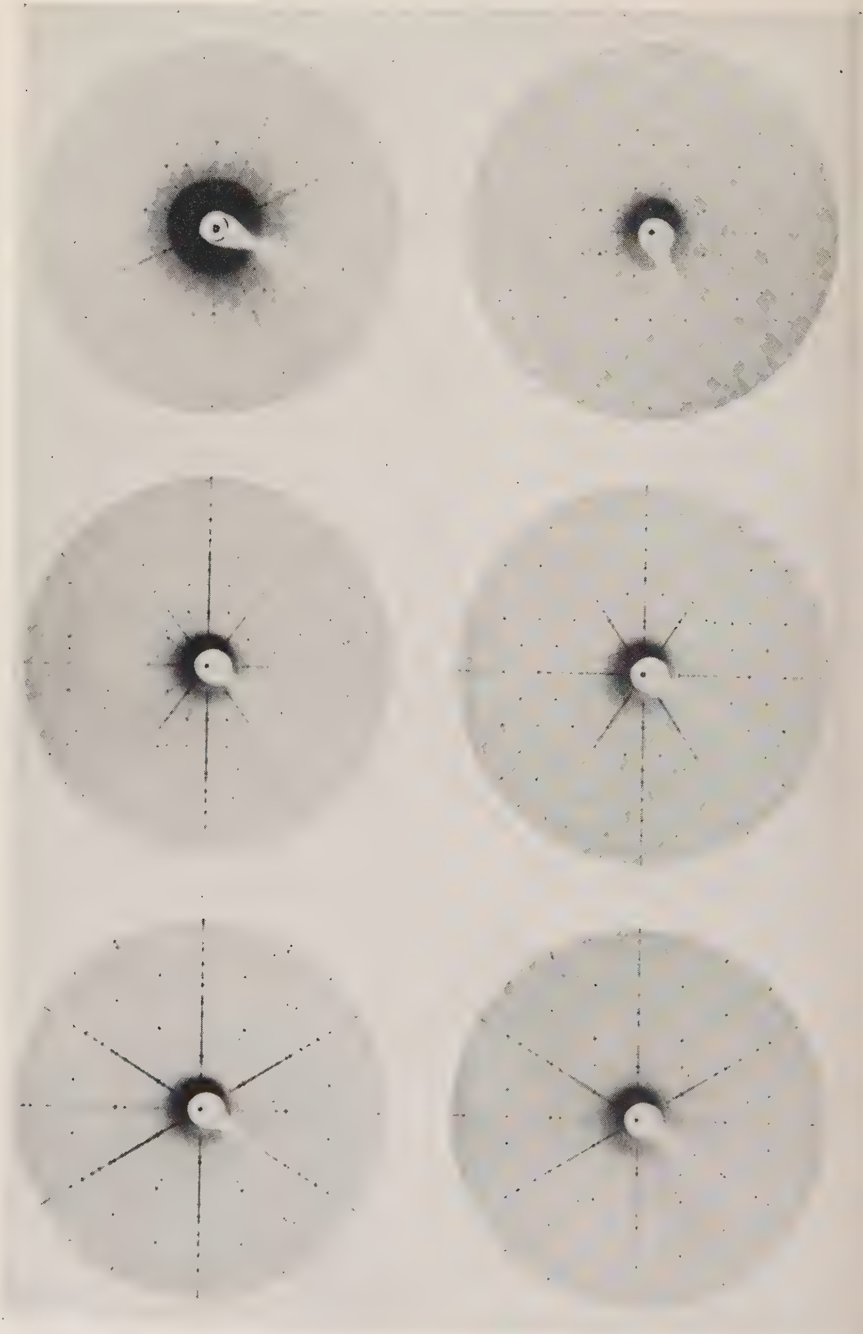

FIG. 1A. Zero level precession photographs ($\sim\frac{1}{2}$ scale) of (left hand column) brackebuschite, (right hand column) pyrobelonite; (top row) a^*c^* nets (a^* vertical); (middle row) b^*c^* nets (b^* vertical); (bottom row) a^*b^* nets (b^* vertical).

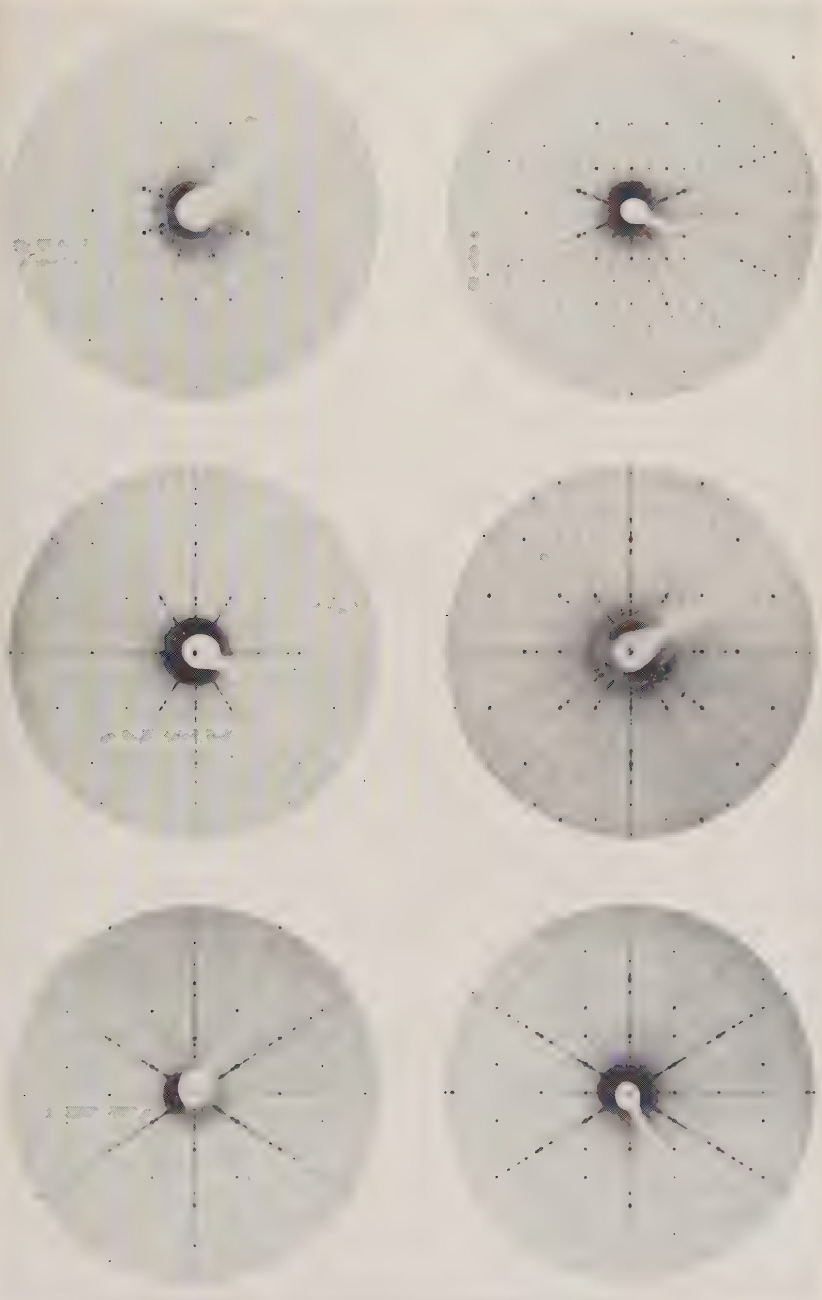

FIG. 1B. Zero level precession photographs ($\sim\frac{1}{2}$ scale) of (left hand column) descloizite, (right hand column) conichalcite; (top row) a^*c^* nets (a^* vertical); (middle row) b^*c^* nets (b^* vertical); (bottom row) a^*b^* nets (b^* vertical).

DESCLOIZITE

1. *Experimental*

The crystals of descloizite (Harvard Museum, 91040) from Los Lamentos, Chihuahua, Mexico, were kindly supplied by Professor Clifford Frondel. They were tabular {010} ({001} in *Pnam* orientation (Dana, 1951, p. 812)), and in many cases the observed faces were curved. The extinction was good and was used to align the crystals on the goniometer head to within ±2°. Some difficulty was experienced in obtaining a small equi-dimensional fragment of reasonably regular shape because the crystals have a conchoidal fracture and no cleavage. Two specimens of about 100 to 150μ, however, were finally obtained by careful cutting; it seemed impractical to use smaller ones. They were mounted with their *a* and *b* axes, respectively, parallel to the goniometer axis and Buerger precession photographs were obtained of the zero and upper levels along each of the three principal axes, using both filtered and unfiltered Mo*K* radiation ($\lambda K\alpha = 0.7107$ Å) with $\bar{\mu} = 25°$. Zonal intensities were estimated visually from multiple exposures with a film-to-film ratio of 3.0 and an over-all exposure ratio of more than 200. They were corrected for the Lorentz-polarization factor by use of the revised calculations of Waser (1951), and for absorption by standard graphical methods. The upper level photographs were examined for absences and general intensity distribution. Intensity data also were obtained from 0*kl* Weissenberg films.

2. *Space group, and preliminary location of lead atoms*

The unit cell dimensions ($a = 7.60_7$, $b = 6.07_4$, $c = 9.44_6$ Å) and the space group (*Pnma*, or *Pn*2*a*) have been reported in an earlier paper (Barnes & Qurashi, 1952), together with a preliminary location of the lead atoms at $\frac{1}{8}, y, \frac{1}{6}; \frac{7}{8}, \frac{1}{2}+y, \frac{5}{6}; \frac{3}{8}, \frac{1}{2}+y, \frac{2}{3}; \frac{1}{8}, y, \frac{1}{3}$, with $y = \frac{1}{4}$ if the space group is *Pnma*. These coordinates were based on a general survey of *hkl* intensities and on preliminary Patterson maps. Thus, no violations of the systematic space group absences were observed on precession films after exposures of ten to twenty hours, from which it was inferred that at least the lead atom, and probably the zinc and vanadium atoms also, must be in *Pnma* (or *Pn*2*a*) positions.* The equivalent positions for *Pnma* are

(*a*) $0, 0, 0; 0, \frac{1}{2}, 0; \frac{1}{2}, 0, \frac{1}{2}; \frac{1}{2}, \frac{1}{2}, \frac{1}{2}$
(*b*) $0, 0, \frac{1}{2}; 0, \frac{1}{2}, \frac{1}{2}; \frac{1}{2}, 0, 0; \frac{1}{2}, \frac{1}{2}, 0$
(*c*) $x, \frac{1}{4}, z; \bar{x}, \frac{3}{4}, \bar{z}; \frac{1}{2}-x, \frac{3}{4}, \frac{1}{2}+z; \frac{1}{2}+x, \frac{1}{4}, \frac{1}{2}-z$
(*d*) $x, y, z; \frac{1}{2}+x, \frac{1}{2}-y, \frac{1}{2}-z; \bar{x}, \frac{1}{2}+y, \bar{z}; \frac{1}{2}-x, \bar{y}, \frac{1}{2}+z;$
$\bar{x}, \bar{y}, \bar{z}; \frac{1}{2}-x, \frac{1}{2}+y, \frac{1}{2}+z; x, \frac{1}{2}-y, z; \frac{1}{2}+x, y, \frac{1}{2}-z$

* In a 200-hour 0*kl* Weissenberg photograph, a few extremely weak reflections have been observed for which $k+l$ is odd (Qurashi, Barnes & Berry, 1953). Their effect on the

Of the $hk0$ reflections, those with $(h/2)+k$ odd are very weak while those with $(h/2)+k$ even are uniformly strong, thus suggesting that the Pb-Pb peaks in the $(hk0)$ Patterson map should appear at $(\frac{1}{4}, \frac{1}{2}, -)$. Now, there are three sets of 4-fold and one set of 8-fold positions in $Pnma$, and these can each be described in terms of one or two sets of $Pn2a$ positions (4-fold). With four lead atoms to place in the cell, the Pb-Pb peaks in the $(hk0)$ Patterson map may be expected at $(2x_{\mathrm{Pb}}, \frac{1}{2}, -)$, and thus $x_{\mathrm{Pb}} \simeq \frac{1}{8}$. The choice of y_{Pb} is arbitrary in $Pn2a$, but in $Pnma$, since x_{Pb} is neither 0 nor $\frac{1}{2}$, the four lead atoms must be in position (c), and therefore $y_{\mathrm{Pb}} = \frac{1}{4}$ (*International Tables*, 1952). (Even if the space group is $Pn2a$, y_{Pb} can still be taken as $\frac{1}{4}$ and the coordinates of the vanadium, zinc, and oxygen atoms can be fixed relative to this.) From the observation that the hkl intensities repeat after $l=6$, and that the strong reflections in the $\{h0l\}$ and $\{0kl\}$ zones vary approximately as $\cos 2\pi(l/6)$, it follows that $z_{\mathrm{Pb}} \simeq \frac{1}{6}$.

These preliminary considerations indicated that no overlapping of lead atoms was to be expected in any of the principal projections, and that a detailed interpretation of Patterson maps should give definite information about the structure.

3. *Patterson maps*

In a structure of any complexity it is desirable to scale the Patterson maps carefully so that peak heights have a quantitative significance. This is particularly important in the case of decloizite if ambiguity between the positions of the vanadium and zinc atoms is to be avoided.

The intensities in each zone were first put on an absolute scale by Wilson's method (1942) of comparing $\bar{I}$ with $\sum_j f_j^2$ summed over all the atoms in the cell, a small estimated correction (10–20%) being introduced to allow for atoms overlapping in projection. The ratios of the three scale factors so obtained were then adjusted slightly on the basis of comparison with the ratios of the intensities of axial rows of reflections common to pairs of zones; in this way an averaged set of scale factors was obtained which was estimated to be correct to within about 10%.

The three Patterson maps, each for one-quarter of the cell, are shown in Fig. 2 with common edges adjacent to each other. The broken lines passing from one map to the next connect peaks that must correspond to the same interatomic vectors in both because they have one component in common. This device facilitates the three-dimensional location and interpretation of a particular interatomic vector. The correctness of

---

structure clearly will be very small and does not affect the present argument. They will be discussed in connection with the refinement of the structure.

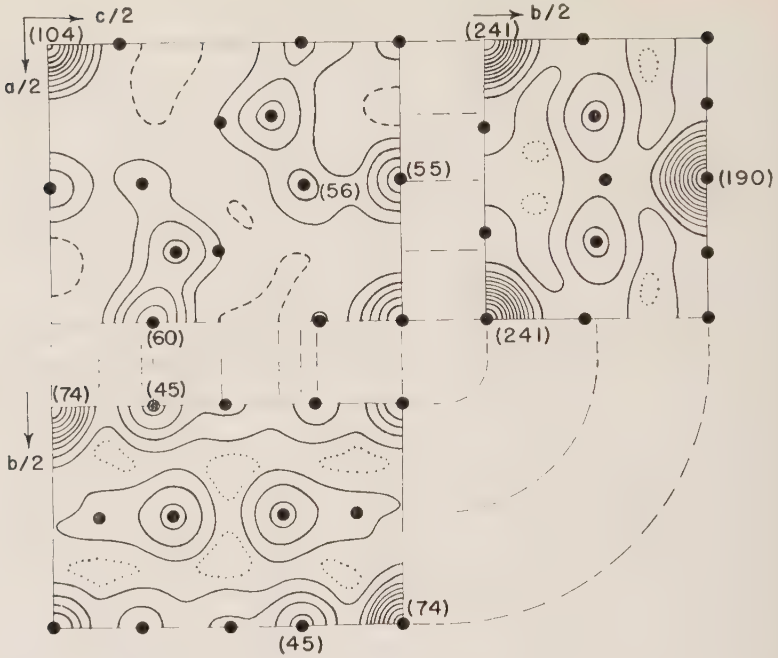

FIG. 2. Patterson maps for the three principal zones of descloizite, each over a quarter of the unit cell. Contours at intervals of 50 units with the 50-contour broken, and an extra contour at 75 units shown dotted in the ($hk0$) and ($0kl$) maps. The numbers in parentheses are the peak-heights remaining after subtraction of the Pb-Pb interactions.

the relative scales for the three maps is confirmed by the heights of the origin peaks; the slightly higher value for the $\{hk0\}$ zone is to be expected because of the appreciable depth of the cell (9.44 Å) and the consequent overlapping. From the values of these peak heights (after allowing for the effect of the lighter atoms), it can be estimated that a Pb-Pb peak of single weight, *i.e.*, one vector per unit cell, should have a height of about $450/4 = 112$. The height of a Pb-X peak of unit weight can then be estimated as follows. Place a Pb atom at (0, 0), an X atom at $(0, \frac{1}{2})$, and an X' atom at $(\frac{1}{2}, 0)$ in any given projection. It can then be shown, by calculating a theoretical Patterson map, that the peak heights, H, are related by

$$H(\text{Pb-Pb}):H(\text{Pb-}X):H(\text{Pb-}X') = \sum_{hk} f_{\text{Pb}}f_{\text{Pb}}:\sum_{hk} f_{\text{Pb}}f_X:\sum_{hk} f_{\text{Pb}}f_{X'}$$

where the products of the scattering factors, $f_{\text{Pb}}f_X$, etc., contain the temperature factor and the converging factor employed in the actual Patterson synthesis.* An approximation to the summations is obtained by an integral of the form

$$\int_0^{(\sin\theta_m)/\lambda} f_{\mathrm{Pb}} f_X \frac{\sin\theta}{\lambda}\, d\left(\frac{\sin\theta}{\lambda}\right) \qquad (1)$$

where θ_m is the maximum value of the Bragg angle used for the Patterson synthesis. The integrals may be evaluated by calculating $f_{\mathrm{Pb}} f_X$, etc., at 0.1 intervals of $\sin\theta/\lambda$ and then applying Simpson's rule. By this means the following values for the heights of peaks of unit weight were obtained:

Pb-Pb, 112; Pb-Zn, 37; Pb-V, 26; Pb-O, 8.5; Zn-Zn, 12.3; V-V, 6.2.

4. *The lead atoms*

On the basis of the preliminary survey of intensities, Pb-Pb peaks of weight 2 are to be expected at $(2x_{\mathrm{Pb}}, \frac{1}{2}, -)$ and at $(\frac{1}{2}-2x_{\mathrm{Pb}}, \frac{1}{2}, -)$ in the $(hk0)$ Patterson map. It is clear from Fig. 2 that only the observed peak of height 640 at $(\frac{1}{4}, \frac{1}{2}, -)$ can be interpreted as due to Pb-Pb, thus confirming $x_{\mathrm{Pb}} = \pm\frac{1}{8}, \pm\frac{3}{8}$ (for the four equivalent positions). The quadruple weight is to be ascribed to overlapping of peaks $(2x_{\mathrm{Pb}} \simeq \frac{1}{2} - 2x_{\mathrm{Pb}})$. Following the broken lines in Fig. 2 from the $(hk0)$ to the $(h0l)$ map, it is apparent that the Pb-Pb peaks in the latter must lie along $x = \frac{1}{4}, \frac{1}{2}$, the vectors being $(\frac{1}{2} \pm 2x_{\mathrm{Pb}}, -, \frac{1}{2})$ of weight 2, $(2x_{\mathrm{Pb}}, -, 2z_{\mathrm{Pb}})$ of unit weight (unless $z_{\mathrm{Pb}} = 0$ or $\pm\frac{1}{4}$), and $\pm(\frac{1}{2}, -, \frac{1}{2} \pm 2z_{\mathrm{Pb}})$ of weight 2 (unless $z_{\mathrm{Pb}} = 0$ or $\pm\frac{1}{4}$). Consideration of the $(\frac{1}{2}, -, \frac{1}{2})$ and $(\frac{1}{2}, -, \frac{1}{2} - \frac{1}{3})$ peaks along $x = \frac{1}{2}$ indicates that $z_{\mathrm{Pb}} = 0$ or $\pm\frac{1}{6}$, with equal probablility.

In the $(0kl)$ Patterson map, Pb-Pb peaks occur along $y = 0$, at $(-, 0, \frac{1}{2} \pm 2z_{\mathrm{Pb}})$ with weight 2 (unless $z_{\mathrm{Pb}} = 0$ or $\pm\frac{1}{4}$). Therefore, in Fig. 2 the only possible values of z_{Pb} are 0, $\pm\frac{1}{6}$, the absence of a strong peak at $(\frac{1}{2}, -, 0)$ in the $(h0l)$ map ruling out $z_{\mathrm{Pb}} = \pm\frac{1}{4}$. On this basis it follows that the lead atoms do not overlap in the $(0kl)$ projection, and, from the coordinates of special positions (c) (*Pnma, International Tables*, 1952), they cannot overlap in the $(hk0)$ projection owing to the operation of translational symmetry elements, thus establishing confidence in the estimate of 450/4 for a Pb-Pb peak of unit weight. Now, $z_{\mathrm{Pb}} = 0$ can be eliminated as a possible coordinate because the $(-, 0, \frac{1}{2})$ peak should have a weight of 4 and, consequently, a height of at least 450, whereas the observed value is only 288. Thus $z_{\mathrm{Pb}} \simeq \pm\frac{1}{6}$ in agreement with the observed peak at $(-, 0, \frac{1}{2} - \frac{1}{3})$ of weight 2 and height 270, and with the earlier estimate based on a qualitative survey of the three-dimensional data.

The coordinates of the lead atom, therefore, are $(\frac{1}{8}, \pm\frac{1}{4}, \pm\frac{1}{6})$ to a sufficient approximation. Examination of the projections in Fig. 3 show that changing the signs of y_{Pb} and z_{Pb}, either singly or together, is merely

---

[*] Because the scattering factor of the Pb atom falls off rather slowly, an extra converging factor of $\exp(-4(\sin\theta/\lambda)^2)$ was used to damp out diffraction ripples caused by the termination of the series at $\sin\theta/\lambda \simeq 0.6$.

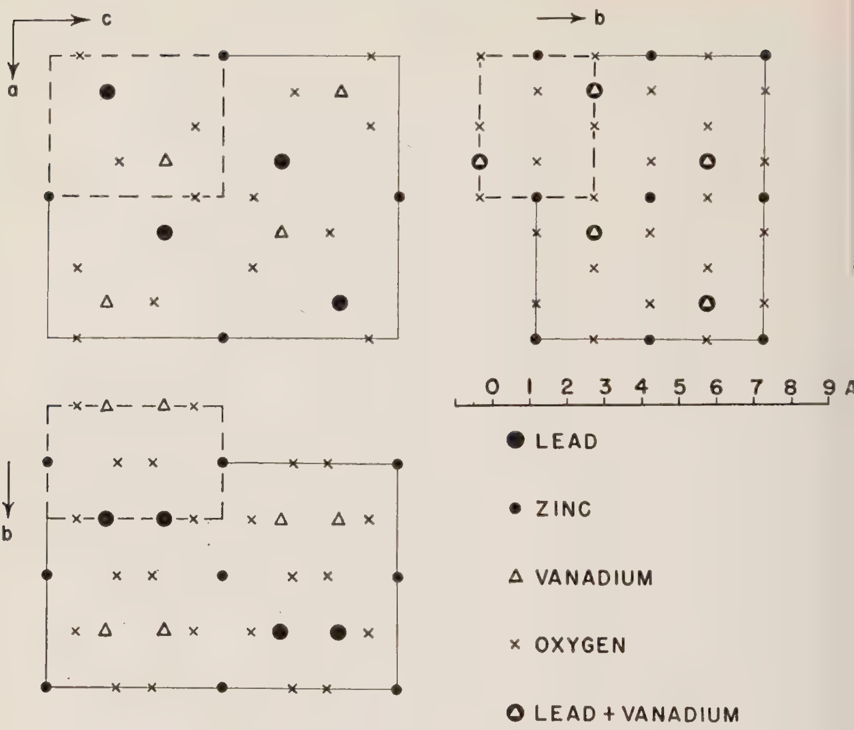

FIG. 3. Approximate structure of descloizite deduced from the Patterson maps.

equivalent to shifting the origin (from (0, 0, 0) to (0, $\frac{1}{2}$, 0), (0, 0, $\frac{1}{4}$), or ($\frac{1}{2}$, $\frac{1}{2}$, $\frac{1}{2}$)). The signs, therefore, can be taken arbitrarily as positive, and the positions of the lead atoms as ($\frac{1}{8}$, $\frac{1}{4}$, $\frac{1}{6}$), etc., represented by the large solid circles in the projections of Fig. 3. It is noteworthy that these sites are somewhat analogous to those occupied by the bismuth atoms in pucherite ($BiVO_4$, *Pnca*, special positions (*c*), $z_{Bi} \simeq \frac{1}{9}$, $c = 12.02$ Å; Qurashi & Barnes, 1953).

5. *The zinc and vanadium atoms*

Having fixed the positions of the lead atoms, the Patterson contributions from the Pb-Pb interactions can be calculated and then subtracted from the observed Patterson peaks. The residual map should represent Pb-X interactions, with perhaps a few X-X' interactions, the latter being in general much the weaker of the two. The subtraction is readily performed with the estimate of 112 for a unit Pb-Pb peak, and the resultant *difference* peak heights are given (in parentheses) beside the Pb-Pb peaks in Fig. 2. The high residual value of the (*hk*0) origin peak, and that of the one at $(\frac{1}{4}, \frac{1}{2}, -)$, suggests that a metal atom overlaps the lead atom in the $(hk0)$ projection; from the peak heights ($\sim$200) it may be either a vanadium or a zinc atom, allowing $\sim$30 for the background. (When estimating the heights of the Pb-metal peaks a reasonable allowance for background is approximately one-half of the average background, which consists largely of Pb-O and X-X' interactions.) Analogy with the pucherite structure (in which Bi and V atoms both occupy the same type of special positions and overlap in the $(hk0)$ projection; Qurashi & Barnes, 1953) favours V as the atom overlapping Pb in the $(hk0)$ projection of descloizite. In any case, however, the effective height of a Pb-X peak in the $(hk0)$ Patterson map is increased by a factor of about $(f_{\mathrm{Pb}}+f_{\mathrm{metal}})/f_{\mathrm{Pb}}\simeq 1.30$ due to this overlap.

All Pb-X peaks in the $(hk0)$ Patterson map must have a weight of at least 4 so that the axial peaks correspond to a unit Pb-X peak of height $\sim\frac{1}{4}((135-35)/1.3)=19$, which is rather small for a Pb-metal peak. On the other hand, the peaks at $(\frac{1}{4}\pm\frac{1}{8}, \frac{1}{4}, -)$ correspond to a unit Pb-X peak of height $\sim\frac{1}{4}((215-35)/1.3)=35$, which is just right for a Pb-metal peak. This places four metal atoms along $y=0$, $\frac{1}{2}$ with $x=0$, $\frac{1}{2}$, or $\pm\frac{1}{4}$. It is clear from both the $(hk0)$ and $(0kl)$ Patterson maps that $y=0$, $\frac{1}{2}$, or $\pm\frac{1}{4}$ for *all* metal atoms in the structure, and it is of interest to note that this is the limitation imposed by the special positions (a), (b), (c) of *Pnma*.

In Fig. 2 the broken connecting lines from the $(hk0)$ map to the $(h0l)$ and $(0kl)$ maps, lead from the peaks at $(\frac{1}{4}\pm\frac{1}{8}, \frac{1}{4}, -)$ to those at $(\frac{1}{4}\pm\frac{1}{8}, -, \frac{1}{4}\pm\frac{1}{12})$ and $(-, \frac{1}{4}, \frac{1}{4}\pm\frac{1}{12})$, respectively. These almost certainly represent Pb-metal vectors because they are effectively the strongest peaks in the "difference Patterson" maps. If they are due to a single Pb-X vector, then, from the $(0kl)$ peaks, the atom X must have $y=0$, $\frac{1}{2}$ and $z=0$, $\frac{1}{2}$, the other possibilities of $z=\frac{1}{6}$, $\frac{1}{3}$, etc. being ruled out by the absence of an equivalent peak at $(-, \frac{1}{4}, 0)$. This allocation gives a unit Pb-X peak of height of $\sim\frac{1}{4}\,(220-27)=48$, which corresponds to a metal atom (probably Zn) together with overlap from some other vectors. From the corresponding $(hk0)$ and $(h0l)$ peaks, it has already been established that $x=0$, $\frac{1}{2}$, or $\pm\frac{1}{4}$. The absence of peaks of height 120 at $(\frac{1}{8}, -, \frac{1}{6})$ and $(\frac{3}{8}, -, \frac{1}{3})$, however, eliminates the possibility of $x=\pm\frac{1}{4}$, and also requires overlapping atoms in the $(h0l)$ projection. Thus the x, z coordinates of the atom X must be $0, \frac{1}{2}$, and $\frac{1}{2}, 0$ which are special positions (b) of *Pnma*; the unacceptable sets $(\frac{1}{4}, \frac{1}{2}; \frac{3}{4}, 0)$ are not consistent with $P2_12_12_1$, *Pn2a*, or *Pnma*, although the y, z coordinates $(0, 0; \frac{1}{2}, 0; 0, \frac{1}{2}; \frac{1}{2}, \frac{1}{2})$ would be.

Consideration of the $(-, 0, \frac{1}{2})$ peak of height 288, and of its associated peaks in the other two maps, shows that if it is also a Pb-X peak, the coordinates of the atom X in this case must be $(-, y_{\mathrm{Pb}}, z_{\mathrm{Pb}}+\frac{1}{2})$, etc., *i.e.*, $(-, \frac{1}{4}, \frac{1}{2}+\frac{1}{6})$, $(-, \frac{1}{4}, -\frac{1}{6})$, etc., and the unit peak height would be $\sim\frac{1}{8}(288-28)=32$, thus corresponding again to a Pb-metal peak. If this is correct, a Patterson peak of height $\sim 32\times 4=128$ should be present at about $(-, \frac{1}{2}, \pm\frac{1}{6})$, (with a symmetrical one at $(-, 0, \frac{1}{2}\pm\frac{1}{6})$), and there is a rather diffuse peak of height 180 at $(-, \frac{1}{2}, \frac{1}{8})$. That this is not an independent peak is apparent from an examination of the peaks in the $(hk0)$ and $(h0l)$ Patterson maps corresponding to the $(0kl)$ peaks of heights 180 and 288. These two sets must correspond to the $(0, 0, -)$, $(\frac{1}{2}, 0, -)$, and $(\frac{1}{4}, \frac{1}{2}, -)$ peaks in the $(hk0)$ "difference Patterson" map (and to no others); they are equivalent to a unit Pb-X peak of height ~ 25, which is just right for a Pb-V peak.

The identification of the $(-, 0, \frac{1}{4})$ peak of height 158 is the next problem. Its associated peaks in the $(h0l)$ Patterson map, however, are not clearly defined, owing partly to the proximity of strong peaks. If it is assumed to represent a Pb-X vector, the coordinates of the atom X are $(-, \frac{1}{4}, \frac{3}{4}\pm\frac{1}{6})$ and the unit peak height $\sim\frac{1}{4}(158-27)=33$, which suggests either two oxygen atoms or an atom of vanadium. This makes the identification of the metal atoms a little less certain. There are, however, only three possible positions from which to choose (see Fig. 3) because the $(h0l)$ Patterson peaks corresponding to the only remaining $(0kl)$ peaks (at $(-, \frac{1}{4}, \frac{1}{4}\pm\frac{1}{6})$) are barely detectable and therefore cannot be Pb-metal peaks.

The uncertainty can be resolved by the following device. In the $(0kl)$ projection place an "average" atom with $f=\frac{1}{3}(f_{\mathrm{Zn}}+f_{\mathrm{V}}+2f_{\mathrm{O}})$ in each of the three possible sites and calculate the structure factors using these "average" atoms together with the lead atoms; assume a centric projection which is valid for $P2_12_12_1$, $Pn2a$, or $Pnma$ because of the rational values of y. In this way enough signs should be established to construct a sufficiently good Fourier map for the identification of the doubtful atoms.

The signs of all but five of the $0kl$ reflections were fixed with reasonable certainty by this means and, of the five whose signs remained uncertain, three were too weak to be observed. The resulting $(0kl)$ Fourier synthesis, calculated with an artificial converging factor of $\exp(-3(\sin\theta/\lambda)^2)$ to reduce diffraction ripples, is plotted in Fig. 5. In order to interpret this Fourier map, theoretical estimates of the various peak-heights were obtained by placing a Pb atom at $y, z, =0, 0$ and atoms X, X' at $y, z=0, \frac{1}{2}$ and $\frac{1}{2}, 0$, respectively, in the $(0kl)$ projection. The Fourier peak heights are then equal to

$$8\pi\int_0^{(\sin\theta_m)/\lambda} f\,\frac{\sin\theta}{\lambda}\,d\left(\frac{\sin\theta}{\lambda}\right) \tag{2}$$

(cf. equation (1)), where f includes any extra converging factor employed. In this way, the following peak-heights were deduced: Pb, 130; Zn, 43: V, 30; O, 9. On the basis of these values, it is apparent from the $(0kl)$ Fourier map (Fig. 5) that the $(-, 0, 0)$ position is occupied by an atom of zinc while that at $(-, -\frac{1}{4}, \frac{1}{6})$ is occupied by an atom of vanadium. In conjunction with the analysis of the Patterson maps, the coordinates of the Zn atoms, therefore, are now completely determined as $(\frac{1}{2}, 0, 0)$, etc.

The information from the Fourier synthesis concerning the y, z, coordinates of the vanadium atoms can now be combined with the data from the Patterson maps to identify the $(-, \frac{1}{2}, 0)$ and $(-, \frac{1}{2}, \frac{1}{8})$ Patterson peaks (heights 288 and 180, respectively) with Pb-V vectors. The corresponding $(hk0)$ and $(h0l)$ Patterson peaks enable $(x_{\mathrm{Pb}}-x_{\mathrm{V}})$ to be fixed as $\frac{1}{4}$, so $x_{\mathrm{V}}=-\frac{1}{8}$. The coordinates of the V atoms, therefore, are $(-\frac{1}{8}, \frac{3}{4}, \frac{1}{6})$, etc.

Thus all the metal atoms are in special positions characteristic of *Pnma*, namely, Pb in (c) at $(\frac{1}{8}, \frac{1}{4}, \frac{1}{6})$, etc., V in (c) at $(-\frac{1}{8}, \frac{3}{4}, \frac{1}{6})$, etc., Zn in (b) at $(\frac{1}{2}, 0, 0)$, etc., as shown in Fig. 3. This confirms one of Hägele's speculations regarding the structure of descloizite.

6. *The oxygen atoms*

Having established the positions of the metal atoms, the heights of the Pb-Pb, Pb-Zn, Pb-V, Zn-Zn, Zn-V, and V-V Patterson peaks can be calculated and then subtracted from the peak heights observed. In this way a set of "second difference Patterson" maps were obtained, the peaks of which should correspond largely to Pb-O, and in some cases to Zn-O and to V-O , interactions. These maps are shown schematically in Fig. 4; the small negative values for the $(hk0)$ and the $(h0l)$ origin peaks are due to insufficient allowance for overlapping when scaling the intensities.

Now from the $(0kl)$ Fourier map (Fig. 5), it is apparent that one O atom must be situated in each of the approximate positions $(-, 0, \frac{1}{5})$ and $(-, -\frac{1}{4}, \frac{1}{12})$. It is highly probable that another O atom is present at $y=\frac{1}{4}$, $z\simeq\frac{1}{20}$, and that the $(-, -\frac{1}{4}, \frac{1}{12})$ Fourier peak is due to two overlapping atoms of oxygen (peak height, calculated, 18; observed, 15). This confirms the $(-, 0, \frac{1}{4})$ and $(-, 0, \frac{3}{8})$ peaks in the "second difference Patterson" maps (Fig. 4) as Pb-(2O) peaks (unit peak height $\sim 76/4=19$), and shows that the rather diffuse peak at about $(-, \frac{1}{4}, \frac{1}{12})$ (Figs. 2, 4) is composed of Pb-O and Zn-(2O) vectors (peak height, calculated, $\sim 32+20=52$; observed, 100). On the basis of the strong $(hk0)$ peaks (Fig. 4), and the known y coordinates for these two pairs of O atoms, $x\sim 1, \frac{1}{4}, \frac{1}{2}, \frac{3}{4}$ for the first pair (for which $y\simeq\pm\frac{1}{4}$) and $x\simeq\frac{1}{8}, \frac{3}{8}, \frac{5}{8}, \frac{7}{8}$ for the second pair (for which $y\simeq 1, \frac{1}{2}$). The extraordinary heights of the $(hk0)$ peaks involved

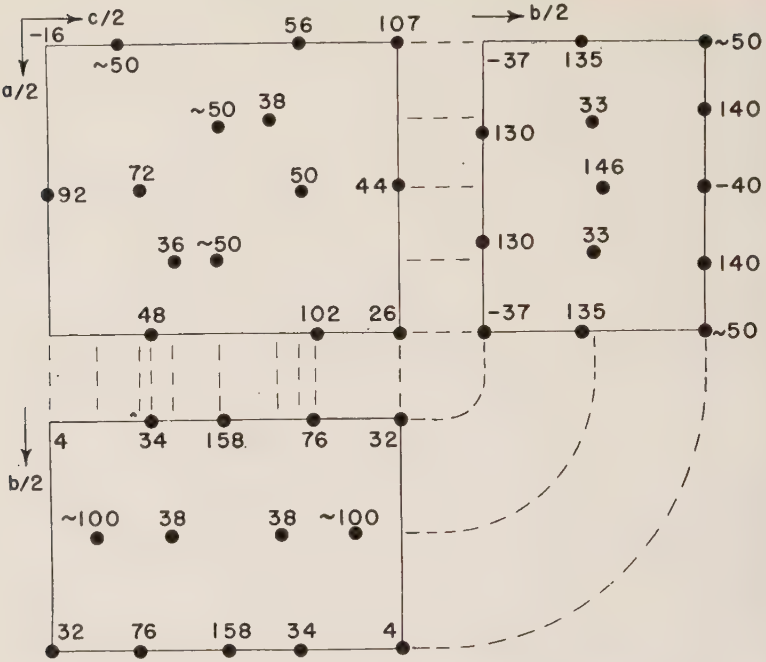

FIG. 4. Second difference Patterson maps obtained by subtracting all metal-metal peaks, thus leaving behind the metal-oxygen peaks plus the negligible oxygen-oxygen peaks.

(Fig. 4) are due to the fact that they represent overlaps of Zn-O and (Pb+V)-O vectors. Comparison with the observed (*h*0*l*) peaks (Fig. 4) now enables the *z* coordinates of the oxygen atoms to be obtained, bearing in mind that the zinc atoms overlap in the (*h*0*l*) projection (Fig. 3), and are therefore nearly as effective as the lead atoms.

The probable positions of most of the oxygen atoms were obtained in this way. The locations, of course, are somewhat uncertain, but ambiguities were largely removed with the aid of Fourier syntheses based on the signs obtained from the coordinates of the metal atoms. The approximate positions of the oxygen atoms are indicated by crosses in Fig. 3.

7. *Preliminary Fourier maps*

In section 5, the *y* and *z* coordinates of the zinc and vanadium atoms have been obtained directly from an (0*kl*) Fourier synthesis with signs determined by placing an "average" atom of scattering power $\frac{1}{3}(f_{\mathrm{Zn}}+f_{\mathrm{V}}+2f_{\mathrm{O}})$ in each of the three possible sites predicted by the Patterson maps. Since the present structure is significantly different from that proposed

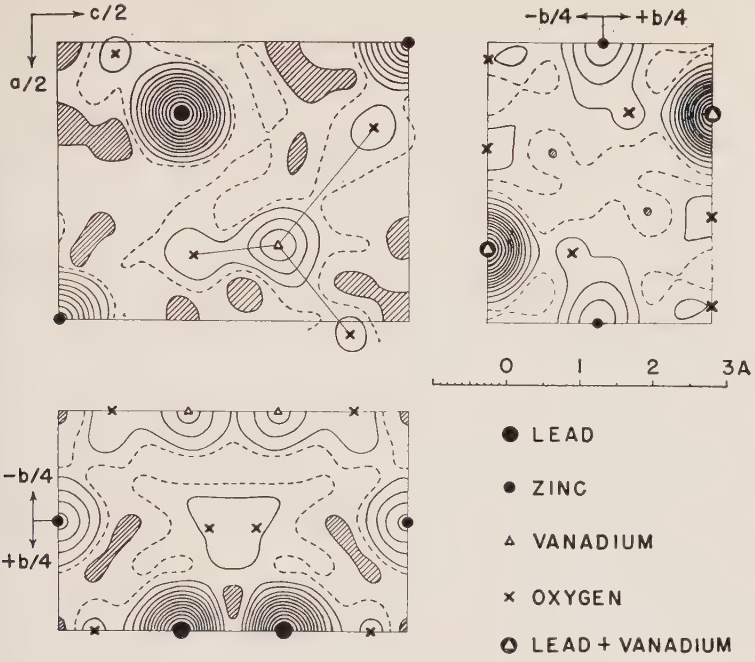

FIG. 5. Preliminary Fourier maps of the descloizite structure. Contours at intervals of 10 $e.\text{Å}^{-2}$; contour at 5 $e.\text{Å}^{-2}$ shown broken; negative regions hatched.

by Bachmann (1953), it is desirable to carry out a similar direct determination for the $\{h0l\}$ and $\{hk0\}$ zones.

From the argument presented in section 5, it is clear that the zinc, the vanadium, and two pairs of oxygen atoms must be located in the four different types of positions indicated in the $(h0l)$ projection (Fig. 3). The same device as that used for the $(0kl)$ projection (*i.e.*, placing an "average" atom in each of these positions) definitely fixed the signs of all but six of the observed reflections in the $\{h0l\}$ zone; the observed F's for these six reflections are between 20 and 40 as against 100 to 300 for the stronger reflections. The $(h0l)$ Fourier map, calculated with the signs obtained in this way, is shown in Fig. 5; it is remarkable for the fact that, in the regions of negative electron density, $-\rho$ nowhere exceeds $6e.\text{Å}^{-2}$. The map leaves little doubt about the essential validity of the previous locations for the zinc, the vanadium, and the two pairs of oxygen atoms. In particular, the absence of distortion in the contours around the peak at $(\frac{1}{2}, -, 0)$, together with the observed height of this peak $(81 = 2 \times 40.5)$, verifies the superposition of two zinc atoms required by special positions (*b*) of *Pmna*. Also, the probable overlapping of the two oxygen atoms at

$(-, -\frac{1}{4}, \frac{1}{12})$, etc. previously mentioned in connection with the $(0kl)$ Fourier map is now confirmed by the two peaks along $z \simeq \frac{1}{2} - \frac{1}{12}$). This also brings out the approximately tetrahedral coordination of oxygen atoms around the atoms of vanadium. The V-O distances are approximately 1.55 to 1.95 Å, and thus compare favourably with those in V_2O_5 (1.57 to 1.92 Å; Ketelaar, 1936; Byström, Wilhelmi & Brotzen, 1950) and in $BiVO_4$ (1.76 to 1.95 Å; Qurashi & Barnes, 1953). The oxygen configurations around the lead and zinc atoms also appear to be normal.

The signs of all but five of the structure factors observed in the $\{hk0\}$ zone were fixed by the same method; the observed values of these five are all less than 32. The resulting Fourier map also is shown in Fig. 5 and confirms the atomic coordinates already established.

It should be noted that in none of the Fourier maps of Fig. 5 are more than four resolved oxygen peaks observed in one-quarter of the cell. However, the coordinates of all five are readily inferred from the peak heights and by a combination of the information from all three maps.

Structure factors have been calculated with these coordinates, and the R-factors are 10%, 12%, and 15%, for the $\{hk0\}$, $\{0kl\}$, and $\{h0l\}$ zones, respectively, when the unobserved reflections are included. To obtain the parameters of the oxygen atoms with satisfactory accuracy, it is essential that the structure be refined by difference methods. This refinement will be discussed in a subsequent paper.

8. *Discussion of the structure proposed by H. Bachmann* (1953)

The principal projections of the structure of descloizite proposed by Bachmann (1953) are shown in Fig. 6. In order that these projections shall be directly comparable with those in Fig. 3, the a, b, and c axes of Bachmann (based on *Pmcn* adopted from Bannister, 1933) have been changed to b, c, and a, respectively, (*Pnma*), and the resulting z parameters (y in Bachmann's paper) have been altered by $\frac{1}{2}$.

It is obvious from Figs. 3 and 6 that, with the exception of the lead-atom positions, the two structures as a whole have nothing in common. On the other hand, individual projections do show certain similarities, and, with the exception of the vanadium in the $(h0l)$ projection, Bachmann has placed the atoms in the neighbourhood of one or other of the peaks of Fig. 5. His separation of the superposed zinc atoms in the $(h0l)$ projection can be attributed to the presence of the neighbouring (double) oxygen peaks. This separation displaces the four zinc atoms from the special positions (b) of *Pnma* into the general (8-fold) positions (d), unless the y coordinates are taken as $\pm\frac{1}{4}$ (instead of $0, \frac{1}{2}$) to give the (4-fold) positions (c). This discrepancy of $\frac{1}{4}$ in the y coordinates of the zinc atoms is the basic difference between the structure (Fig. 3) deduced from

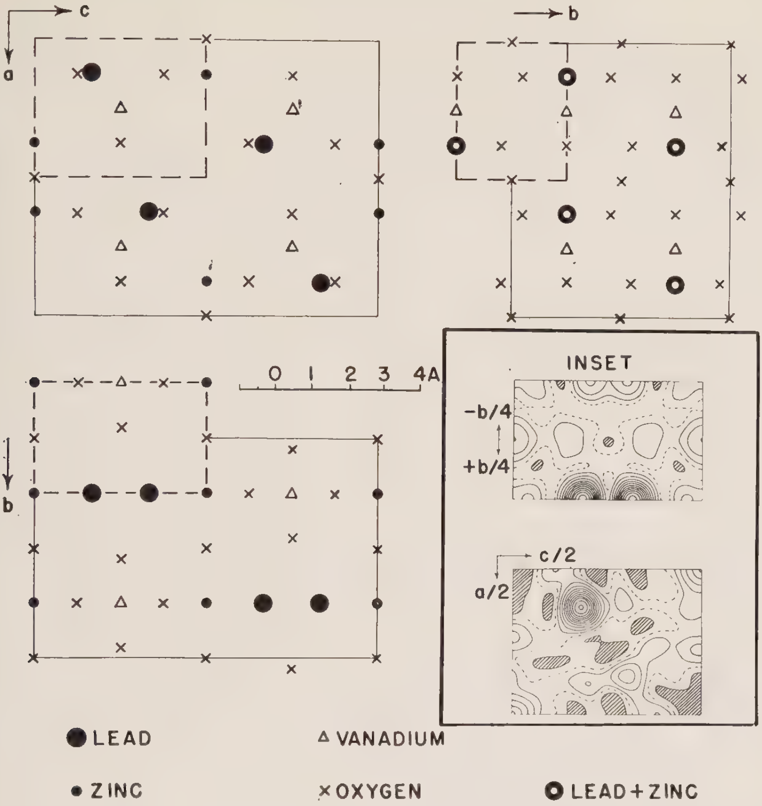

FIG. 6. Schematic representation of descloizite structure proposed by Bachmann; atoms designated as in Figs. 3, 5; note that Pb and Zn now overlap in the (*hk*0) projection. Inset: (0*kl*) and (*h*0*l*) Fourier maps obtained with magnitudes of the structure factors used in the present paper but signs fixed by Bachmann's structure; the similarity with Fig. 5 is apparent.

the Patterson maps, and that (Fig. 6) proposed by Bachmann; other differences, such as Bachmann's location of the vanadium atom in what is probably a diffraction ripple around the lead atom, can be ascribed to the use of assumed coordinations.

Finally, (*h*0*l*) and (0*kl*) Fourier maps, obtained by the use of only those structure factors whose signs are fixed definitely by the coordinates of Bachmann (*i.e.*, omitting terms for which $|F_c|$ is very small while $|F_o|$ may be large), are shown in Fig. 6) (inset). In spite of the conditioning effect of the signs, these maps correspond essentially to the structure of Figs. 3 and 5 rather than to that of Fig. 6.

CONICHALCITE

1. *Experimental and unit cell data*

The crystals of conichalcite (Harvard Museum, 92923), from the type locality, Bisbee, Arizona, also were kindly supplied by Professor Clifford Frondel. As in the case of descloizite, the lack of a cleavage, and the uneven fracture, made it difficult to obtain ideally shaped crystals for the structure investigation. Two fragments, however, about 150 μ in linear dimensions and approximately cubical, were cut and then mounted with their a and b axes, respectively, along the goniometer axis; a complete set of zero and upper level precession photographs were taken using both filtered and unfiltered MoK radiation. The intensities were estimated, corrected, and put on an absolute scale exactly as described for descloizite.

The dimensions of the unit cell are $a = 7.40$, $b = 9.21$, $c = 5.84$ Å (Berry, 1951) and the space group is $P2_12_12_1$ (Qurashi, Barnes & Berry, 1953).

2. *Patterson maps*

Patterson maps covering a quarter of the cell for each of the three principal zones are plotted in Fig. 7; an extra converging factor of $\exp(-4(\sin\theta/\lambda)^2)$ was used for uniformity with descloizite. These maps bear a striking resemblance to the corresponding ones for descloizite (see Fig. 2); in fact, there is a peak-by-peak correspondence between them as far as the peak positions are concerned. This strongly suggests that the structure of conichalcite is approximately related to that of descloizite by appropriate replacement of Pb, Zn, and V atoms by atoms of Ca, Cu, and As, for which further support comes from a detailed examination of the heights of the various peaks. Also, the replacement of vanadium by arsenic, and of lead and zinc by calcium and copper, makes the $(0kl)$ Fourier map almost exactly symmetrical about $y = \frac{1}{2}$ and $z = \frac{1}{2}$, this feature being apparent even from inspection of the $0kl$ precession photographs (Fig. 1B) in which reflections with either k or l odd are very weak. Thus the $(0kl)$ Patterson map (Fig. 7) appears approximately symmetrical about $y = \frac{1}{4}$ and $z = \frac{1}{4}$. Finally, a number of peaks that are incipient or not observable in the descloizite Patterson maps emerge fairly clearly in those of conichalcite because of the lower scattering power of the heavy atoms in conichalcite which decreases their masking effect. Typical examples are the $(0, \frac{1}{2}, -)$ Patterson peak and the $(h0l)$ Patterson peaks corresponding to the $(0kl)$ peak at $(-, \frac{1}{4}, \frac{1}{7})$.

The interpretation of the Patterson maps for conichalcite, therefore, is essentially the same as for descloizite, providing the effect of the few very weak reflections that contradict the n and a glides of $Pnma$ (Qurashi,

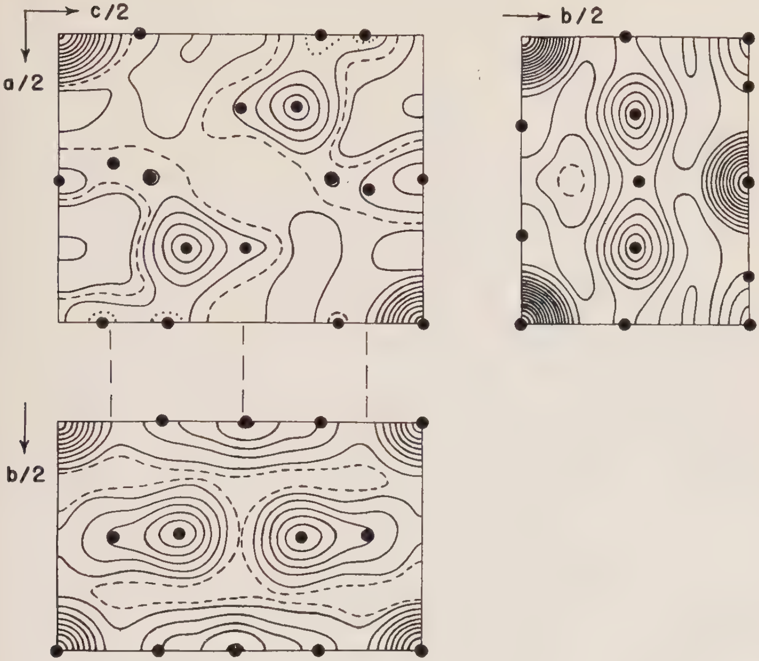

FIG. 7. Patterson maps for the three principal zones of conichalcite, each over a quarter of the unit cell. Contours at intervals of 10 units with the 45-contour broken, and sections of the 55-contour shown dotted.

Barnes & Berry, 1953) is ignored. This is justifiable because the effect will merely be to move some of the atoms slightly from the positions demanded by *Pnma* (or *Pn2a*) symmetry and it can best be taken into account during final refinement of the parameters. The problem, however, arises as to whether the lead atoms in the descloizite structure are replaced by the calcium atoms or by the copper atoms in conichalcite. The answer is not readily obtained from the Patterson maps. One solution would be to place an "average" atom with $f=\frac{1}{2}\,(f_{\mathrm{Ca}}+f_{\mathrm{Cu}})$ in each of the two possible positions (*i.e.*, those occupied by lead and zinc in descloizite), to calculate the signs of the structure factors, and then to identify the atoms from the Fourier peak heights. A better method is to plot difference syntheses, which will give directly the excess or deficit of the actual peak heights over the assumed values.

3. *Partial difference syntheses*

Since it was anticipated that the oxygen atoms in conichalcite might occupy different sites from those in descloizite, the signs for the first set

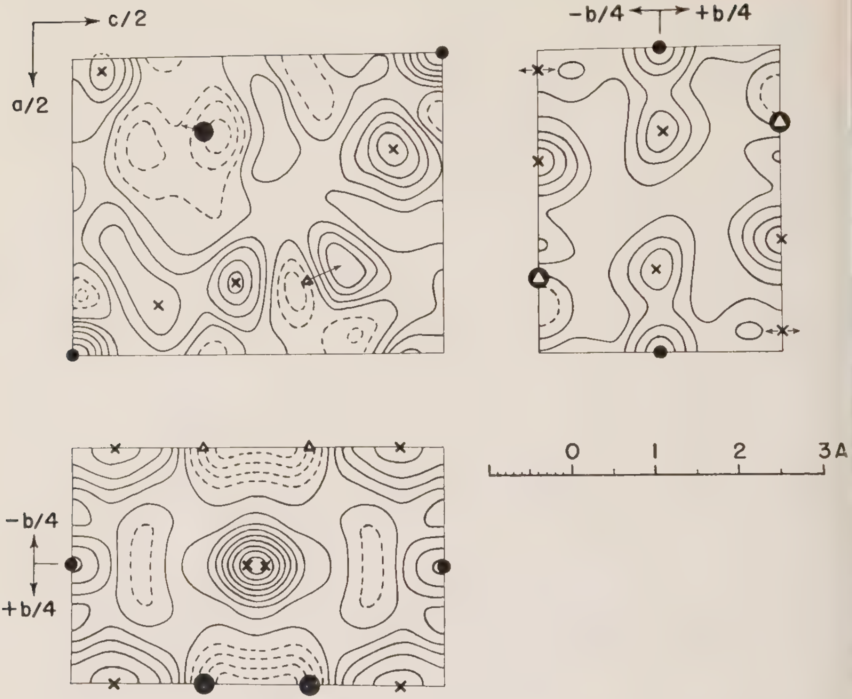

FIG. 8. Partial difference syntheses for conichalcite obtained by subtracting out the contributions of As and of $\frac{1}{2}$(Ca+Cu) placed in the possible positions for Ca and for Cu. Contours at intervals of 2 $e.\text{Å}^{-2}$ with the zero-contour and negative contours shown broken. Large solid circles, Ca; small solid circles, Cu; open triangles, As; crosses, O. The small arrows indicate the directions of some of the shifts.

of difference syntheses were calculated from the three metal atoms only, distributed as suggested in section 2. This procedure determined the signs of all but one of the observed reflections in the $\{hk0\}$ zone, and all but eleven of the observed reflections in the $\{h0l\}$ zone. For the $\{0kl\}$ zone, it was necessary to ignore all the terms with k odd because the calculated values are zero; the consequent error, however, is not large because, as mentioned previously, the observed F's for all such terms are small. The difference syntheses for the three zones are given in Fig. 8. Comparison with the Fourier maps of descloizite (Fig. 5) shows that the peaks corresponding to the zinc atoms are all positive (about $8e.\text{Å}^{-2}$ per zinc atom) from which it follows that copper replaces zinc. The peaks corresponding to lead atoms are negative in all three difference syntheses, although the effect in the $(hk0)$ and $(0kl)$ difference maps is diminished somewhat by effective overlapping with arsenic, and possibly by an additional oxygen in the $\{hk0\}$ zone. The negative peaks, however, confirm that calcium (in conichalcite) must occupy the position of lead (in descloizite).

The three difference syntheses also give some information about the positions of the oxygen atoms. These are essentially the same as in the descloizite structure except that the two overlapping oxygen atoms along $x=\frac{3}{8}$ in the $(h0l)$ projection of descloizite (Figs. 3, 5) appear (Fig. 8) to have separated in conichalcite; this separation, however, turns out to be largely spurious on refinement of the structure. It is of interest that the $(hk0)$ difference map (Fig. 8) already gives indications of the shift of one oxygen atom away from special positions (c) of $Pnma$ with $y=\pm\frac{1}{4}$.

The present R-factors for the conichalcite structure are 12%, 22%, and 22% for the $\{hk0\}$, $\{0kl\}$, and $\{h0l\}$ zones, respectively, when all the unobserved reflections are included. The refinement of the structure and the introduction of the weak reflections contradicting the n and a glides of $Pmna$ will be considered at the same time as the refinement of the descloizite structure.

REFERENCES

BACHMANN, H. G. (1953): Die Kristallstruktur des Descloizit, *Acta Cryst.*, **6,** 102; Beiträge zur Kristallchemie natürlicher und künstlicher Schwermetallvanadate; II. Die Kristallstruktur des Descloizit, *N. Jahrb. Min.*, Mh., 9/10, 193–208.

BARNES, W. H., & QURASHI, M. M. (1952): Unit cell and space group data for certain vanadium minerals, *Am. Mineral.*, **37,** 407–422.

BANNISTER, F. A. (1933): The identity of mottramite and psittacinite with cupriferous descloizite, *Min. Mag.*, **23,** 376–386.

BERRY, L. G. & GRAHAM, A. R. (1948): *X*-ray measurements on brackebuschite and hematolite, *Am. Mineral.*, **33,** 489–495.

BYSTRÖM, A., WILHELMI, K. A. & BROTZEN, O. (1950): Vanadium pentoxide—a compound with five-coordinated vanadium atoms, *Acta Chem. Scand.*, **4,** 1119–1130.

DANA, J. D. & E. S. (1951): *System of Mineralogy*, **2,** ed. 7, by C. Palache, H. Berman & C. Frondel, New York.

HÄGELE, G. (1939): Adelit und Descloizit, *N. Jahrb. Min.* Abt. A, Beil.-Bd. **75,** 101–109.

International Tables for X-Ray Crystallography (1952), Birmingham.

KETELAAR, J. A. A. (1936): Die Kristallstruktur des Vanadinpentoxyds, *Zeit. Krist.*, (A)**95,** 9–27.

QURASHI, M. M. & BARNES, W. H. (1953): The structure of pucherite, $BiVO_4$, *Am. Mineral.*, **38,** 489–500.

QURASHI, M. M., BARNES, W. H. & BERRY, L. G. (1953): The space group of conichalcite, *Am. Mineral.*, **38,** 557–559.

RICHMOND, W. E. (1940): Crystal chemistry of the phosphates, arsenates, and vanadates of the type $A_2XO_4(Z)$, *Am. Mineral.*, **25,** 441–479.

WASER, J. (1951): The Lorentz factor for the Buerger precession method, *Rev. Sci. Instr.*, **22,** 563–566.

WILSON, A. J. C. (1942): Determination of absolute from relative x-ray intensity data, *Nature*, **150,** 152.

DETERMINATION OF COLUMBIUM IN ORES BY *X*-RAY FLUORESCENCE[1]

JOHN S. STEVENSON, *McGill University, Montreal, Quebec.*

ABSTRACT

Analyses for columbium in pyrochlore ores from North Bay, Ontario, have been made successfully by using *x*-ray fluorescence techniques. It was necessary to use, as in methods of optical spectroscopy, an internal standard for this work. The choice of a suitable internal standard for a particular metal in a specific mineral association or ore-type requires consideration of the characteristic *x*-ray spectrum and absorption edges not only of the metal to be analysed for but also of the metals with which it is associated. For these reasons, molybdenum was found to be a suitable internal standard for columbium in the analyses of these ores.

INTRODUCTION

X-ray spectroscopy has been used recently with very satisfactory results to supplement optical spectroscopy in the spectrochemical analysis of metals in ores and minerals.

Because of the current demand for columbium, research was started in April, 1953, in the *x*-ray laboratory of the Department of Geological Sciences of McGill University on methods of *x*-ray analysis for columbium in ores of the metal. A method using *x*-ray spectroscopy was set up and many routine analyses for columbium in ore samples were run during the following months with excellent results.

THEORY

Secondary x-radiation

X-ray spectroscopy involves an analysis of the secondary *x*-ray or fluorescence spectrum of an atom or element when that atom is subjected to primary *x*-radiations from a separate *x*-ray tube. Because each element possesses a characteristic emission spectrum, an analysis of its spectrum will serve to identify the element. The concentration of an element present in a sample is proportional to the intensity of the characteristic lines in its emission spectrum and therefore measurement of these intensities will give the percentage of the element present.

The emission spectrum of an element consists of characteristic wave-lengths depending on its atomic structure. These wave-lengths may be grouped into several series according to the electron-shells or energy levels of the atom, but wave-lengths from only two, the K and the L series, are commonly used in x-ray spectroscopy, and within these series the characteristic wave-lengths or lines most commonly used are the $K\alpha_1$, $K\beta_1$ in the K series, and the $L\alpha_1$, $L\beta_1$, and $L\beta_2$ in the L series.

---

[1] EDITOR'S NOTE.—The 15th meeting of the International Union of Pure and Applied Chemistry, in 1949, agreed to use the name *niobium* instead of *columbium* for element 41. The element is still best known as columbium to mineralogists in North America, in future the newly accepted name should be used.

The analysis of a secondary x-ray emission spectrum of an element is made by the separation or dispersion and the identification of the characteristic wave-lengths present in the spectrum. This dispersion is accomplished by using the diffraction grating supplied by suitably spaced atomic planes of a crystal. For our present purposes, the most satisfactory planes were the $(33\bar{1})$ planes of a mica crystal. The diffracted wave-lengths are identified by their reflection angles as given by the Bragg equation $n\lambda = 2d \sin \theta$ in which n is the order of the reflection, λ the diffracted wave-length, d the spacing in Ångstrom units of the diffracting atomic planes, and θ is the spectrometrically measured angle of incidence of the x-rays on the diffracting planes.

A Geiger counter mounted on a goniometer is used to intercept and identify the wave-lengths in terms of the Bragg angle and also to measure the intensities of radiations for each wave-length, in terms of quanta of radiation per second. The Geiger counter does this by passing on the impulses received from the quanta to an electronic scaling and counting unit.

The proportionality constant of the intensity of a particular line of the element in relation to the percentage of the element present in a sample is determined by reference to intensity measurements made on the same line, the reference line, in standard samples containing known amounts of the element to be determined. In practice, a calibration curve giving percentage of element in terms of intensities for a specific line in the spectrum of that element is prepared by measuring line intensities on prepared samples. This proportionality relation depends not only on the percentage of that element but also on the kind and percentage of other elements present in the sample, *i.e.*, on the composition of the matrix. However, as long as the composition of the matrix of an unknown sample remains approximately the same as the matrix of the reference or standard sample, the proportionality between intensity of reference line and percentage of element will be constant. These conditions usually obtain in samples of steels and alloys, and standard samples with varying proportions of the same elements may be prepared and analysed and a calibration curve set up for a particular element on the standard.

Should the matrix of the unknown be different from that of the standard samples, as it usually is in ores and minerals, then the proportionality between the percentage of an element and the intensity of a reference line of that element may be altered from what it is in the standard samples from which the calibration curve was prepared. This is so because, if a change is made in the concentration of some other element that possesses one or more lines that may have absorption or excitation effects on the particular reference line used in the intensity measurements, then the measure of the intensity of that line will also be changed and the proportionality of measured intensity to the amount of the element present also changed.

Internal standard

The disturbing effect of the matrix may be minimized in the analyses of ores and minerals by the use of an internal standard. In this method a known amount of an element, the internal standard, is added to the standard samples and the same amount to the unknown samples. If the internal standard contains an emission line whose wave-length is close to that of a line in the element to be analysed for, then the absorption or excitation of the two nearby lines by the matrix will be in very nearly the same ratio. The intensity ratios of these references lines in the two elements, the internal standard and the element to be analysed, are then determined in standard samples prepared to contain different percentages of the one element and a constant percentage of the internal standard. In a sample of unknown composition to which the same percentage of the internal standard has been added, it is only necessary then to measure the intensities of the reference lines, calculate the intensity ratio, and by reference to the calibration curve prepared from the standard samples, determine the percentage of the sought-for element present.

The ores or minerals should not contain in abundance an element or elements that will either suppress by absorption or enhance by secondary radiation more of the one reference line than the other. Knowing what elements might be expected in a sample, reference is made to wave-length tables (von Hevesy, 1932, p. 148) of absorption edges and emission lines. From these it can be determined whether there are any edges with wave-lengths between those of the reference lines. If there is such an edge, there will be a greater absorption and suppression of the reference line with the shorter wave-length, and consequently a change, for a given amount of the internal standard, in the intensity ratio of the reference lines. For analogous reasons, the unknown sample should not contain elements with lines whose wave-lengths lie either between the absorption edges of the reference lines of the sought-for element and the internal standard, or on the short wave-length side of their absorption edges. Otherwise there will be an enhancing by excitation of one or the other of the reference lines and a change in the intensity ratio of the lines.

The possibilities of disturbing effects from lines of other elements in a sample can be minimized by the selection of an internal standard that possesses a reference line very close to a reference line in the sought-for element, and also possesses an absorption edge close to the absorption edge of that same line.

EQUIPMENT

In this investigation, a General Electric SPG Fluorescent *X*-ray Spectrometer was used, with an XRD-3 General Electric Spectrogoniometer and *X*-ray Detector. The primary *x*-radiation was obtained from tungsten-target Machlett AEG-50T tube and a sample area $\frac{3}{4}$-inch square irradiated. The secondary *x*-ray or fluorescent radiation from the sample was diffracted through a bent mica crystal arranged for transmission with a *d* spacing of *ca* 1.5 Å, and detected by a Geiger-counter spectrometer. An electronic circuit provided for the chart recording (Fig. 1) of location and relative intensities of the lines in the emission spectrum of the sample.

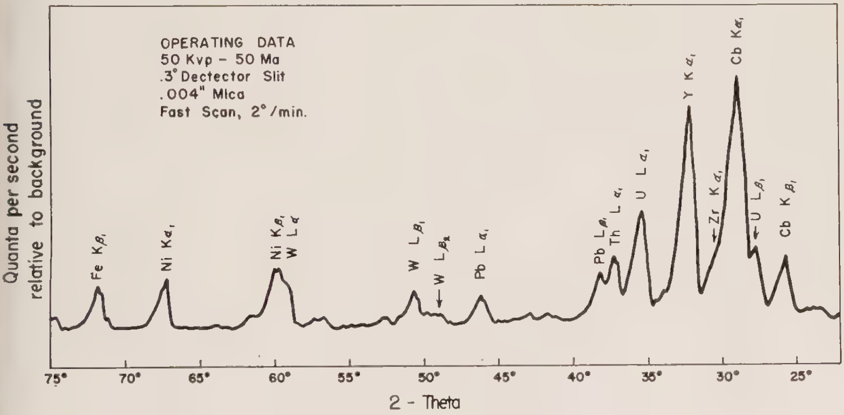

FIG. 1. Secondary *x*-ray spectrum from an ore-sample; scanning for qualitative analysis only.

Automatic scanning and the chart-recorder were used only for qualitative analyses of unknown samples. For quantitative work, the goniometer of the spectrometer was set at the 2-theta angle for each of the reference lines, one in the sought-for element and one in the internal standard. The time required for a pre-set number of counts or quanta from each setting was recorded by a timer; from this the total intensity determined as counts or quanta per second and intensity ratios calculated. Because the counts due to the effect of extraneous background are normally the same under similar operating conditions for the elements in the unknown samples and for the elements in the standard samples, the net number of counts due to the element alone is not determined.

EXPERIMENTAL PROCEDURE

Mineralogy of the ore to be analysed

The problem undertaken was the development of an accurate and relatively rapid method of determining columbium in a complex columbium ore from North Bay, Ontario. This ore contained the following non-metallic minerals, listed in approximate order of decreasing abundance: calcite, orthoclase, quartz, apatite, biotite, garnet, sodic pyroxene, pyrochlore, fluorite, albite, scapolite, and small amounts of uraninite. The metallic minerals included small amounts of pyrite, magnetite, and hematite. Not all these minerals were necessarily present in all samples of the ore. It may be noted that no molybdenum minerals were present.

Choice of an internal standard

In choosing an internal standard, many samples were scanned to determine what elements might be expected to occur in troublesome amounts. From a study of the spectral charts so obtained and from tables of the principal *x*-ray spectral lines and of absorption edges, molybdenum was chosen as the internal standard, and the $K\alpha_1$ lines of this element and of columbium chosen as reference lines. Since molybdenum did not occur

TABLE 1. PRINCIPAL *X*-RAY SPECTRAL LINES OF THE ELEMENTS[1]

Wave-length XU[2]	Element	Line	Absorption Edge, XU
616	Rh	$K\alpha_2$	533
620	Mo	$K\beta_2$	618
630	Th	$L\gamma_2$	627
631	Mo	$K\beta_1$	618
642	Ru	$K\alpha_1$	558
646	Ru	$K\alpha_3$	558
652	Th	$L\gamma_1$	627
708	Mo	$K\alpha_1$	618
708	U	$L\beta_3$	569
712	Mo	$K\gamma_2$	618
718	U	$L\beta_1$	592
739	Y	$K\beta_1$	726
745	Cb	$K\alpha_1$	650

[1] von Hevesy, 1932, pp. 141–142.

[2] XU = *X*-ray wave-length unit; 1000 XU = 1kX = 1.00202 Å.

in the ores on which work was done, the amount present would always be only the amount added as the internal standard.

A study of the preceding Table will show the lines that come between the K absorption edges at 618XU and 650XU for molybdenum and columbium respectively. Not only are these intervening lines relatively weak lines, but the possible interfering elements, ruthenium and thorium, occur in the ores in no more than trace amounts.

Reference to a table of absorption edges (von Hevesy, 1932, p. 156) showed that the only edges between $K\alpha_1$ at 708XU for molybdenum and $K\alpha_1$ at 745XU for columbium were the L absorption edge for uranium at 721XU and the K absorption edge for yttrium at 726XU. Although uranium is present in the ores, the L absorption edge is weak; and although the K of yttrium edge is relatively strong, the amount of yttrium present is small. The effect of these elements on the $K\alpha_1$ intensity ratios of columbium and molybdenum would therefore be negligible. For these reasons, the $K\alpha_1$ line of molybdenum was chosen as a suitable reference line for the $K\alpha_1$ line of columbium in the North Bay ores, and standards using molybdenum as the internal standard for columbium were set up.

Technique

Standards were prepared to contain the same percentage (5%) of MoO_3 (C.P.) and the following percentages of Cb_2O_5: 0.15, 0.30, 0.90, 1.00, 2.00, 2.50. This was the range expected in the material to be analysed, as previously determined from chemical analyses of selected typical samples.

Because of the abundance of orthoclase feldspar in the ore, feldspar, ground to pass 100-mesh, was used as a matrix for the mixtures of molybdenum and columbium oxides. However, runs were also made with other prepared samples using calcite and quartz as a matrix, and satisfactory checks were obtained.

To ensure getting samples as uniform as possible—uniform both as to particle size and as to the mixing of Cb_2O_5 and MoO_3—each sample, after addition of the oxides, was ground the same length of time, ten minutes, in a mechanically operated agate mortar and pestle. A ten-minute grind of the powdered oxides into the 100-mesh feldspar matrix appeared to be the optimum to give reproducible results with a minimum amount of sample preparation.

From a 10-gram initial sample, a $2\frac{1}{2}$-gram sample, enough to fill two sample trays, an original and a duplicate, was cut for analysis.

The sample trays consist of small rectangular blocks $2'' \times 1\frac{1}{4}'' \times \frac{3}{16}''$ into which a rectangular cavity $\frac{7}{8}''$ square $\times \frac{3}{32}''$ deep has been routed. The blocks were cut from a sheet of cold-setting plastic.[1] The area of the cavity, $\frac{7}{8}$-inch square, is a little larger than the opening, $\frac{3}{4}$-inch square, for the irradiating x-rays, but this oversize ensures a constant area of irradiation for all samples. Data are lacking on the minimum thicknesses of powder in a sample tray that will produce maximum fluorescence under specified operating conditions. Other conditions being the same, a thickness less than the minimum will produce less intensity of a particular spectral line, but a greater thickness will not produce a greater intensity. For a metallic element Glucker (in Koh & Caugherty, 1952) has estimated this thickness to be in the order of 0.1 mm. Since there was no shortage of material for analysis, a convenient depth of $\frac{1}{32}$-inch for the sample cavity was used, a depth well in excess of that necessary for maximum fluorescence yield.

The filled trays were packed lightly with the powdered sample and smoothed off with a glass slide. The trays, one at a time, are then placed in a holder where they are held at an angle of 30 degrees from the horizontal. The holder, with its sample, is so placed below the lower part of the x-ray tube that a vertical beam of x-rays irradiates the exposed surface of the sample and is reflected horizontally from this surface through the mica crystal to the Geiger tube. It is our experience that none of the sample is lost from the tray with this arrangement. The intensity of the radiations of the selected lines, $K\alpha_1$ in the emission spectra were then determined for columbium and molybdenum. This was done by setting the goniometer at the 2 θ angles for the $K\alpha_1$ lines respectively of columbium and molybdenum and obtaining the time for a predetermined number of quanta from each of these two $K\alpha_1$ lines. Five time-counts were made on each line for each sample, the average time taken, and from this time, the intensity in terms of quanta per second determined for each line. The logarithm of the intensity ratio of these lines, $I\mathrm{Cb}K\alpha_1$ to $I\mathrm{Mo}K\alpha_1$ was then plotted against log per cent Cb_2O_5, and the working curve (Fig. 2), with molybdenum as an internal standard, obtained.

In practice, all unknown samples for analysis are ground to pass 100-mesh, 5 per cent MoO_3 added to each sample, and, as with the standards, given a 10-minute mixing grind in a mechanical mortar and pestle. For each sample, the intensity ratio, $I\mathrm{Cb}K\alpha_1$ to $I\mathrm{Mo}K\alpha_1$, is determined and from this ratio the percentage of Cb_2O_5 present in the sample is read from the working curve.

Because of the low intensity of secondary radiations from amounts of Cb_2O_5 less than 0.1 per cent and resulting inaccuracy of results, no attempt was made to determine amounts of Cb_2O_5 less than this; that is, less than 0.07 per cent Cb. For the present investigation the upper limit

---

[1] Polyester Resin Laminac manufactured by American Cyanamid Co., N. Y.

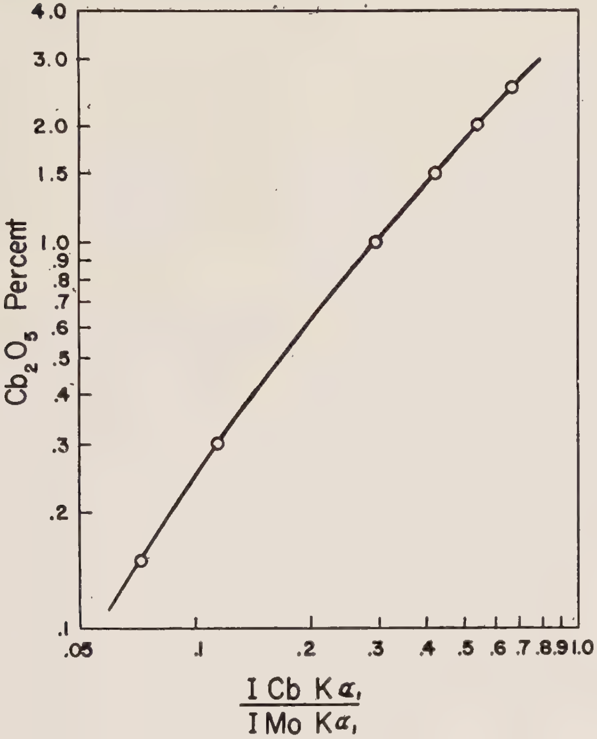

FIG. 2. Working or calibration curve for columbium using molybdenum as an internal standard.

for which standards were prepared was 2.5 per cent Cb_2O_5.

Using the technique outlined above with molybdenum as the internal standard, about 2,500 ore-samples have been analysed for columbium in the University laboratory from May, 1953 to November, 1953, inclusive, and very consistent results have been obtained.

Acknowledgements

The writer gratefully acknowledges the helpful advice of Dr. S. C. Robinson and Mr. E. J. Brooker of the Geological Survey of Canada, during the initial stage of the development of this procedure. He also wishes to thank Professor J. E. Gill of McGill University for his critical reading of the manuscript.

References

KOH, P. K. & CAUGHERTY, B. (1952): *X*-ray fluorescent analysis—*Jour. App. Phys.*, **23**, 429.

VON HEVESY, G. (1932): *Chemical Analysis by X-rays and its Applications*—New York.

STUDIES OF RADIOACTIVE COMPOUNDS: VII -PHOSPHURANYLITE AND DEWINDTITE

D. D. Hogarth, *Geological Survey of Canada, Ottawa*

AND

E. W. Nuffield, *University of Toronto, Toronto.*

Abstract

Phosphuranylite from Urgeirica, Portugal is orthorhombic, *Bmmb* with *a* 15.85, *b* 17.42, *c* 13.76 Å. Dewindtite from Kasolo, Belgian Congo is isostructural as shown by Frondel (1950), with *a* 16.00, *b* 17.62, *c* 13.66 Å. Calculations of unit cell contents do not lead to unique chemical formulas for the minerals. Available chemical analyses suggest that the chemical formulas of phosphuranylite and dewindtite are not analogous.

Recently Frondel (1950) found a remarkable similarity in the *x*-ray powder patterns of phosphuranylite and dewindtite and suggested that the two minerals are isostructural and exhibit at least partial isomorphous replacement between calcium (phosphuranylite) and lead (dewindtite). Three incomplete analyses by Hallowell (in Frondel) on minute quantities however, led to the formula $Ca(UO_2)_7(PO_4)_4(OH)_4 \cdot 10H_2O$ for phosphuranylite in contrast to the accepted formula for dewindtite $Pb_3(UO_2)_5(PO_4)_4(OH)_4 \cdot 10H_2O$ (Dana, 1951).

Frondel's material was unsuitable for single crystal *x*-ray studies and as a result the calculation of unit cell contents which might have explained this discrepancy, could not be made. An opportunity to provide these data came to us when we obtained a small specimen from Urgeirica, Portugal showing numerous tiny laths of phosphuranylite.

The optical properties of this specimen were found to be biaxial negative, $2V$ small, indices of refraction for Na light: nX 1.669 (pale yellow), nY 1.710 (golden yellow), nZ 1.710 (golden yellow). They are in good agreement with the optical constants given by Frondel for phosphuranylite from the Ruggles Mine, New Hampshire and from Carrasca, Portugal. The indices of lead-bearing phosphuranylite are substantially higher. A spectrographic analysis of our specimen showed only a trace of lead. A tiny lath gave the following data from *x*-ray rotation and Weissenberg films: orthorhombic, *Bmmb*; *a* 15.85, *b* 17.42, *c* 13.76 Å. In this orientation the direction of elongation is parallel to [001] and the flattening is parallel to (100) or (110).

The specimen of dewindtite which was available to us proved to be fine-grained and without visible crystal form. Close examination showed that it was interlayered with meta-torbernite. A few small grains of pitchblende were seen as well as a considerable quantity of an orange mineral of about the same specific gravity as dewindtite. It was practical to separate only enough dewindtite for *x*-ray powder study.

X-ray powder patterns with copper radiation[1] and using a camera of diameter 114.59 mm. were now prepared of both minerals. The pattern of phosphuranylite was indexed with the aid of the cell constants derived by the Weissenberg study to $d = 2.88$ Å. The practically identical dewindtite pattern was then indexed by analogy with phosphuranylite (Table 1). The spacings for three planes ($d_{400} = 4.00$, $d_{204} = 3.14$, $d_{440} = 2.96$ Å) were used to calculate the cell dimensions: *a* 16.00, *b* 17.62, *c* 13.66 Å. Although care was taken to obtain an undistorted *x*-ray powder pattern and corrections were made for the personal error in measurement, the values probably have an error of about ±0.1 Å because only the low

TABLE 1. *X*-RAY POWDER DATA

PHOSPHURANYLITE			*hkl*	DEWINDTITE		
I	*d*(meas.)	*d*(calc.)		*I*	*d*(meas.)	*d*(calc.)
3	10.34	10.39	101			
10	7.91	7.92	200	10	8.01	8.00
5	5.83	5.86	220	10	5.89	5.92
½	4.92	4.93	301	2	4.99	4.97
			212			4.98
2	4.73	4.75	311	2	4.77	4.78
3	4.42	4.44	032			
		4.41	103	4	4.37	4.38
1	4.30	4.29	321			
6	3.96	3.96	400	7	4.00	4.00
3	3.88	3.87	232	1	3.90	3.89
3	3.81	3.82	240	1	3.86	3.86
2	3.44	3.44	004			
		3.43	402			
1	3.37	3.38	014			
		3.37	412	5	3.40	3.39
6	3.15	3.16	204	7	3.14	3.14
6	3.10	3.11	052			
		3.10	214			
		3.10	143			
		3.09	501	5	3.07	3.09
			511			3.07
1	2.93	2.93	440	5	2.96	2.96
6	2.88	2.90	060			
		2.89	252			
		2.85	351	9	2.88	2.87

---

[1] Using Cu $K\alpha = 1.5418$ Å.

order reflections could be indexed with assurance and used for the calculations.

The specific gravity of phosphuranylite is not accurately known. Frondel set the value at about 3.2; Branche, Chervet & Guillemin (1951) stated that it sank in methylene iodide of density 3.31. Schoep (1922) determined the specific gravity of dewindtite crystals as 5.03 at 17° C. with a pycnometer.

The chemical composition of phosphuranylite, like the specific gravity, is difficult to determine accurately. This difficulty lies in the problem of obtaining sufficient material free from contamination. Two of the three partial analyses of Hallowell are reproduced in Table 2 (IA, IB) after subtracting insoluble matter and recalculating to 100%. The unit cell contents have been calculated for an assumed specific gravity of 3.5 (IIA, IIB) and 4.0 (IIIA, IIIB). The most probable cell contents for analysis A (IVA) are

TABLE 2. PHOSPHURANYLITE, ANALYSES AND UNIT CELL CONTENTS

	Analysis A				*Analysis B*			
	I	II	III	IV	I	II	III	IV
CaO	3.43	4.9	5.6	6	2.3	3.3	3.8	4
UO_3	72.94	20.4	23.3	24	77.8	22.3	25.5	24
P_2O_5	10.65	6.0	6.9	6	11.3	6.4	7.3	8
H_2O	[12.98]	57.7	66.0	66	[8.6]	38.2	43.7	44
			calc. S. G. =	4.03				3.94

I. The chemical analyses of Hallowell (nos. 2 & 3 in Frondel, 1950) recalc. to 100% after subtracting insol. II. Calc. unit cell contents for assumed S. G. of 3.5. III. Calc. unit cell contents for assumed S. G. of 4.0. IV. Possible ideal unit cell contents.

$$6CaO \cdot 24UO_3 \cdot 6P_2O_5 \cdot 66H_2O \text{ or } 6[Ca(UO_2)_4(PO_4)_2(OH)_4 \cdot 9H_2O]$$

which have a calculated specific gravity of 4.03. Analysis B (IVB) suggests the cell contents

$$4CaO \cdot 24UO_3 \cdot 8P_2O_5 \cdot 44H_2O \text{ or } 4[Ca(UO_2)_6(PO_4)_4(OH)_2 \cdot 10H_2O]$$

The calculated specific gravity is 3.94.

The analyses of dewindtite by Schoep (1925) are reasonably consistent. The most recent of these analyses is presented in Table 3 (I) and recalculated to 100% (II). The calculated unit cell contents (III) using Schoep's measured specific gravity, 5.03 suggest three alternative ideal cell contents

$$\text{IV: } 4[Pb_3(UO_2)_5(PO_4)_4(OH)_4 \cdot 10H_2O]$$
$$\text{V: } 4[Pb_3(UO_2)_6(PO_4)_4(OH)_6 \cdot 10H_2O]$$
$$\text{VI: } 6[Pb_2(UO_2)_4(PO_4)_3(OH)_3 \cdot 7H_2O]$$

TABLE 3. DEWINDTITE, ANALYSIS AND UNIT CELL CONTENTS

	I	II	III	IV	V	VI
PbO	24.85	25.43	13.3	12	12	12
UO_3	54.80	56.08	22.9	20	24	24
P_2O_5	10.14	10.38	8.5	8	8	9
H_2O	7.93	8.11	52.6	48	52	51
	97.72	100.00	calc. S.G. = 4.54		5.01	5.06

I. Chemical analysis by Schoep (1925). II. Analysis recalc. to 100%. III. Unit cell contents calculated for analysis. IV. $4[Pb_3(UO_2)_5(PO_4)_4(OH)_4 \cdot 10H_2O]$, calc. S.G. = 4.54. V. $4[Pb_3(UO_2)_6(PO_4)_4(OH)_6 \cdot 10H_2O]$, calc. S.G. = 5.01. VI. $6[Pb_2(UO_2)_4(PO_4)_3(OH)_3 \cdot 7H_2O]$, calc. S.G. = 5.06.

The first formula is identical with the generally accepted formula. The calculated specific gravity 4.54, is so much lower than the measured value that this formula may be ruled out of consideration. The calculated specific gravities for the remaining two formulas (5.01 and 5.06 respectively) agree closely with the measured gravity. The cell contents are equally compatible with the calculated cell contents for Schoep's analysis. The calculations therefore, do not lead to a unique choice for the cell contents for either phosphuranylite or dewindtite.

Neither dewindtite formula is strictly analogous to either of the possible phosphuranylite formulas although there is some similarity. The main difficulty is with the lead and calcium content. The lead in dewindtite is much higher relative to other constituents than is the calcium of phosphuranylite. At this time it is not possible to say whether the discrepancy in the formulas of the two minerals is real or is due to the difficulty of obtaining accurate chemical data.

ACKNOWLEDGMENT

A grant in aid of research from the Research Council of Ontario (to E. W. N.) is gratefully acknowledged.

REFERENCES

BRANCHE, G., CHERVET, J. & GUILLEMIN, C. (1951): Nouvelles espèces uranifères françaises, *Soc. franç. minéral., Bull.*, **74**, 457.

DANA, J. D. & E. S. (1951): *System of Mineralogy*, **2**, ed. 7, by C. Palache, H. Berman & C. Frondel, New York.

FRONDEL, C. (1950): Studies of uranium minerals (V): Phosphuranylite, *Am. Mineral.*, **35**, 756.

SCHOEP, A. (1925): Nouvelles recherches sur la dewindtite. *Soc. franç. minéral., Bull.*, **48**, 77.

STUDIES OF URANIUM MINERALS (XIV): RENARDITE*†

CLIFFORD FRONDEL AND FRANK CUTTITTA, *Harvard University, Cambridge, Mass. and U. S. Geological Survey, Washington 25, D. C.*

ABSTRACT

A new chemical analysis of renardite from Katanga has confirmed the formula $Pb(UO_2)_4(PO_4)_2(OH)_4 \cdot 7H_2O$. *X*-ray single-crystal study established the unit cell as orthorhombic, with the dimensions *a* 16.01 Å, *b* 17.5, *c* 13.7. Renardite is isostructural with both dewindtite (*a* 16.07 Å, *b* 17.50, *c* 13.62) and phosphuranylite. The chemical composition of dwindtite, however, cannot be reconciled with that of renardite on this basis. Phosphuranylite probably is the calcium analogue of renardite, with the formula $Ca(UO_2)_4(PO_4)_2(OH)_4 \cdot 7H_2O$.

RENARDITE

Renardite was originally described from Katanga, Belgian Congo, by Schoep (1928, 1930) and it has since been identified at several localities in France by Branche *et al.* (1951). A new analysis of Katanga material cited in line 2 of Table 1, confirms the composition

$$Pb(UO_2)_4(PO_4)_2(OH)_4 \cdot 7H_2O$$

earlier derived by Schoep and by Branche *et al.*

Several minute crystals were examined by *x*-ray rotation and Weissenberg methods in copper radiation. The orthorhombic unit cell dimensions obtained are cited in Table 2. The specific gravity, given as slightly more than 4 by Schoep and as 4.35 by Branche *et al.*, indicates that the unit cell contents are $6[Pb(UO_2)_4(PO_4)_2(OH)_4 \cdot 7H_2O]$. The calculated specific gravity then is 4.34. Crystals of renardite are tablets or laths flattened on {100} with {010} and {001} or {010} and {101} as the only other forms. The orientation and partial morphological unit of Schoep corresponds to the *x*-ray unit. The average measured ρ value of {101} is 39° 47′ ±2° (Schoep), 40° 07′ ±1° (present study), and the ρ value calculated from the *x*-ray cell is $\sim 40\frac{1}{2}°$. The *x*-ray powder spacing data are given in Table 3.

Optically the material described here has slightly higher indices of refraction than that described in earlier reports (Table 4). Some of our crystals had lower indices (as low as $nX = 1.704$) and a few crystals varied in index along the elongation or showed concentric zones with the outer parts having the highest indices. The differences perhaps are due

---

* Contribution from the Department of Mineralogy and Petrography, Harvard University, No. 347.

† Publication authorized by the Director, U. S. Geological Survey.

TABLE 1. CHEMICAL ANALYSES OF RENARDITE

	BaO	PbO	UO_3	P_2O_5	H_2O+	H_2O-	Rem.	Total
1.		13.16	68.92	8.37	9.55			100.00
2.	0.91	12.95	69.08	9.17	3.11	4.78		100.00
3.		12.26	64.82	8.15	3.77	4.97	6.53	100.50
4.		12.3	67.6	8.0	8.7		3.2	99.8

1. Theoretical weight percentages of $Pb(UO_2)_4(PO_4)_2(OH)_4 \cdot 7H_2O$.

2. Renardite from Katanga, Belgian Congo. Microanalysis by F. Cuttitta. Recalculated to 100 after deducting Al_2O_3 0.31, Fe_2O_3 0.62, SiO_2 1.54 from original sum of 100.21. Spectrographic analysis also showed the presence of Ca, Mg, Cu, Mn, Ni, Y, and V.

3. Renardite from Katanga, Belgian Congo (Schoep, 1928). Rem. includes $(Fe, Al)_2O_3$ 3.68, MoO_3 0.74, and quartz 2.11.

4. Renardite from Grury, France (Branche, *et al.*, 1951). Rem. is CaO 0.9, Al_2O_3 0.7, Fe_2O_3 0.9, SiO_2 0.7.

TABLE 2. UNIT CELL DIMENSIONS OF RENARDITE, DEWINDTITE, AND PHOSPHURANYLITE

	(Present Study)		(Hogarth & Nuffield, 1953)	
	Renardite	Dewindtite	Dewindtite	Phosphuranylite
a_0	16.01 Å	16.07 Å	16.00 Å	15.85 Å
b_0	17.5	17.50	17.62	17.42
c_0	13.7	13.62	13.66	13.76
Space group				Bmmb

TABLE 3. *X*-RAY POWDER SPACING DATA FOR RENARDITE

(*Copper radiation, nickel filter, d in* Å)

d	*I*	*d*	*I*	*d*	*I*
10.25	5	3.40	4	2.00	1
8.86	1	3.11	9	1.896	3
7.95	10	2.88	8	1.851	1
6.38	1	2.72	1	1.780	1
5.86	6	2.59	1	1.718	2
5.53	1	2.44	1	1.669	1
4.97	1	2.22	2	1.594	1
4.75	1	2.16	2	1.540	2
4.43	6	2.09	2	1.512	1
3.96	7	2.05	2	1.438	1

TABLE 4. OPTICAL PROPERTIES OF RENARDITE

	Orientation		n	Pleochroism
Renardite from Katanga (Schoep, 1928)	X	a	1.715	colorless
	Y	c	1.736	yellow
	Z	b	1.739	yellow
	$r>v$			
Renardite from Katanga (present study)	X	a	1.721	colorless
	Y	c	1.741	yellow
	Z	b	1.745	yellow
	$r>v$			
	$2V\sim45°$			
Renardite from France (Branche *et al.*, 1951)	X	a	1.716	colorless
	Y	c	1.736	yellow
	Z	b	1.740	yellow

to a varying substitution of Ba or Ca for Pb. Phosphuranylite, presumably the Ca analogue of renardite, shows a similar variation in the indices of refraction due to the substitution of Pb for Ca.

RELATION OF RENARDITE TO DEWINDTITE AND PHOSPHURANYLITE

The x-ray powder pattern of renardite is virtually identical with those of dewindtite and phosphuranylite, as are the unit cell dimensions (Table 2), and these three minerals must be presumed to be isostructural. The isostructural relation of dewindtite and phosphuranylite was earlier indicated by Frondel (1950) and by Hogarth & Nuffield (1953). The unit cell dimensions reported by the latter authors for dewindtite were here confirmed (Table 2) on an unanalyzed specimen that answered the description of Schoep (1930).

Renardite, dewindtite, and phosphuranylite should have analogous chemical formulas if they are isostructural, but the formulas reported for these minerals cannot be reconciled on this basis. The principal difficulty is with dewindtite. Dewindtite and renardite are both hydrated lead uranyl phosphates, and as their x-ray powder and single-crystal photographs are the same, they may be presumed to be identical. The four chemical analyses reported of dewindtite, however, are reasonably consistent and are near to the formulas $Pb_2(UO_2)_5(PO_4)_4(OH)_4 \cdot 10H_2O$ (Schoep) or $Pb_3(UO_2)_6(PO_4)_4(OH)_6 \cdot 9H_2O$ (Hogarth & Nuffield)—quite different from the formula of renardite, $Pb(UO_2)_4(PO_4)_2(OH)_4 \cdot 7H_2O$. Further, the specific gravity of dewindtite is 5.03 as compared to 4.35 for renardite; and the indices of refraction of the two minerals are different. Possibly the x-ray and other measurements reported for dewindtite were not all made on the same mineral.

Our knowledge of phosphuranylite is scant and contributes little to the general problem. The three partial analyses reported of this mineral show that it is a hydrated calcium uranyl phosphate, but the ratios of the analyses are widely divergent. One of the analyses (No. 2 in Table 4 of Frondel, 1950), however, has virtually the same ratios as renardite, with $CaO:UO_3:P_2O_5=1:4.1:1.2$. The formula of phosphuranylite probably is $Ca(UO_2)_4(PO_4)_2(OH)_4\cdot 7H_2O$ analogous to renardite, rather than $Ca_3(UO_2)_6(PO_4)_4(OH)_6\cdot 9H_2O$ analogous to dewindtite. New analyses of type dewindtite and of phosphuranylite are desirable.

Study of authentic specimens of dumontite, $Pb_2(UO_2)_3(PO_4)_2(OH)_4\cdot 3H_2O$, and of parsonsite, $Pb_2(UO_2)(PO_4)_2\cdot 2H_2O$, has shown that these minerals are not related to the minerals at hand.

This work was supported in part by the U. S. Geological Survey on behalf of the Division of Raw Materials of the Atomic Energy Commission.

REFERENCES

BRANCHE, G., CHERVET, J., & GUILLEMIN, C. (1951): Nouvelles espèces uranifères françaises, *Soc. franç. minéral. Bull.*, **74**, 457–488.

FRONDEL, C. (1950): Studies of uranium minerals (V): phosphuranylite, *Am. Mineral.*, **35**, 756–763.

HOGARTH, D. D., & NUFFIELD, E. W. (1953): Studies of radioactive compounds: VII-phosphuranylite and dewindtite, *Geol. Soc. America, Bull.*, **64**, 1434 (abs.). *Am. Mineral.*, **39**, 444–447, 1954.

SCHOEP, A. (1928): La renardite, nouveau minéral uranifère, *Soc. franç. minéral., Bull.*, **51**, 247–252.

——— (1930): Les minéraux du gîte uranifère du Katanga, *Ann. Musée du Congo Belge*, ser. 1 minéralogie, Tome 1, fasc. 2, 31–34.

AN ASSOCIATION OF TRACE ELEMENTS AND MINERALIZATION AT SUDBURY*

H. B. Stonehouse, *Illinois State Geological Survey, Urbana.*

Abstract

The Ti, Mn, Ni, V, Co and Ga concentrations in 330 samples of norite taken adjacent to mineralized areas in the Sudbury basin, have been determined spectrographically. A pattern in the behaviour of the concentration as the distance from the mineralized areas increased is revealed, and is characteristic for each element.

The area known as the Sudbury basin is formed by an elliptical ring the outcrop of a norite-micropegmatite instrusive said to be of Keweenawan age. It is approximately 37 miles long from northeast to southwest and 17 miles wide from northwest to southeast. The width of this outcrop varies from a maximum in the south range of slightly less than 4 miles to a minimum in the north range of slightly less than 1 mile. The dip of the intrusive is inward for the most part; on the southern boundary however, it is vertical or steeply dipping outward in some places. An assumed average inward dip of 38° gives a calculated thickness of $1\frac{1}{4}$ miles for the intrusive.

The lower, or outside portion of the intrusive is commonly known as norite, but has also been referred to as quartz gabbro, diorite or quartz diorite. The composition varies somewhat, but the difficulty of naming the rock is due to the rarity of completely fresh specimens.

Walker (1897) suggested that the present relative position of the norite and the micropegmatite is due to "gravitative differentiation" of homogenous magma, intruded as a flat sill and folded after solidification to its present shape. Phemister (1925) thought that the two portions of the intrusive may have been emplaced at different times, the magma for each intrusion perhaps coming from the same underground reservoir after differentiation, and the second intrusion occurring before the complete solidification of the first had taken place. Knight (1917) was of the opinion that the intrusive is in the form of a ring-like mass injected around a down faulted block, now preserved within the igneous outcrop, and Yates (1948) says "that a large syncline, existing previously, controlled the position and shape of the norite. The apparent differentiation is more likely a form of 'deuteric alteration,' the initial crystallization taking place at the outer margins with the gases and more residual acid solutions collecting near the upper part, with just enough leakage of the convex roof to allow continued movement of residual altering solutions upward. The intense granitization of the agglomerate and tuffaceous cover is good evidence of such escape."

---

* An extract from a thesis for a Ph.D. degree at the University of Toronto.

Chemical analyses and specific gravity determinations summarized by Collins (1934) do not indicate any significant differentiation in the norite.

The nickeliferous orebodies of the Sudbury district are found at the lower edge of the norite, or in "offsets" in the older rocks below the norite. The mineralization in these bodies is in the form of pyrrhotite, chalcopyrite and pentlandite, with minor amounts of arsenides and rare sulphides. Gold and silver occur native and as tellurides, and metals of the platinum group are found. Selenium is recovered from the ore, though selenium minerals are rare. Galena, marcasite, sphalerite, violarite and some silver minerals occur in late stage veins (Yates, 1948).

The ore is always associated with quartz diorite, either replacing it or occurring in other rocks close to it, with the exception of the Levack orebody, where a granite breccia takes the place of quartz diorite. The quartz diorite is petrologically similar to the norite, but the exact relationships between the two rocks are not known. The sulphides are found massive and disseminated, when massive they may occur in stringers in shattered and brecciated country rock of any description.

The various theories of genesis of the ore deposits range from those of Coleman (1913) and others who favour separation of an immiscible sulphide melt and its segregation, to those of Knight (1917) and others, who postulate a hydrothermal replacement of the country rock by the ore minerals. Bateman (1917) suggests that the sulphides were injected in a molten condition into their present position after separation from the norite magma, and Yates (1948) classifies the deposits as epigenetic replacement bodies, in part high temperature hydrothermal, and in part deep seated contact metamorphic. There appears to be agreement on the fact that the mineralization is genetically related to the norite.

In order to determine the nature of any association of trace elements and mineralization, samples were taken in areas close to orebodies, and analysed spectrographically.

As norite is adjacent to all the orebodies sampled and was considered more homogenous with respect to its primary trace element content than sedimentary beds or lava flows, all samples were taken from the norite.

Sampling was commenced at some point beyond the limits of the economic orebody, and called for convenience the contact of mineralization. This contact is an arbitrary line and was fixed visually. In some cases, its position was influenced by the presence of a fault plane, the edge of a shear zone, the contact of two different rock types, or a combination of these conditions, but the main factor governing its position was the sulphide content of the rock on either side of the line, and the rate of decrease of this amount in a direction away from the orebody. The presence of too much sulphide in the sample affects its behaviour in the arc during spectrographic analysis, so that the results obtained from these samples cannot be directly compared with the results from those samples containing little or no sulphide. The contact of mineralization was fixed so that the results from all the samples taken could be compared directly, and though visible sulphide was present in some samples, this did not amount to more than 2 per cent and did not affect the behaviour of the sample in the arc. Variations in the position of the contact of mineralization with respect to such factors as distance from the orebodies, intensity and type of mineralization, and perhaps relation to different rock types and faults are unavoidable.

Samples were taken on traverse lines run roughly perpendicular to and away from the orebodies. 20 traverses were run and a total of 330 samples were taken. It was reasoned that any variations in the trace element content of the rock due to the mineralization, would be more more pronounced closer to it, and therefore frequency of sampling was greater at the start of each traverse. Sampling was commenced 1 inch from the contact of mineralization, and the interval between samples doubled for successive pairs. Where samples were taken close together, they necessarily had to be small, but an attempt was made to take them all of approximately the same size, that is, about 2 inches diameter. As far as possible they were taken where there were no obvious local differences in the rock, and any geological features such as shears, dikes, veinlets or local accumulations of sulphides were recorded. Sampling was at such a depth to ensure that the rock had been unaffected chemically by weathering.

The samples were washed to remove all adhering material, heated for 5 minutes to red heat and quenched in distilled water, as suggested by Ahrens (1950) to facilitate grinding. About 10 grams was then ground in an agate mortar to about minus 150 mesh. 0.1 gram of sample was then weighed accurately into a sample vial, and to this was added a similar amount of spectrographically pure carbon powder as buffer, and 0.01 gram of spectrographically pure tin oxide powder as internal standard.

The addition of an internal standard, and the closely related behaviour of standard element and unknown element during handling and and arcing, compensates for many factors likely to introduce errors. Differences in photographic material and processing will be minimized also. Unless several internal standards are used, one for each element or group of elements to be determined, it is impossible to satisfy all requirements for the best one. It is essential that the internal standard element should be absent or present in the material to be analysed in concentrations sufficiently small so as not to interfere with the spectrographic line intensity due to the added internal standard, or present in sufficiently large concentrations that any variation in concentration will again not affect the line intensity. Tin oxide was chosen as Clauson (1947) has shown that tin is absent from the norite at Sudbury, and the oxide was a convenient medium to introduce the tin.

The relative amounts of sample, buffer and internal standard were chosen after experimental arcing had indicated that they would give suitable line intensities.

This material was then shaken for 5 minutes with two stainless steel balls of $\frac{1}{4}$ inch diameter, a method employed by Smith & Hoagbin (1946) to mix samples. After mixing, the material was introduced into a $\frac{1}{4}$ inch external diameter, center post, undercut carbon electrode, with a capacity of about 40 milligrams of sample. The powder was then moistened with a saturated solution of sugar in alcohol to "cake" it, and dried for 10 minutes. The sample was then arced under the following conditions:

Sample electrode—anode
D.C. arc
Voltage—250 volts
Current—13 amps.
Time—90 seconds
Arc gap—5 mm.

The spectrograph used was, an A.R.L. 2 meter grating type, with 24,400 lines per inch on the grating and a resolution of 5.2 A per mm. in the first order. Light from the arc was filtered to 12% to give a suitable exposure, and passed through a slit set at 40 microns, to give a suitable line width for densitometric determinations, all of which were made on an A.R.L. densitometer.

Eastman Kodak Spectrum Analysis Film No. 2 was used for recording the spectrum. It was developed in D-19 developer at 70° F. for $2\frac{1}{2}$ minutes. washed for 30 seconds and fixed for 2 minutes in acid fixer, washed and dried.

During handling of the sample care was taken to ensure that mechanical losses and decontamination were reduced to a minimum, and that all samples were treated identically. The similarity in the intensity of the internal standard line in practically all the samples is an indication of the similarity of arcing conditions and photographic processing which existed. When internal standard line intensity varied only slightly, and when the intensity ratios of the trace elements, particularly gallium, varied in the opposite sense, or when internal standard line intensities varied appreciably, a repeat analysis was made.

A reproducibility test was run on one of the samples, and gave standard deviations for 16 determinations as follows:

Ga	± 4.4%
Mn	±13.4%
V	±16.1%
Ti	±16.9%
Co	±25.7%

These values are designated very good for gallium, fair for manganese, vanadium and titanium, and poor for cobalt, by Ahrens (1950).

Intensity relationships are used in the method of spectrographic analysis involving internal standardization. In this method, a constant proportion of an element, the internal standard is added to each sample, and the intensity ratio of a line of the element to be determined, and the internal standard line chosen, is observed. Since the internal standard is present in non-variant concentration in the samples, and line intensities are proportional to concentration, other factors being equal, this ratio is proportional to the concentration of the element to be determined. To enable this relationship to be transformed into direct rather than relative concentrations, standards are used containing different but known amounts of the trace elements to be analysed for, in a matrix.

Claffy (1947) states that "it has been found . . . that the state of chemical combination of an element as well as the nature of the matrix have great influence on the intensity of spectral lines." In order to obtain reliable trace element concentrations, an attempt was made to simulate the matrix of the rock samples as closely as possible, both physically and chemically, in standards.

To obtain a suitable matrix composition, Collins' (1934) average analysis of norite from the Sudbury area was recalculated with the exclusion of TiO_2, P_2O_5, H_2O, MnO, CO_2, and S. Spectrographically pure chemicals were mixed in proportion to the recalculated analysis, and this material was used as a matrix. Calculated amounts of spectrographically pure trace element compounds were added to a portion of the matrix, such that a 1% concentration of each element resulted in the mixture. Controlled dilution of this 1% mixture by matrix material gave mixtures which were used as a set of standards.

Since all the spectrographically pure chemicals used were in the form of oxides or carbonates, and hence not physically similar to the material in the rock samples, which is mostly in the form of silicates, a fusion of the standards was made and a homogenous glass obtained. Investigation of this material showed that both major and minor elements had been lost during the fusion, and this material was discarded.

Ahrens (1950) and Mitchell (1948) recommend sintering of the standards, and this was done at 1000° C. for 24 hours. It was found that the standards then burnt smoothly in the arc, and the spectrogram obtained resembled closely that of the average rock sample. Both powdered carbon buffer and tin oxide internal standard were added to the standards prior to arcing in the same proportions as to the samples.

Trace elements are considered to be those elements not common in the upper lithosphere, that is, all elements other than oxygen, silicon, aluminium, iron, calcium, sodium, potassium and magnesium (Rankama & Sahama, 1949). Clarke & Washington (1924) state that the "minor constituents are generally found in very small amounts, rarely more than 2 per cent for any one, or as much as 5 per cent for all of them in any one rock." They have been divided into two groups with respect to their presence in igneous rocks; those elements which form independent minerals, generally the accessory minerals, and those elements which rarely form specific minerals, but which occur in solution in other minerals of the rock (Rankama & Sahama, 1949). Some elements belong to both groups.

Goldschmidt (1937) advanced a hypothesis governing the distribution of those trace elements of the second group occurring in solution in other minerals of the rock. The partition of these elements between the silicate, sulphide and oxide phases depends on the affinity of each element for the particular phase, the relative abundance of suitable phases present, and the conditions prevailing at the time of partition. The affinity of an element for a particular phase is related to its atomic structure, its ionic structure, and its ionization potential (Goldschmidt, 1937). The presence of an element in a mineral depends, of course, on the presence of that element in the solution or melt from which the mineral crystallized, and the concentration in the mineral depends on the concentration in that solution or melt, its affinity for the particular phase, the conditions prevailing at the time of crystallization, and the atomic or ionic size of the element.

Among other factors, the state of oxidation is important in determining the amount of an element present in a mineral. Under reducing conditions, chromium will be obliged to enter the sulphide daubréelite rather than form an oxide (Goldschmidt, 1937) and possibly under oxidizing conditions, the amount of iron available for entry into pyroxene may be limited.

Atoms or ions fit into positions in a crystal structure unique for any particular mineral, that is formed during crystallization of that mineral.

The unit of this structure is comparatively rigid, and only small changes in dimensions are possible, so that atoms or ions included will be chosen, among other reasons, according to their size. This is represented by the radius of the atoms or ions, which, since atoms or ions are not solid particles, is a variable quantity depending on the coordination, nature of the bonding to adjacent atoms or ions, and the ionic charge.

The rigidity of the crystal structure is such that when diadochy takes place, as the substitution of different elements in identical positions in a crystal structure without disruption of that structure is known, the radii of the two atoms or ions involved must not vary by more than 10 to 15 per cent of the larger of the two (Goldschmidt, 1945). Rankama & Sahama (1949) raise this tolerance to about 15 per cent, but indicate that there are exceptions to this rule. Variations of temperature and pressure affect the tolerances, which are increased for increasing temperature and vice versa. The effect due to pressure is probably in the opposite sense.

Coordination and crystal structure influence diadochy in some cases. An element may substitute for another element frequently and completely in one type of structure, while doing so rarely and in limited amount in another. An example of this is given by the substitution of large amounts of aluminium for magnesium in the spinels, but the restricted substitution of aluminium and sodium for magnesium which takes place in the pyroxenes. Another example is the extensive substitution of barium for potassium in feldspars, and the limited or lack of substitution of barium for potassium in mica. There are many more examples.

When substitution takes place, the electrostatic charges in the structure must be satisfied.

The relative bond strength of two atoms or ions in identical positions in a structure is the final criterion which decides whether substitution will or will not take place at any particular time, and thus is important in fixing the sequence of incorporation of a number of elements into a structure. The atom or ion providing stronger bonds will be substituted for that providing weaker bonds preferentially (Goldschmidt, 1937).

Within allowable tolerances under prevailing conditions, for atoms or ions of similar valency charge, the larger will weaken the bond, and for atoms or ions of similar size, the larger valency charge will strengthen the bond, except where strong directed bonds may distort a structure. When a trace element replaces a major element of similar valency "camouflage" takes place, when the major element has the lower valency "capturing" occurs, and when the major element has the higher valency the replacement is known as "admission" (Goldschmidt, 1937). During crystallization from a magma, captured trace elements will be concentrated in early crystallized minerals, or early phases of a mineral, and where these separate, in the early more basic rock fraction. Admitted trace elements will be concentrated in later crystallizing minerals and later phases of a mineral, and consequently in the more acid rock fractions. With regard to atomic or ionic size, within limits of diadochy, the smaller atom or ion will be concentrated early, and the larger one later.

This can be illustrated by the following figures, which show that scandium* (Sc^{3+} 0.83 kX), captured by magnesium (Mg^{2+} 0.78 kX) is concentrated in basic rocks, while lithium (Li^{+} 0.78 kX) is admitted by magnesium and concentrated in acid rocks.

	Sc ppm.	*Li ppm.*
Pyroxenite	46[1]	
Dunite, eclogite		2.3[2]
Granite	1.3[1]	179.4[2]

[1] Goldschmidt (1934, 1937*b*).
[2] Strock (1936).

This concentration of the ion with the highest valency in basic rocks is also indicated by the enrichment of calcium (Ca^{2+} 1.06 kX) over sodium (Na^{+} 0.98 kX) in basic igneous rocks.

	% Ca	*% Na*
Gabbro	7.85	1.85
Granite	1.42	2.58

Data taken from Daly (1933).

With regard to the similarity of charge, the smaller ion (Ni^{2+} 0.78 kX) is concentrated in basic rocks rather than the larger one (Zn^{2+} 0.83 kX).

	Ni ppm.	*Zn ppm.*
Peridotite, dunite	3160[1]	
Gabbro		90[2]
Granodiorite		200[2]
Granite	2.4[1]	

[1] Goldschmidt (1937).
[2] Lundegårdh (1948).

The changes in the iron (Fe^{2+} 0.83 kX) to magnesium ratio in igneous rocks, based on figures from Daly (1933) also show this trend.

	Fe:Mg
Dunite	0.2
Granite	4.9

---

* All atomic and ionic radii are taken from Rankama & Sahama (1949).

Predictions can be made on this basis as to the trends of concentrations of trace elements in differentiated igneous rock complexes, and in the minerals in those rocks. Nockolds & Mitchell (1948) studied four complexes, and Wager & Mitchell (1951) studied the highly differentiated Skaergaard intrusion. The results obtained showed the form of these trends, and confirmed the hypothesis advanced by Goldschmidt (1937) and mentioned above.

Apart from the trace elements studied quantitatively here, titanium, manganese, nickel, vanadium, cobalt and gallium, relative concentrations of chromium, silver, copper and zinc were determined. Of these, titanium and possibly nickel, copper and lead in part occur as specific minerals in the rocks, the first as ilmenite and the remainder as sulphides. The remaining elements and possibly some nickel, copper, silver, zinc and lead, do not form common rock forming minerals and are considered therefore to occur by substitution in the silicates, oxides or sulphides of the rock. The occurrence and behaviour of some of these trace elements in igneous rocks in general, and in the Sudbury norite in particular, is discussed below.

Titanium Ti^{4+} (0.64 kX)

Titanium is not classed with the trace elements by Nockolds & Mitchell (1948) or by Wager & Mitchell (1951), perhaps because it is usually determined by chemical methods in rock analysis, but by definition, it must be considered as a trace element. It is the only element here discussed which occurs mainly in the first group of the division made by Rankama & Sahama (1949), those elements which form independent minerals, generally the accessory minerals, but titanium is found in pyroxene, hornblende and biotite, besides ilmenite, titanomagnetite, sphene and rutile in igneous rocks.

The average titanium concentration of the Sudbury norite is 2500 ppm. This is considerably lower than values for other gabbros and norites, which range from 4200 ppm. (v. Tongeren, 1938) to 6800 ppm. (Daly, 1933). The curve drawn of the average trace element concentra-

Description of Diagrams

The accompanying curves show the average Trace Element Concentration, in parts per million, plotted against the distance from the Contact of Mineralization, in feet, on a logarithmic scale. Data for individual samples is plotted as short horizontal lines, with the exception of high and low values, which are indicated in the boxes above the curves and which are not used in computing the averages. The length of the horizontal lines is proportional to the number of samples with the same concentration values in any one sample position, for any one element.

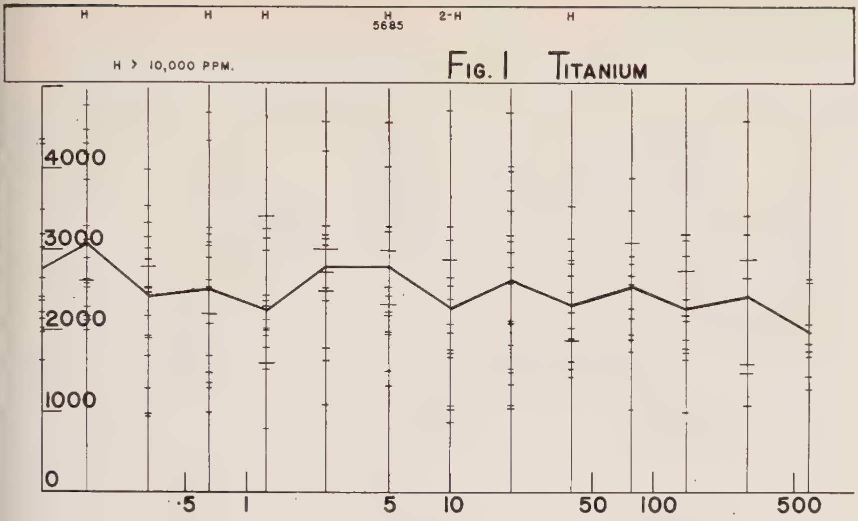

Fig. 1 Titanium

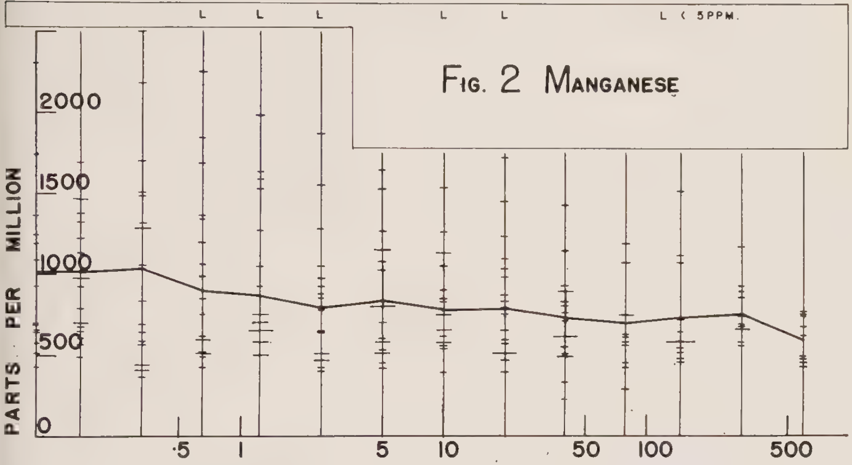

Fig. 2 Manganese

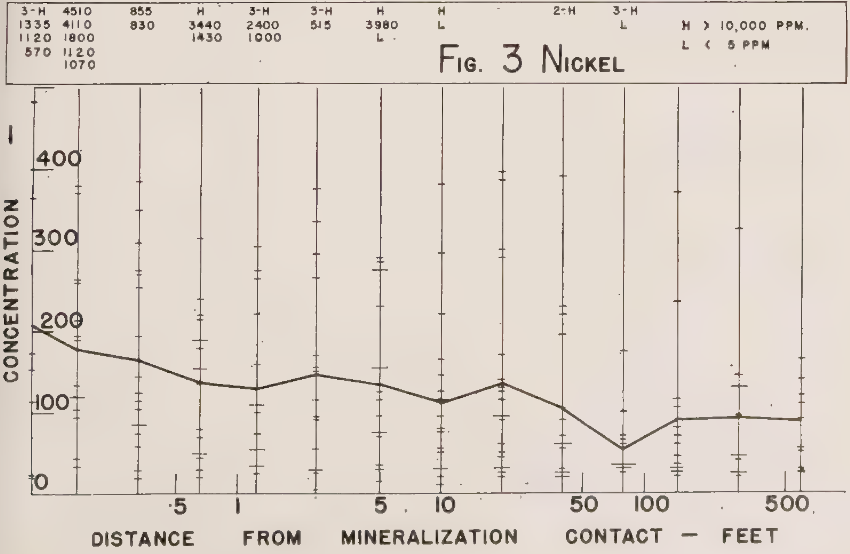

Fig. 3 Nickel

Fig. 4 Vanadium

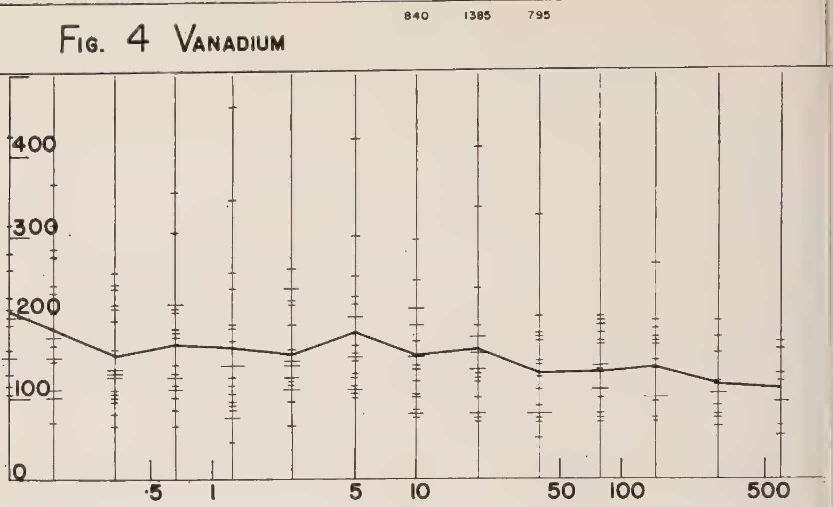

Fig. 5 Cobalt

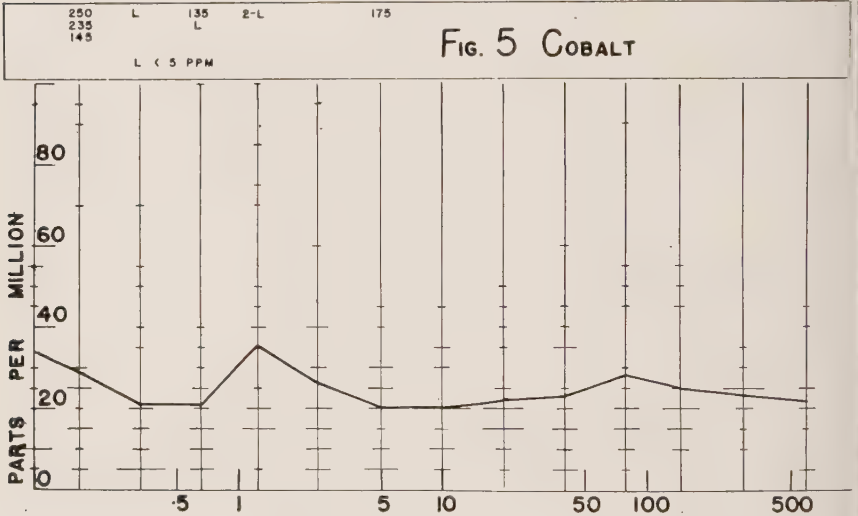

Fig. 6 Gallium

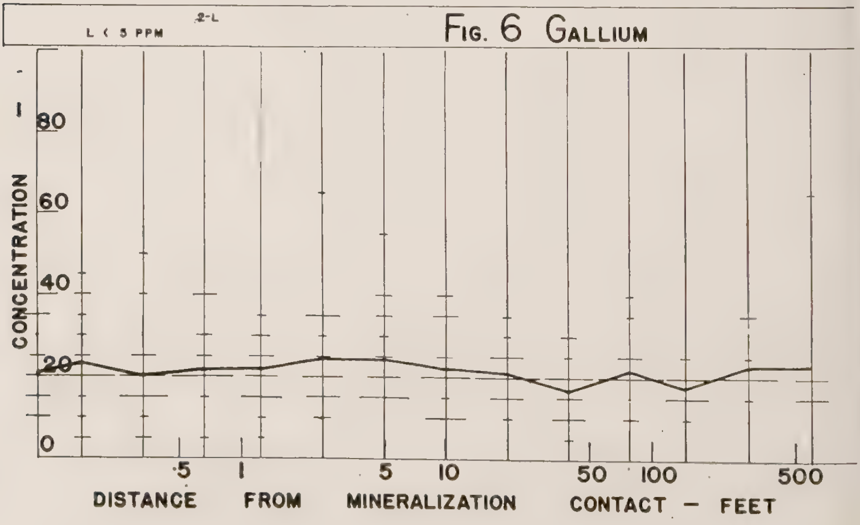

tion for each sample position against distance from the contact of mineralization (Figure 1), shows that the titanium concentration decreases as the distance from the contact of mineralization increases. When a similar curve is drawn for samples from each individual traverse, though the titanium concentration decreases overall as the distance from the contact of mineralization increases, there is usually a pronounced peak 10 to 20 feet from the start of the curve, which often coincides with a peak drawn in the curve drawn for vanadium. This peak is present in sample position 9 in the average curve, and would be more obvious if 2 high values were suppressed in each of sample positions 6 and 7, these 4 values being among the 7 highest recorded for titanium.

Manganese Mn^{2+} (0.91 kX)

Specific manganese minerals do occur in igneous rocks, but they are of minor importance. Manganese commonly occurs in silicates and oxides; sulphides are relatively free of manganese.

Manganese occurs mainly as the diavalent ion (Rankama & Sahama, 1949), and can substitute for iron (Fe^{2+} 0.83 kX), calcium (Ca^{2+} 1.06 kX), magnesium (Mg^{2+} 0.78 kX) and sodium (Na^{+} 0.98 kX), the first being the most common substitution. Data from Daly (1933) and Otto (1936) indicate that manganese is concentrated in early differentiates, but that the manganese to iron ratio remains fairly constant throughout differentiation. However, Nockolds & Mitchell (1948) and Wager & Mitchell (1951) show that while the manganese to iron ratio remains fairly constant, manganese tends to concentrate in late differentiates. Work by Landergren (1948) shows that the manganese to iron ratio increases in acid rocks.

Manganese can occur in all of the primary minerals present in the Sudbury norite. Data concerning its distribution between these minerals is poor, but it occurs in plagioclase and biotite from a diorite according to Nockolds & Mitchell (1948) as follows:

	ppm.
Plagioclase	80
Biotite	100

and in

Plagioclase	50
Pyroxene	2700

in an olivine free gabbro (Wager & Mitchell, 1951)

The manganese content of the Sudbury norite, 825 ppm., is also below that of other norites and gabbros which range from 1000 ppm. (Otto, 1936) to 3100 ppm. (v. Tongeren, 1938). In Figure 2 is illustrated the curve drawn for the manganese concentration versus the distance from the mineralization contact. The concentration shows a steady decrease in value as the distance increases, and this is similar to the majority trend as observed for the individual traverses.

It has been shown that manganese concentrates in late differentiates, and if differentiation had taken place in the norite, it would be expected that the manganese concentration would rise as the distance from the bottom of the norite, that is, the contact of mineralization in every case, increased.

Nickel Ni^{2+} (0.78 kX)

Nickel occurs primarily in four ways in igneous rocks, in silicates, sulphides, oxides and rarely in iron-nickel alloys. The most important method of occurrence is in silicates, where nickel is camouflaged by magnesium (Mg^{2+} 0.78 kX) and is concentrated in early formed olivine, orthopyroxene and clinopyroxene, and to a less extent in amphibole (Vogt, 1923). In sulphides, nickel is present in pentlandite and pyrrhotite in larger amounts than in associated pyrite (Gavelin & Gabrielson, 1947); in pyrite and pyrrhotite, nickel presumably replaces iron, the atomic radii being identical (1.24 kX). In oxides, nickel is found in magnetite and ilmenite, perhaps as the nickel spinel trevorite, in solution

Nickel is distributed in the lithosphere in the following manner:

	ppm.
Silicate meteorites	3300[1]
Peridotite	3160[2]
Gabbro	158[2]
Diorite	40[2]
Granite	2.4[2]

[1] Goldschmidt (1937*a*).
[2] Goldschmidt (1937).

It is seen that nickel is concentrated in early basic rocks, and it occurs in these rocks substituting for magnesium. However, the nickel to magnesium ratio is also enhanced in these early crystallates, despite the identical ionic size and valency (Wager & Mitchell, 1951). Goldschmidt (1944) states that nickel has a tendency to homopolar bonding in compounds, which increases the bond strength and consequently is responsible for the preferential concentration with respect to magnesium in early crystallates.

Nickel is present in hypersthene, augite and biotite from a diorite, as shown by Nockolds & Mitchell (1948) in the following amounts:

	ppm.
Plagioclase	—
Hypersthene	300
Augite	200
Biotite	150

and in pyroxene, ilmenite and magnetite from an olivine free gabbro (Wager & Mitchell, 1951),

	ppm.
Plagioclase	—
Pyroxene	50
Magnetite	50
Ilmenite	100

Nickel may also occur in hornblende; these minerals are all present in the norite sampled.

The average of the three most frequently occurring values for the nickel concentration of the Sudbury norite is 25 ppm., and this figure gives a more representative measure of the nickel content of the rock away from the mineralized areas. The average of all the analyses is 240 ppm. Both of these values are within the range of the nickel content of other norites which is from 0.2 ppm. (Lundegårdh, 1947) to 350 ppm. (Vogt, 1923).

Figure 3 shows that the nickel content of the norite decreases as the distance from the contact of mineralization increases, and finally levels off at a value of about 80 ppm. This trend is similar to the trends displayed by the individual traverses which often show in addition, one or more high values not present in the average curve.

These high values, which are most prominent and numerous close to the mineralization contact, are probably due to the incorporation of nickeliferous pyrrhotite or pentlandite particles in the sample, as they are often associated with visible sulphide. Chemical analyses of the norite and the sulphide separated therefrom showed that while the nickel in both the rock, determined spectrographically, and the nickel in the sulphide, determined chemically, varied in the same sense, there was no relation between the nickel and sulphur contents of the rock, the latter also determined chemically. Visible pyrite and chalcopyrite in some samples indicates that the sulphur is not all associated with pyrrhotite or pentlandite.

A spectrographic analysis for nickel in the acid resistant portion of the heavy mineral fraction of six samples chosen from the beginning, middle and end of two traverses, showed that there was little variation in the nickel content of this portion of the norite from these traverses. This portion of the heavy mineral fraction of the rock was found to consist mainly of pyroxene and amphibole, and the results obtained showed that there had been no segregation of nickel rich, or early crystallizing pyroxene or amphibole in the area covered by these traverses.

Vanadium V^{4+} (0.61 kX)

Vanadium occurs extremely rarely in igneous rocks in a distinct mineral, ardennite, a member of the epidote group, and it must therefore be sought in the other minerals of the rocks. It probably exists as the quadrivalent ion, and in that state would be captured by aluminium (Al^{3+} 0.57 kX) or iron (Fe^{3+} 0.67 kX), and camouflaged by titanium (Ti^{4+} 0.64 kX). According to Wager & Mitchell (1951) vanadium exists as the trivalent ion (0.65 kX) and is camouflaged by ferric iron. Leutwein (1941) suggests that the ferric ion would be reduced to the ferrous ion, as trivalent vanadium is a strong reducing agent, and replacement could no then take place.

Nockolds & Mitchell (1948) show that vanadium is concentrated i the first crystallized biotite, in muscovite, ilmenite, and to a less exten in pyroxene and amphibole. Wager & Mitchell (1951) find that it i similar to chromium in its behaviour and shows a preference for magnetite, ilmenite and pyroxene in that order. Other authors are in accord with this, and the association of vanadium with magnetite, ilmenite and rutile to a less extent, is common.

When vanadium substitutes for titanium or ferric iron, it should be concentrated preferentially in the earliest crystallates. Predictions with regard to its behaviour when substituting for aluminium cannot be made, as relative bond strengths due to ionic size and valency are in opposition.

Vanadium can occur in all the primary minerals of a norite. Nockolds & Mitchell (1948) show that vanadium distribution is as follows in a diorite:

	ppm.
Plagioclase	20
Hypersthene	100
Augite	200
Biotite	400

and Wager & Mitchell (1951) give the following data for an olivine free gabbro:

	ppm.
Plagioclase	10
Pyroxene	100
Magnetite	800
Ilmenite	300

The vanadium concentration in the Sudbury norite is 165 ppm. This is between the lowest value of 50 ppm. (Sahama, 1945) and the highest of 350 ppm. (Lundegårdh, 1947) for other gabbros and norites.

The curve represented in Figure 4 shows that the vanadium concentration of the norite decreases as the distance from the mineralization contact increases, but an obvious feature is the peak present in sample position 9. This peak is obvious in the curves drawn for individual traverses, and frequently coincides with the titanium peak mentioned above. An inspection of the titanium to vanadium ratios for the individual traverses, shows that it is remarkably constant throughout any one traverse. This obvious association of titanium and vanadium is emphasized further by the similarity of the titanium to vanadium ratio of 2 rock samples and of the ilmenite separated from them, all determinations being spectrographic. This would indicate that probably the vanadium occurs mainly in ilmenite or perhaps associated with titanium in other minerals.

As mentioned above, when vanadium substitutes diadochally for titanium, it should be concentrated in the earliest crystallites of any mineral containing both elements. The lack of systematic variation in the titanium to vanadium ratio with respect to the position of the samples in the traverses, shows that these relatively vanadium rich early crystallites have not been separated and concentrated preferentially in any portion of the norite covered by the traverses. This evidence of lack of differentiation is confirmed by the similarity of the concentration of nickel in the pyroxene and amphibole along a traverse, and by a study of the distribution of manganese in the norite, as discussed above.

Cobalt Co^{2+} (0.82 kX)

The occurrence of cobalt in igneous rocks is similar to that of nickel, with the exception that no iron-cobalt alloys are known. It is camouflaged by iron (Fe^{2+} 0.83 kX) and is concentrated in early crystallizing fractions (Nockolds & Mitchell, 1948, Wager & Mitchell, 1951). Sandell & Goldich (1943) found that the trend between basic and acid igneous rocks shown by the cobalt to magnesium ratio is more apparent than that shown by the cobalt to iron ratio, and is linear over a wide range. This trend is, however, opposite to that expected by Goldschmidt's theory, which predicts that cobalt, being the larger ion, would be concentrated in the later differentiates with respect to magnesium. Nockolds & Mitchell (1948) show that the cobalt to magnesium ratio is highly variable, and no definite trend is apparent.

On account of its smaller size, the nickel ion would be expected to concentrate relative to cobalt in early differentiates, for despite the fact that these two elements replace different major elements, they occur in the same structural positions. This has been found to be the case by

Goldschmidt (1937), Lundegårdh (1947) and Wager & Mitchell (1951).

Cobalt is preferentially concentrated in pyrite rather than pyrrhotite in any one association of these two sulphides (Gavelin & Gabrielson, 1947), but comparisons between these sulphides from different occurrences cannot be made. In oxides, cobalt occurs in both magnetite and ilmenite (Wager & Mitchell, 1951) and in both oxides and sulphides, presumably replaces iron.

Cobalt is found in all the primary minerals which occur in the norite studied. It is present in the minerals of a diorite according to the following data (Nockolds & Mitchell, 1948):

	ppm.
Plagioclase	15
Hypersthene	100
Augite	70
Biotite	50

and in minerals from an olivine free gabbro as follows:

	ppm.
Plagioclase	—
Pyroxene	60
Magnetite	80
Ilmenite	100

(Wager & Mitchell, 1951). Cobalt also occurs in hornblende.

Cobalt is found in norites and gabbros in concentrations between 25 ppm. (Lundegårdh, 1947, Sahama, 1945) and 80 ppm. (v. Tongeren, 1938). The average concentration in the Sudbury norite is 30 ppm.

Figure 5 shows that the average cobalt concentration for the various sample positions plotted against the distance from the contact of mineralization, is quite uniform, but there are some erratic high values. These high values are a feature of the curves drawn for the cobalt concentration versus distance from the mineralization contact for the individual traverses, and often coincides with extremely high nickel values, though occasionally the latter occur without the former. These high values are thought to be due to the presence of cobalt bearing sulphide in the sample, perhaps nickeliferous pyrrhotite or pentlandite, though some of this material must be cobalt free, or perhaps pyrite associated with the pyrrhotite or pentlandite. Most of the pyrite in the rock, however, is cobalt free.

Gallium Ga^{3+} (0.62 kX)

Gallium does not form independent minerals in rocks, and the similarity in size between the gallium ion and the aluminium ion (0.57 kX) indicates that camouflage of gallium by aluminium will take place. This happens in both 4-fold and 6-fold coordination positions (Rankama & Sahama, 1949) as is shown by the occurrence of a synthetic gallium spinel (Barth & Posnjak, 1931) and a synthetic compound formed by replacing aluminium by gallium in the feldspar structure (Goldsmith, 1950). However the larger size of the gallium ion indicates that it should be relatively concentrated in later differentiates of an igneous magma. This has been shown to be the case by Wager & Mitchell (1951), Goldschmidt & Peters (1931) and others, but this trend is only indicated in hornblende and biotite in the Caledonian plutonic rocks studied by Nockolds & Mitchell (1948), and is not apparent in the rocks as a whole, which show a comparatively non-variant gallium to aluminium ratio between acid and basic rocks. Wickman (1943) explains that the constancy of this ratio is due to the fact that gallium may be camouflaged by chromium (Cr^{3+} 0.64 kX) and iron (Fe^{3+} 0.67 kX) and admitted by titanium (Ti^{4+} 0.64 kX), and will thus occur in chromite, magnetite and ilmenite, which he assumes are early crystallizing minerals in a differentiation sequence. Thus gallium may be concentrated without reference to aluminium in basic rocks, by association with these oxides, and it is concentrated in acid rocks relative to aluminium by direct substitution. A suitable combination of these circumstances results in a roughly invariant gallium to aluminium ratio throughout a differentiation sequence. That gallium occurs in magnetite and ilmenite has been shown by Wager & Mitchell (1951), but its presence in chromite has yet to be determined.

Among the primary minerals occurring in the norite at Sudbury, gallium is to be found in feldspars, pyroxene, amphibole, biotite, magnetite and ilmenite. Nockolds & Mitchell (1948) show that the distribution in a diorite is as follows:

	ppm.
Plagioclase	30
Hypersthene	1
Augite	8
Biotite	12

and in an olivine free gabbro, Wager & Mitchell (1951) show the following distribution:

	ppm.
Plagioclase	50
Pyroxene	—
Magnetite	30
Ilmenite	3

The average gallium concentration of the Sudbury norite is 20 ppm., which agrees with the other figures of 20 ppm. (Sahama, 1945) and 35 ppm. (v. Tongeren, 1938) for gabbros and norites.

The curve of the average gallium concentration values versus the distance from the contact of mineralization (Figure 6), shows that there is very little variation in the gallium content of the rock. Owing to the high reproducibility of the gallium analyses, small variations in the values would be significant. Thus the gallium concentration is seen to be low close to the mineralization, to rise to the sixth and seventh sample positions, to fall to a low between the tenth and twelfth sample positions and to rise again. This is the trend exhibited by the majority of the individual traverses, but as with them, does not appear to be related to the trends of any of the other trace elements.

Chromium Cr^{3+} (0.64 kX)

Chromium occurs in rocks as chromite, rarely as chrome spinels, and in silicates. The most important occurrence is in silicates, where chromium is camouflaged by aluminium (Al^{3+} 0.57 kX) and iron (Fe^{3+} 0.67 kX), and apparently captured by magnesium (Mg^{2+} 0.78 kX) and iron (Fe^{2+} 0.83 kX).

Chromium appears to be highly concentrated in early differentiated silicates (Wager & Mitchell, 1951; Nockolds & Mitchell, 1948 and Goldschmidt, 1937). That it shows a distinct preference for pyroxene rather than olivine is indicated by Wager & Mitchell (1951), but the high concentration reported by Goldschmidt (1937) in dunite and that by Sahama (1945) in "ultrabasics" appears contradictory. Perhaps the abundance in pyroxene may be explained by the presence of chrome diopside.

Chromium may be present in all the ferromagnesium minerals in norite, but it is not found in plagioclase. In a diorite (Nockolds & Mitchell, 1948) it occurs as follows:

	ppm.
Plagioclase	—
Hypersthene	200
Augite	1500
Biotite	800

and in an olivine free gabbro (Wager & Mitchell, 1951) as follows:

	ppm.
Plagioclase	—
Pyroxene	—
Magnetite	800
Ilmenite	300

Chromium intensity ratios, proportional to the chromium concentration, vary similarly to the manganese concentration in the Sudbury norite, that is, for the most part, the chromium concentration decreases as the distance from the mineralization contact increases.

Copper Cu^{2+} (0.83 kX)

Copper has a strong affinity for sulphur and occurs in igneous rocks mainly as the sulphide chalcopyrite, but probably replaces iron in minerals containing that element, and sodium (Na^{+} 0.98 kX) in plagioclase feldspars. It occurs in apatite but is not found in the potash feldspars (Nockolds & Mitchell, 1948).

According to Sandell & Goldich (1943) copper is concentrated in early crystallates. Wager & Mitchell (1951) show that copper concentrates towards the end of differentiation, but add that the possible reason for this late concentration in the case they studied is that insufficient sulphur was present to remove all the copper in the early precipitated sulphides, though the sulphur content of the rock under discussion (500 ppm.) is close to the average given by Goldschmidt (1937*a*) and Clarke & Washington (1924).

Vogt (1923) shows that the copper content of ores associated with norite is higher than that of those associated with more basic rocks. This would indicate that the copper content of a magma increases as differentation proceeds.

Copper generally appears to be absent from hornblende (Nockolds & Mitchell, 1948), but is present in all the other primary minerals which may occur in norite.

	ppm.
Plagioclase	—
Hypersthene	150
Augite	100
Biotite	300

are the amounts present in minerals from a diorite (Nockolds & Mitchell, 1948) and

	ppm.
Plagioclase	15
Pyroxene	50
Magnetite	30
Ilmenite	50

is present in the minerals from an olivine free gabbro (Wager & Mitchell, 1951).

There is apparently no trend in the copper concentration of the Sudbury norite, and the values obtained show that the copper distribution is spotty and erratic.

Lead, Zinc and Silver

Lead is present in only nine samples and zinc occurs in four of these. Silver generally occurs in the samples containing lead, but it is present in other samples. The samples containing lead have a high copper content and often a high nickel content, suggesting that the lead may be present as the sulphide. These elements are too sparsely distributed to be of any but general interest, and the values are too erratic.

Summary

There appears to be then, associated with the mineralization which produced the orebodies, a relative concentration of titanium, vanadium, manganese, nickel and chromium adjacent to the mineralized zone, which decreases as the distance from the zone increases. There is a slight peak concentration in the case of titanium and vanadium away from the mineralized zone, but overall along the traverse, the concentration of these two elements decreases. Gallium is depleted close to the mineralized zone and concentrated further away. The cobalt content of the rock appears to be unaffected with relation to the mineralized zone. Copper concentration is erratic and is probably primarily due to chalcopyrite disseminated throughout the rock. Silver, lead and zinc are not present in a sufficient number of samples for conclusions to be drawn regarding their association with mineralization.

The variation of these trace elements is certainly associated spatially with the mineralized zones, and thus the orebodies. It seems probable that the variations in the trace element concentrations are caused by agencies connected with the emplacement of the sulphide mineralization, but this has not been proven, and perhaps the distribution of these trace elements in the present manner took place after mineralization. It is likely that the concentration of the trace elements is additive, and not due to their rearrangement in the rock, but this is only surmise.

Despite the fact that the samples were taken from widely varying locations around the Sudbury basin, and that all of the orebodies with which they were associated may not have been formed by the same processes (Davidson, 1948, Yates, 1948), there is no distinction between the results from one traverse and any other. There are also no great differences in the trace element content of samples from different locations.

The distribution of the manganese and nickel and the constancy of the titanium to vanadium ratio shows that there has been no significant differentiation of those portions of the norite covered by this sampling.

In connection with this research, I wish to thank the following for assistance: International Nickel Co. of Canada Ltd. and Falconbridge

Nickel Mines Ltd., The National Research Council of Canada, D. A. Moddle and W. O. Taylor of the Ontario Department of Mines, and Staff and Students at the University of Toronto.

References

Ahrens, L. H. (1950): *Spectrographic Analysis*, Cambridge, Mass.

Barth, T. W. F. & Posnjak, E. (1931): The spinel structure: An example of variate atom equipoints, *Jour. Wash. Acad. Sci.*, **21**, 255–258.

Bateman, A. M. (1917): Magmatic ore deposits, Sudbury, Ontario. *Econ. Geol.*, **12**, 391–426.

Claffy, E. W. (1947): Spectrochemical analysis of rocks and minerals. *Am. Jour. Sci.*, **245**, 35–48.

Clarke, F. W. & Washington, H. S. (1924): *U. S. Geol. Surv.*, *Prof. Paper* 127.

Clauson, V. (1947): Geology of the Sudbury basin area, *Ph.D. Thesis, University of Washington.*

Coleman, A. P. (1913): The nickel industry, *Can. Dept. Mines, Mines Branch.*

Collins, W. H. (1934): The life history of the Sudbury nickel irruptive—I Petrogenesis. *Trans. Roy. Soc.* Canada, **28**, Sec. IV. 123–177.

Daly, R. A. (1933): *Igneous Rocks and the Depths of the Earth*, New York.

Davidson, S. (1948): Falconbridge Mine, *Structural Geology of Canadian Ore Deposits. Symposium, Can. Inst. Min. Met.*, 618–626.

Gavelin, S. & Gabrielson, O. (1947): Spectrochemical investigations of sulphide minerals from the ores of the Skellefte district, *Sver. Geol. Undersök.*, Ser. C, **491**, 1–45.

Goldschmidt, V. M. (1934): Drei Vorträge über Geochemie, *Geol. Fören. Förh.*, **56**, 385.

——— (1937): The principles of distribution of chemical elements in minerals and rocks, *J. Chem. Soc.*, Part I, 655–673.

——— (1937*a*): Geochemische Verteilungsgesetze der Elemente, IX Die Mengenverhältnisse der Elemente und der Atom-Arten, *Norsk. Vid.-Akad. Mat.-Natur. Kl., Skr.*, No. 4, 1–148.

——— (1937*b*): Geochemie und periodisches System der chemischen Elemente, *Travaux du Congres jubilaire Mendeleev*, **2**.

——— (1944): Crystal chemistry and geochemistry, *Chem. Products*, **7**, 29.

——— (1945): The geochemical background of minor-element distribution, *Soil Sci.*, **60**, 1–7.

——— & Peters, C. (1931): Zur Geochemie des Galliums, *Nach. Ges. Göttingen, Math.-phys., Kl.* III; *Fachgr.* IV, *Geol. Miner.*, 165.

Goldsmith, J. R. (1950): Gallium and germanium substitutions in synthetic feldspars, *Jour. Geol.*, **58**, 518–536.

Knight, C. W. (1917): Royal Ontario nickel commission report, *Ont. Depart. Mines.*

Landergren, S. (1948): On the geochemistry of swedish iron ores and associated rocks, *Sver. Geol. Undersök.*, *Ser.* C, **496**, 1–182.

Leutwein, F. (1941): Geochemie und Verkommen des Vanadiums, *Berlin Freib. Geol. Gest.*, **18**, 73.

Lundegårdh, P. H. (1947): Rock composition and development in central Roslagen, Sweden. *Ark. Kem. Min. Geol.*, **23**A, No. 9.

——— (1948): Aspects of the geochemistry of chromium, cobalt, nickel and zinc. *Sver. Geol. Undersök.*, **43**, No. 513.

Mitchell, R. L. (1948): The spectrographic analysis of soils, plants and related materials, *Commonwealth Bur. Soil Sci.*, *Tech. Commun.* **44**.

Nockolds, S. R. & Mitchell, R. L. (1948): The geochemistry of some Caledonian plutonic rocks; A study in the relationship between major and trace elements of igneous rocks and their minerals, *Trans. Roy. Soc. Edin.*, **61,** (ii), 533.

Otto, H. (1936): Die Rolle des Mangans in der Mineralien. *Min. Petr., Mitt.* **47,** 89–140.

Phemister, T. C. (1925): Igneous rocks of Sudbury and their relation to the ore deposits, *Ont. Dept. Mines,* **34** (8).

Rankama, K. & Sahama, T. G. (1949): *Geochemistry,* Chicago.

Sahama, T. G. (1945): Spurenelement des Gestein in südlichen Finnisch-Lappland, *Bull. Comm. Géol. Finlande,* No. 135.

Sandell, E. B. & Goldich, S. S. (1943): The rarer metallic constituents of some American igneous rocks, *Jour. Geol.,* **51,** 99–115 and 167–189.

Smith, R. W. & Hoagbin, J. E. (1946): Quantitative spectrographic analysis of ceramic materials, *Jour. Am. Ceram. Soc.,* **29,** 222.

Strock, L. W. (1936): Zur Geochemie des Lithiums, *Nach. Ges. Göttingen, Math.-phys., Kl.* III, *Fachgr.* IV, *Geol. Miner.,* 171.

v. Tongeren, W. B. C. (1938): On the occurrence of rarer elements in the Netherlands East Indies, *D. B. Centens, Amsterdam.*

Vogt, J. H. L. (1923): Nickel in igneous rocks, *Econ. Geol.,* **18,** 307–353.

Wager, L. R. & Mitchell, R. L. (1951): The distribution of trace elements during strong fractionation of basic magma—A further study of the Skaergaard intrusion, East Greenland. *Geochim. Cosmochim. Acta,* **1,** 129–208.

Walker, T. L. (1897): Geological and petrographic studies of the Sudbury nickel district, *Quart. Jour. Geol. Soc.* London, **53,** 40–66.

Wickman, F. E. (1943): Some aspects of the geochemistry of igneous rocks, *Geol. Fören. Förh.,* **65,** 371.

Yates, A. B. (1948): Properties of the International Nickel Company of Canada, *Structural Geology of Canadian Ore Deposits, Symposium, Can. Inst. Min. Met.,* 596–617.

X-RAY MEASUREMENTS ON ARGENTOPYRITE

J. Murdoch and L. G. Berry, *University of California at Los Angeles and Queen's University, Kingston, Ontario, Canada.*

Abstract

New observations on argentopyrite from Freiberg and Joachimstal lead to the following data for the species:

Orthorhombic, probable space group D_{2h}^{13}—*Pmmn;* unit cell with $a=6.64$, $b=11.47$, $c=6.45$ Å and $a:b:c=0.5789:1:0.5623$, contains $4[AgFe_2S_3]$; specific gravity, 4.25 (meas.) 4.27 (calc.). The crystals are markedly pseudohexagonal due to interpenetrating twinning; lamellar twinning is also present. Crystals display the forms b {010}, m {110}, n {120} x {011} and c {001}, the termination faces are usually rough. The x-ray powder diffraction data index completely with the lattice dimensions.

Argentopyrite is classified in Dana's System of Mineralogy (1944) as an incompletely described mineral, possibly dimorphous with sternbergite ($AgFe_2S_3$). The prismatic six-sided twinned crystals of argentopyrite were originally described as monoclinic. Schrauf (1871) showed that the mineral is orthorhombic and pseudohexagonal by twinning. Weisbach (1877) described brittle, apparently hexagonal prismatic crystals from Marienberg which are clearly argentopyrite but differ in specific gravity from the original material. Weisbach also described "argyropyrite" as non-brittle pseudohexagonal twinned crystals with a perfect basal cleavage from Himmelsfurst mine, Freiberg. Streng (1878) described crystals of "Silberkies" from Andreasberg which are pseudohexagonal twins, and similar in silver content and specific gravity to Weisbach's material from Marienberg. In connection with a study of frieseite the late Professor M. A. Peacock also made some observations on a specimen of argentopyrite (87701) from the Holden Collection of Harvard University. Peacock (1942) published his observations on frieseite together with new data on sternbergite in a brief abstract; his observations on argentopyrite remain unpublished. The present report combines these unpublished observations with new data obtained from other specimens of this mineral.

The specimens which we have studied are from Freiberg and Joachimstal, one (Freiberg) supplied by Ward's Natural Science Establishment, one from the Royal Ontario Museum (M13001) and one from the National Museum at Washington (R541). The specimen from Ward's carries a crust of prismatic crystals of argentopyrite, practically all tarnished iridescent or blackened. These crystals appear as simple hexagonal prisms (even those appearing most perfect have striations on the faces of the prism zone), or as more or less deeply grooved prisms with reentrant angles sharply marked. Most show no definite terminations, but some show a low pyramidal development, sometimes six more or less imperfect faces, at other times fewer which are recognizable. Even the best of these, when examined on the reflecting goniometer, give very poor signals. The average rho angle for these is close to 29°, representing, as will be shown later, (011) faces. A considerable number, particularly of the larger individuals, show an irregular core of foreign material, slightly harder than argentopyrite. Polished sections, made perpendicular to the prism show this core to be isotropic. Micro-chemical reactions indicate silver and iron, but the amount is too small for further identification to be possible. Associated minerals are gypsum, appearing in tiny water clear crystals perched on a crust of argentopyrite and other minerals, and dull gray, botryoidal crusts of arsenic (identified from x-ray powder pattern). Some proustite and occasional grains of pyrite, and possible other sulphide minerals were observed.

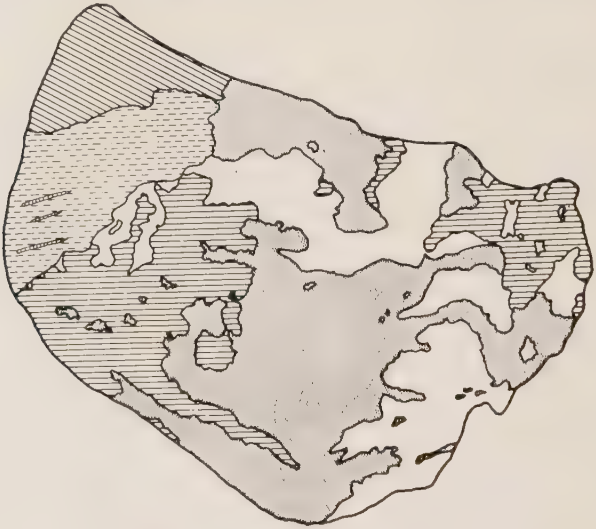

Fig. 1. Argentopyrite; polished section on (001) in polarized light with crossed nicols. Intricate interpenetration twinning shown by the distribution of patterns. Each pattern represents an individual.

Polished surfaces were made of some of the larger individuals, normal to the prism zone. These show in polarized light under crossed nicols an extremely intricate intergrowth of numerous individuals, revealed by rather intense interference colors, ranging from very deep blue through paler shades of blue gray, to bright grayish white which is the color in ordinary light. The very strong anisotropism in this orientation, and the presence of intergrowths, further confirm the non-hexagonal character of the mineral. The complexity of intergrowth is not confined to the basal plane, as one crystal, mounted with a prismatic (probably 010) face in reflecting position showed equal irregularity of grain shape as well as occasional lamellae with trace of plane parallel to *c*. Some idea of the complexity of these intergrowths is indicated in the accompanying drawing (Figure 1) made from observations of a specimen in polarized light with crossed nicols.

The Royal Ontario Museum specimen (Joachimstal) also showed rather brightly tarnished crystals, but in some areas the argentopyrite was essentially fresh, bronze brown in color, and giving excellent reflection signals from prism zone faces. Even here, the terminal faces were poor in quality. Few or no cored individuals were noted on this specimen. Earlier than argentopyrite, dull gray rosette-like cubic crystal aggregates of chloanthite are abundant. This mineral also was identified by its *x*-ray powder pattern and micro-chemical tests for nickel and arsenic, cobalt was absent. Considerable associated proustite was noted in the specimen.

On the National Museum specimen the crystals of argentopyrite are sharp hexagonal prisms, rarely striated parallel to *c* and with a low roughly pyramidal termination. The crystals are tarnished, green, blue, yellow and purple. The crust of argentopyrite is underlain by ruby silver, and rhombohedrons of siderite are also present.

Geometrical Crystallography

M. A. Peacock measured 2 crystals of argentopyrite from Joachimstal, leaving sketches and measurements of these crystals. One crystal is a psuedohexagonal twin showing the form {010} represented by 5 large faces (Figure 2), the form {120} with 2 faces bevelling each (010) face. Adjacent (120) faces of different individuals meet in a deep re-entrant notch. Narrow re-entrant grooves formed by two (120) faces also occur in two of the (010) faces. The crystal is terminated by six faces of the form {011} and a rough face approximating the basal pinacoid. Peacock's second crystal is much more complex showing pseudohexagonal twinning and fine lamellar twinning. A third small crystal, apparently a simple hexagonal prism (0.5×0.1 mm.), was selected for *x*-ray measurements.

Some interfacial angles from the literature are shown in Table 1 in comparison with measured angles from Peacock's notes and our recent measurements. Schrauf's (1871) elements fit the measured angles fairly well. Schrauf's observed form *n*{130} becomes {310} in the present setting although erroneously written as {130} in Dana (1892). It is worth noting that the angle 110∧310 is very close to the angle 110∧120

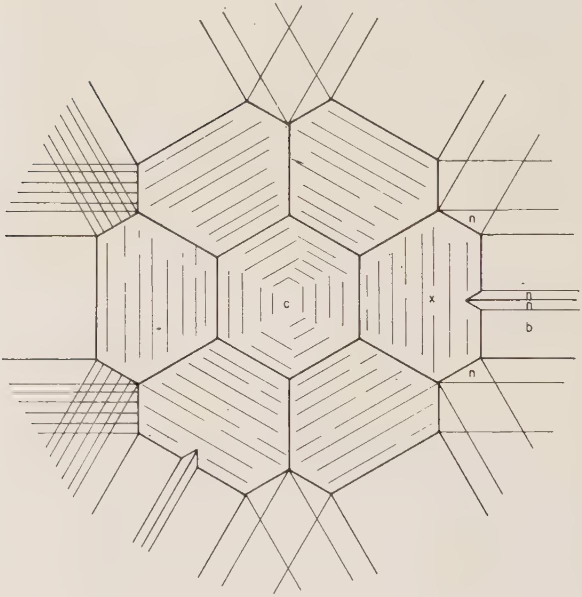

FIG. 2. Idealized drawing, from a working sketch by M. A. Peacock, of a twinned crystal of argentopyrite from Joachimstal showing faces of *c*{001} rough, *x*{011} striated parallel to edge with *b*(010); *b*{010} and *n*{120} folded into the plane of the drawing along the intersection with faces of *x*{011}. Faces of *n*{120} often form grooves on (100), some (120) faces are striated vertically.

(Table 1). Peacocks' crystal (Figure 2) clearly shows two faces (120) adjoining each of the five (010) faces on each side at polar angles of about 40°. In this case the indexing is established without ambiguity. It is probable then that Schrauf's *n*{310} is really {120}. Murdoch's more complex crystal shows polar angles in the prism zone of about 40° which requires that some faces be indexed (120). Streng (1878) records the face (130) which we have not seen on our crystals. The *c* length in Schrauf's axial ratio has been doubled and the one terminal face which is well established has here been indexed (011), in keeping with the structural lattice described in the next section.

STRUCTURAL CRYSTALLOGRAPHY

Small six-sided prismatic crystals of argentopyrite suitable for single crystal *x*-ray studies were readily available on the museum specimens of this mineral. M. A. Peacock, in 1940, made rotation and Weissenberg films on a small crystal from Joachimstal. Specimens from Joachimstal (U.S.N.M. R541, labelled "frieseite"), (R.O.M. M13001) and Freiberg

TABLE 1. ARGENTOPYRITE: CRYSTAL MEASUREMENTS
$a:b:c=0.5812:1:0.5498$ (Schrauf, 1871)

		Observed			Calculated
		Average	Range	Obs.	
Joachimstal (Schrauf, 1871)	010∧110		59°30′–59°52′		59°50′
	010∧010 tw.		60 10 –60 30		60 20
	110∧310		19 05 –19 30		19 $12\frac{1}{2}$
	110∧120				19 07
	010∧011		60 40 –61 12		61 12
	110∧112		61 20		61 15
Andreasberg (Streng, 1878)	010∧010 tw.		59 45 –60 50		59 20 60 20
	010∧130		29 29 –31 09		29 50
	010∧011		57 36		61 12
Joachimstal (M. A. Peacock)	010∧110	58°45′	58 –59 30	(2)	59 50
	010∧010 tw.	59 36	59 31 –59 41	(2)	59 20
		60 13	59 57 –50 43	(4)	60 20
	010∧120	40 30	38 44 –40 35	(7)	40 43
	010∧011	01 03	60 15 –62 11	(9)	61 12
Freiberg (J. M.)	010∧010 tw.	58 47	57 41 –59 52	(2)	59 20
		60 38	60 02 –61 25	(4)	60 20
	010∧120	40 31	40 04 –40 50	(6)	40 43
Joachimstal (J. M.)	010∧011		60 30 –63 00	(5)	61 12

(U.C.L.A.) also yielded crystals suitable for single crystal measurements.

The single crystal *x*-ray films yield the lattice dimensions given in Table 2. The Weissenberg films with iron radiation show almost perfect hexagonal symmetry with *h*00, *h*01, etc., indistinguishable from $h\cdot 3h\cdot 0$, $h\cdot 3h\cdot 1$, etc., and *hh*0, *hh*1, etc., indistinguishable from 0*k*0, 0*k*1, etc. The high order reflections 6003≃90 and 330≃060 are split into two spots on most films with iron radiation but it is not possible to index these points correctly unless we assume that the *a*:*b* ratio is greater than 0.5773:1 $(1:\sqrt{3})$. On Peacock's films (Cu*K* radiation), which have more reflections in the high θ region, there is a visible lack of symmetry in the intensities of the high order reflections on either side of *hh*0 and $h\cdot 3h\cdot 0$ while symmetry is present on either side of *h*00 and 0*k*0. This demon-

TABLE 2. ARGENTOPYRITE: LATTICE DIMENSIONS[1]

	a	b	c	Observer	Radiation
Joachimstal (H.M.M. 87701)	6.65 Å 0.5813	11.44 Å 1	6.43 Å 0.5620	Peacock	CuK
Joachimstal (U.S.N.M. R541)	6.63 0.5775	11.48 1	6.45 0.5618	L.G.B.	FeK MoK
Joachimstal (R.O.M. M13001)			6.44	J.M.	Fe$K\alpha$
Freiberg (U.C.L.A.)	6.63 0.5775	11.48 1	6.46 0.5627	J.M.	Fe$K\alpha$
Freiberg (from powder pattern)	6.64 0.5784	11.48 1	6.47 0.5636	J.M. & L.G.B.	Fe$K\alpha$
Average	6.64 0.5789	11.47 1	6.45 0.5623		
Axial ratio	0.5812	1	0.5498	Schrauf (1871)	

[1] Using Mo$K\alpha$ 0.7107; Cu$K\alpha$ 1.5418; Fe$K\alpha$ 1.9373.

strates clearly that the lattice is not hexagonal either in symmetry or dimension. Peacock's cell dimensions have an $a:b$ ratio which differs significantly from $1:\sqrt{3}$ and agrees closely with the morphological $a:b$ ratio. The morphological $b:c$ ratio, which is based on rather poor observations of one form only, agrees rather poorly with the x-ray measurements. The x-ray powder lines which index as pinacoid reflections (Table 4) lead to the dimensions given in Table 2, line 8. The average cell dimensions then are

$$a=6.64,\ b=11.47,\ c=6.45\text{ Å}$$

These dimensions are used to index the powder pattern given later in Table 4.

The Weissenberg films about the c axis give the pattern shown in lower part of Figure 3. The solid circles appear on the zero layer and all points shown, in general, appear on the upper layers. Indexing in the normal way would require doubling all the h and k indices shown, in order to give rational indices to the points not indexed. We know however that crystals of argentopyrite show complex pseudohexagonal twinning. If we apply the operations of this type of twinning to the indexed points of the reciprocal lattice in Figure 3 the open circle points with $h+k=2n+1$

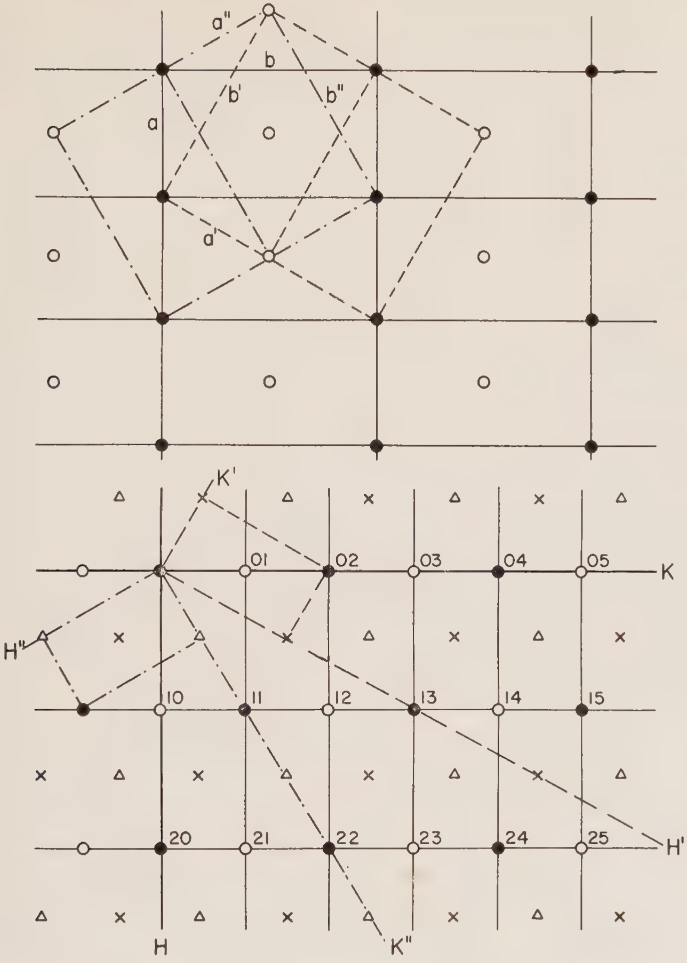

FIG. 3. Upper; plan of direct lattice of argentopyrite perpendicular to c, with $a=6.64$, $b=11.47$ Å; $a'b'$ and $a''b''$ direct lattice in twinned position by rotation of ab about $[1\bar{1}0]$ and[110].

Lower; reciprocal lattice projection of Weissenberg films. Solid points appear on zero layer (except origin); all points in general, appear on upper layers. Twinning by rotation about $[1\bar{1}0]$ brings the open circles into the X positions with axial directions $H'K'$ and about [110] brings the open circles into the Δ positions with axial directions $H''K''$; these axial directions are the reciprocal lattice axes corresponding to the direct lattice in twinned position $a'b'$ and $a''b''$.

fall on the points marked with triangles and crosses, and the solid points are common to all three orientations (indicated by HK; $H'K'$ and $H''K''$). Therefore all observed diffractions can be indexed in terms of a cell with the dimensions given above.

A rotation film, taken on a crystal rotating about the *b* axis (the normal to one of the large prism faces) shows strong zero and sixth layer lines and weak first to fifth, seventh and eighth layer lines. This rotation film leads to a period of 22.97 Å, double the *b*-period given above. Considering the twinning however, this axis of rotation is the *b* axis in one individual and the axes [310] and $[\bar{3}10]$ in the two twinned individuals, furthermore it will be seen in Figure 3 that the odd layer lines will be made up of reciprocal lattice points from the two twinned lattices. In the direct lattice drawing it is obvious that the period $[310] \simeq 2b$.

The observed diffractions for the untwinned cell are: *hkl*, all present; *hk*0 present only with *h* and *k* even; 00*l* present only with *l* even; these are characteristic of the space group D_{2h}^{13}—*Pmmn*. This is the probable space group if the crystals are holohedral.

Specific Gravity and Composition

The early descriptions of argentopyrite give specific gravity determinations which fall in three distinct ranges. The variety "argyropyrite" was distinguished from argentopyrite partly by the specific gravity. Some of the published values are given below, along with new unpublished determinations made by Dr. F. G. Smith with a Berman balance at the University of Toronto in 1940–41.

Argentopyrite		
Joachimstal	6.47	von Waltershausen (in Dana, 1944)
	5.33	Schrauf (1871)
Marienberg	4.06–4.12	Weisbach (1877)
Andreasberg	4.18	Streng (1878)
"Argyropyrite"		
Freiberg	4.206	Weisbach (1878), with cleavage (001)
Argentopyrite		
Andreasberg		
(H.M.M. 81808)	4.23	F. G. Smith
(U.T. 592)	4.26, 4.27	
Himmelsfurst, Freiberg		
(H.M.M. 81792)	4.19	
Joachimstal		
(H.M.M. 81807)	4.03	
no locality	4.13	
	4.14	
	4.25	

From this tabulation it appears that the early high values of von Waltershausen and Schrauf are in error, since no likely minerals have high enough specific gravity to affect the determination materially. A value

TABLE 3. ARGENTOPYRITE: ANALYSES AND UNIT CELL CONTENTS ($M=1257$)

	Joachimstal (von Waltershausen, 1866)				*Andreasberg (Streng, 1878)*			
	1	2	3	4	5	6	7	8
Ag	26.50	3.09	3	26.72	32.89	3.84	4	34.17
Fe	39.30	8.84	9	41.51	35.89	8.10	8	35.37
S	[34.20]	13.41	12	31.77	30.71	12.07	12	30.46
Total	100.00			100.00	99.74			100.00
G	6.47?		4.09		4.18		4.27	

1,5. Analyses. 2,6. Unit cell content for cell with $a=6.64$, $b=11.47$, $c=6.45$ Å and G $=4.25$. 3,7. Idealized cell content with calculated specific gravity. 4. Composition for $3[AgFe_3S_4]$. 8. Composition for $4[AgFe_2S_3]$.

of 4.25 appears closely to represent the specific gravity of argentopyrite. The analyses of argentopyrite also show considerable variation. One complete analysis and one partial analysis are given in Table 3 together with the unit cell contents, using the measured specific gravity of 4.25. Single silver determinations of 22.3 per cent (Schrauf 1871) and 28.8 per cent (Weisbach 1877) also appear in the literature. The analysis of argyropyrite (Weisbach 1877) is similar but we have no new observations that will help settle the status of this material. In considering the unit cell content we are inclined to give most weight to the complete analysis by Streng; indeed the numbers of atoms obtained from this analysis appear most reasonable. This cell content $4[AgFe_2S_3]$ leads to a calculated specific gravity 4.27 in close agreement with the measured values, and is more in keeping with the atomic positions in the space group if the structure is centrosymmetrical. The cell content given by the older and incomplete analysis (von Waltershausen, 1866) gives poor agreement between the measured and calculated specific gravity and includes odd numbers of silver and iron atoms. In preparing material for analysis it would be almost impossible to be certain of the absence of pyrite or marcasite and analyses are very likely to be low in silver. The silver minerals which have been reported in association with argentopyrite would be more readily removed in purification and if present should supply additional elements to the analysis.

The most likely cell content for argentopyrite, $4[AgFe_2S_3]$ supports the suggestion that this mineral is dimorphous with sternbergite $8[AgFe_2S_3]$. It is then possible that argyropyrite is a paramorph of sternbergite after argentopyrite. There is a close similarity between the cell dimensions of argentopyrite and sternbergite.

Table 4. Argentopyrite—$AgFe_2S_3$: *X*-ray Powder Pattern[1]
Orthorhombic *Pmma*; $a=6.64$, $b=11.47$, $c=6.45$ Å, $Z=4$

I(Fe)	*d*(meas)	*hkl*	*d*(calc)
3	5.81 Å	110	5.747 Å
		020	5.735
½	5.68	011	5.622
2	4.67	101	4.627
2	4.30	111	4.291
		021	4.283
5	3.624	121	3.600
10	3.341	200	3.320
		130	3.313
10	3.318	031	3.289
1	3.226	002	3.225
4	3.110	012	3.104
1	2.962	201	2.952
		131	2.947
3	2.902	102	2.901
3	2.878	220	2.873
		040	2.867
½	2.816	112	2.812
		022	2.810
1	2.633	221	2.624
		041	2.620
2	2.591	122	2.588
½	2.523	032	2.465
3	2.434	141	2.437
1	2.323	231	2.337
1	2.276	212	2.268
1	2.178	310	2.173
		240	2.170
		150	2.168
		051	2.161
1	2.120	013	2.113
½	2.040	103	2.045
		142	2.039
½	2.017	113	2.014
		023	2.013
1	1.988	232	1.979
5	1.931	123	1.926
4	1.908	060	1.912
		330	1.915
½	1.869	052	1.869
7	1.808	251	1.811
		203	1.804
		133	1.803
1	1.749	322	1.738
1	1.673	143	1.665
1	1.660	400	1.660
		260	1.657
1	1.613	004	1.612
1	1.597	162	1.596
1	1.544	421	1.548
		351	1.546
		171	1.544
		303	1.542
1	1.458 Å	072	1.461 Å
½	1.450	204	1.450
		134	1.450
½	1.436	214	1.439
		271	1.432
½	1.429	333	1.430
		063	1.428
		422	1.429
		352	1.428
		172	1.427
½	1.383	144	1.375
½	1.366	181	1.369
2	1.321	054	1.319
		510	1.319
		370	1.317
		280	1.316
2	1.311	403	1.314
		263	1.312
½	1.264	105	1.266
		025	1.258
		115	1.258
1	1.236	125	1.236
		334	1.233
		064	1.232
2	1.203	205	1.202
		135	1.202
		363	1.200
½	1.156	404	1.156
		264	1.156
½	1.135	451	1.140
½	1.126	503	1.130
1		292	1.116
1	1.118	305	1.114
		1.10.1	1.113
		523	1.108
1	1.107	434	1.107
		600	1.107
		390	1.104
1	1.090	601	1.091
		391	1.088
1	1.081	533	1.084
		453	1.083
		193	1.082
		006	1.075
½	1.043	602	1.046
		392	1.045
		612	1.043
½	1.019	514	1.021
		374	1.020
		284	1.020

---

[1] Using Fe*Kα* 1.9373 (manganese filter) and a 114.59 mm. diameter powder camera.

sternbergite *Cmma* $a=6.63$, $b=11.60$, $c=12.68$ Å Peacock (1941)
argentopyrite *Pmmn* $a=6.64$, $b=11.47$, $c=6.45$ Å

X-RAY POWDER PATTERN

The *x*-ray powder pattern data for argentopyrite are listed in Table 4 together with the indices and spacings calculated from the lattice dimensions. The patterns for crystal powders from different specimens show a few weak lines which do not appear on all patterns. These lines compare closely in spacing with the strong lines of arsenic, argyrodite, marcasite and smaltite (chloanthite) and have been omitted from the data in Table 4. Some of M. A. Peacock's powder films of materials from the Harvard Museum show strong pyrite lines.

ACKNOWLEDGMENTS

The authors wish to thank Dr. George Switzer of the United States National Museum and Dr. V. B. Meen of the Royal Ontario Museum for their cooperation in loaning specimens for study. The junior author also wishes to acknowledge a grant for equipment from the Committee on Scientific Research of Queen's University, which has helped make this research possible.

REFERENCES

DANA, J. D. & E. S. (1892): *System of Mineralogy*, ed. 6, New York.

——— (1944): *System of Mineralogy*, **1**, ed. 7, by C. Palache, H. Berman & C. Frondel, New York.

PEACOCK, M. A. (1942): On sternbergite and frieseite, *Am. Mineral.*, **27**, 229 (abstract).

SCHRAUF, A. (1871): Mineralogische Beobachtungen III–XXIV Argentopyrite, *Ak. Wien, Sitzungber.*, **64** (1), 192–199.

STRENG, A. (1878): Ueber den Silberkies von Andreasberg, *N. Jahrb. Min.*, 785–799.

VON WALTERSHAUSEN, S. (1866): *Ges. Wiss. Göttingen, Nachr.*, **9**, 66 (in Dana, 1944)

WEISBACH, A. (1877): Ueber die Silberkiese, *N. Jahrb. Min.*, 906–913.

THE DISTRIBUTION OF MAJOR AND MINOR ELEMENTS AMONG SOME CO-EXISTING FERROMAGNESIAN SILICATES[1]

E. H. Nickel,[2] *Mines Branch, Ottawa, Canada.*

Abstract

Co-existing chlorite, biotite, and hornblende from a schist have been analyzed spectrographically for major and minor constituents. It is found that the relative amounts of the elements in the three minerals can be explained by a consideration of electronegativities.

The amount of aluminium in the silicon positions seems to depend upon the relative electronegativities of the oxygens surrounding this site, which is in turn governed by the degree of polymerization in the silicate structure, and other structural differences. The extent to which aluminium replaces silicon in the tetrahedra influences the concentration of elements in the octahedral sites. The elements with similar electronegativities behave in a similar fashion. Cobalt, nickel, chromium, titanium, and vanadium are iron-like; manganese, zirconium, and scandium are more similar to magnesium.

The minerals used in this study were taken from a relatively small schist body in the Michipicoten District of Ontario. In the central portion of this schist is a zone of irregular quartz-scheelite veins. The schist is bordered on two sides by granodioritic masses. Portions of the schist are conglomeratic in appearance, suggesting a clastic origin.

The silicate minerals analyzed include biotite, hornblende, and chlorite. A study has also been made of the trace element distribution in the pyrite, and is discussed in the following paper (Nickel, 1954). Other minerals in the schist include quartz, calcite, albitic plagioclase, and minor epidote. Microcline is present locally.

It is suggested that the minerals were more or less in equilibrium with each other at the time of their formation and that, therefore, the distribution of a particular element approaches an equilibrium state as determined by the particular physico-chemical conditions at that time. It is generally true that the different structures of the silicate minerals distinguish between ions that exhibit dissimilar properties. Size and charge of the ion are major factors in determining its position in the structure but as Shaw (1953) has pointed out, these factors are not sufficient to adequately explain trace element distribution. Fyfe (1951) and Ramberg (1952) have suggested that electronegativity is of importance in governing the relative distribution of ions among various minerals.

---

[1] Extracted from a thesis for the Ph.D. degree, University of Chicago.

[2] Now with Mineragraphic Laboratory, Mines Branch, Department of Mines and Technical Surveys, Ottawa, Canada.

Electronegativity, a measure of the bond character of an atom, is considered to be a combination of the ionization potential and electron affinity of the atom (Fyfe, p. 538). In the succeeding pages the writer will endeavor to show the importance of this property in determining the distribution of some major and minor elements among co-existing chlorite, hornblende, and biotite.

The elements here considered are, of course, those that could be detected by spectrographic analysis, and only those are included that occur in tetrahedral and octahedral sites in the mineral structures. This excludes, then, elements such as potassium, calcium, and sodium. These large ions are not considered here because the amount of these elements is more or less fixed in certain of the minerals. Biotite, for example, requires one atom of potassium in its formula, while chlorite and hornblende do not generally have any of this element.

The electronegativity values to be used in the discussion have been obtained from Fyfe (1951) and are listed in Table 1.

Table 1. Electronegativities of Some Elements

$Mg^{\cdot\cdot}$	1.2	$V^{\cdot\cdot\cdot\cdot}$	1.6
$Sc^{\cdot\cdot\cdot}$	1.3	$Fe^{\cdot\cdot}$	1.65
$Zr^{\cdot\cdot\cdot\cdot}$	1.4	$Ni^{\cdot\cdot}$	1.7
$Mn^{\cdot\cdot}$	1.4	$Co^{\cdot\cdot}$	1.7
Al	1.5	$Si^{\cdot\cdot\cdot\cdot}$	1.8
$Cr^{\cdot\cdot\cdot}$	1.6	$Fe^{\cdot\cdot\cdot}$	1.8
$Ti^{\cdot\cdot\cdot\cdot}$	1.6	O	3.5

PROCEDURES

The minerals for analysis were separated by means of a magnetic separator and heavy liquid methods.

The analyses were carried out spectrographically on a Jarrell-Ash 21-foot grating instrument with a D.C. arc source. A complete description of the analytical methods can be found in Nickel (1953), but a brief outline will be given here.

Separate burnings were made for the determination of the major and minor constituents. For the major element analysis, the silicate samples together with the internal standards—cobalt, molybdenum, and strontium—were fused with boric acid and lithium carbonate. The bead was crushed, mixed with graphite, and arced in a graphite electrode. Spectrum evaluation was carried out as described by Honerjaeger-Sohm & Kaiser (1944). For the minor constituents, the sample was mixed with palladium internal standard and graphite. This was pre-heated to drive the water from the hydrous silicates, then arced. Because of the considerable range of wavelengths of the spectrum lines used in the evaluation, the "bridge" or external standard method described by Kaiser (1944) was used. A pure iron spectrum was used as external standard.

For the purpose of better comparing the behavior of the cations in the silicate minerals analyzed, the weight percentages, as determined spectrographically, have been recalculated to atomic fractions of their sites in the mineral structures. The average values of these atomic fractions are given in Table 2.

Table 2. The Atomic Fractions of the Element Sites in Biotite, Hornblende and Chlorite

(*Average values from* 13 *biotite,* 13 *hornblende, and* 8 *chlorite analyses*)

	Biotite	*Hornblende*	*Chlorite*
Al in tetrahedral position	0.390	0.108	0.298
Al in octahedral position	—	—	0.160
Fe in octahedral position	0.298	0.200	0.207
Mg in octahedral position	0.631	0.733	0.533
Co in octahedral position	1.72×10^{-4}	1.16×10^{-4}	1.28×10^{-4}
Ni in octahedral position	2.20×10^{-3}	1.30×10^{-3}	1.95×10^{-3}
Cr in octahedral position	4.20×10^{-3}	1.05×10^{-3}	2.89×10^{-3}
Ti in octahedral position	2.16×10^{-2}	0.902×10^{-2}	0.484×10^{-2}
V in octahedral position	8.33×10^{-4}	5.00×10^{-4}	2.90×10^{-4}
Mn in octahedral position	3.78×10^{-3}	4.80×10^{-3}	3.17×10^{-3}
Zn in octahedral position	1.60×10^{-4}	2.29×10^{-4}	0.836×10^{-4}
Sc in octahedral position	0.324×10^{-4}	1.43×10^{-4}	0.086×10^{-4}

Silicon and Aluminium

Aluminium can occupy both four and six coordinated positions in silicate structures. Reference to the generalized formulae of biotite—$K(Mg,Fe,Al)_3(Si,Al)_4O_{10}(OH)_2$, hornblende—$Ca_2(Mg,Fe,Al)_5(Si,Al)_8O_{22}(OH)_2$, and chlorite—$(Fe,Mg,Al)_3(Si,Al)_2O_5(OH)_4$ shows that the number of atoms in the tetrahedral (Si,Al) positions are four, eight, and two, respectively. Thus, if the total aluminium and silicon in these minerals is greater than the above values, some of the aluminium can be considered to be in octahedral coordination. The atomic fractions of aluminium and silicon in the biotite samples analyzed add up to approximately four, with few exceptions, showing that all or almost all of the aluminium in biotite is in tetrahedral coordination. In hornblende the aluminium and silicon atomic fractions add up to approximately eight, indicating that the same is true of this mineral. In chlorite, however, there is a considerable excess of aluminium and silicon atomic fractions over two. This excess is probably in octahedral sites in the chlorite.

In Table 2 the values of Al/Al&Si (for aluminium in tetrahedral position) are based on total aluminium for biotite and hornblende. In the case of chlorite, only that quantity is used that, together with silicon, adds up to an atomic fraction of two.

As can be seen from Table 2, both biotite and chlorite have a higher Al/Al&Si ratio than hornblende. There is a relationship between increasing polymerization in silicate structures and increasing tendency for aluminium to replace silicon (Ramberg, 1952). This is clearly shown by the analyses, since biotite and chlorite have sheet structures, and hornblende a double chain structure.

The reason for less aluminium in the tetrahedral positions of chlorite than in biotite can be explained by structural differences in these two minerals. *X*-ray diffraction analysis of the analyzed chlorite indicates that it has the McMurchy structure (the powder patterns exhibit a fairly strong 14 kX reflection). It can thus be considered to consist of alternating mica-like and brucite-like layers (Bragg, 1937). The degree to which aluminium replaces silicon depends on the relative electronegativity of the oxygens at the four corners of the tetrahedra (Ramberg 1952, p. 344). The most striking difference in the environment of these oxygen atoms in biotite and chlorite is that in biotite the oxygens forming the base of the polymerized sheet are weakly attached to potassium, whereas in chlorite they are bound to (OH). Now the electronegativity of (OH) is more similar to that of oxygen than is potassium, therefore in chlorite the O—OH bond is probably more covalent than the O—K bond in biotite. This will tend to make the basal oxygens of the sheet more electronegative in biotite than in chlorite, which in turn will make the tetrahedral site in biotite more favorable for aluminium than that in chlorite. This is indeed shown to be the case in the samples analyzed. The distribution of tetrahedrally coordinated aluminium and silicon depends, of course, on the bonding from layer to layer, which is in turn dependant on the distribution of divalent and trivalent cations in the two types of layers; the latter may in turn well be dependant on the aluminium-silicon relationships. In circular reasoning of this type one must begin somewhere, so the writer has here, as in the case of hornblende and biotite, started with the aluminium and silicon.

Iron and Magnesium

The octahedral sites of hornblende, biotite, and chlorite can be occupied by magnesium, iron, and aluminium, as well as by most of the trace elements analyzed—namely chromium, nickel, cobalt, titanium, vanadium, manganese, zirconium, and scandium. The major elements will be considered first, because the behavior of the minor elements is largely influenced by that of the major ones.

H. Ramberg (1952) has shown that the replacement of silicon by aluminium will decrease the electronegativity of the non-bridging oxygen, resulting in an increase of the iron-magnesium ratio (p. 345). This same factor should also influence the amount of aluminium in six-fold position.

It was shown above that the aluminium in silicon position increases from hornblende to chlorite to biotite. This, then, would tend to progressively decrease the electronegativity of the oxygen atoms surrounding the octahedral sites in these minerals. Therefore hornblende, with its non-bridging oxygens having the highest electronegativity, would favor those cations of lowest electronegativity; biotite, on the other end of the scale, would be more likely to favor cations of high electronegativity. The cations under consideration have the following electronegativities: $Mg^{\cdot\cdot}$1.2; $Al^{\cdot\cdot\cdot}$1.5; and $Fe^{\cdot\cdot}$1.65. Thus they should preferentially occupy the sites in hornblende, chlorite, and biotite, respectively.

This is the case in the samples analyzed. Biotite has a higher atomic fraction of iron than either hornblende or chlorite (Table 2); chlorite is the only mineral that contains appreciable aluminium in the octahedral site; and hornblende has a higher magnesium content than either biotite or chlorite (Table 2).

It is not certain which of these three cations is preferred by the brucite-like layer in chlorite. Since the octahedrally-coordinated aluminium is present in significant quantities only in the chlorite, which can be expected on the basis of the above reasoning applying to the mica-like layer, it appears, that the selective effect of the brucite-like layer is not very great, or is similar to that of the mica-like layer.

It is reasonable to expect the minor elements in six-fold coordination to behave like iron, magnesium, or aluminium, depending on their respective geochemical similarities to these elements. Figure 1 illustrates the relative amounts of these cations in the octahedral sites in biotite, chlorite, and hornblende (in chlorite this includes octahedral sites in both layers). The iron and magnesium values represented are the average values from Table 2, while the aluminium is the average octahedrally-located aluminium from Table 2, which was by subtracting tetrahedral aluminium from total aluminium. If only iron and magnesium were to be considered as governing the behavior of the minor elements, the iron-like ions should be highest in biotite, and equal in chlorite and hornblende (See Fig. 1). The magnesium-like elements should increase from chlorite through biotite to hornblende. But one would expect the aluminium content of chlorite to affect this distribution. If the iron-like elements are favorably affected by the presence of aluminium, their content in chlorite would probably be greater than that in hornblende; if unfavorably, then the reverse would be the case. The magnesium-like minor elements should behave in an analogous manner.

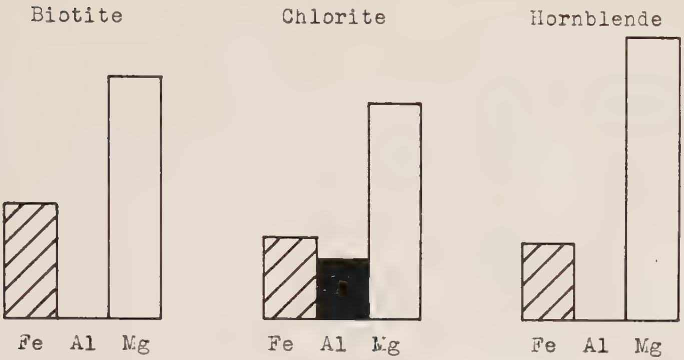

FIG. 1. Diagrammatic representation of relative amounts of iron, magnesium, and aluminium in six-fold coordination.

COBALT, NICKEL AND CHROMIUM

Cobalt, nickel, and chromium behave similarly in that they are most abundant in biotite, least in hornblende, and intermediate in chlorite, as shown in Table 2. Their distribution, in part, parallels that of iron since they are highest in biotite. This is to be expected because of the similarity of the electronegativities of these elements: $\mathrm{Fe}^{\cdot\cdot}$1.65; $\mathrm{Co}^{\cdot\cdot}$1.7; $\mathrm{Ni}^{\cdot\cdot}$1.7; and $\mathrm{Cr}^{\cdot\cdot\cdot}$1.6. Since cobalt, nickel, and chromium are higher in chlorite than in hornblende, one must assume that the six-coordinated aluminium favors the presence of these ions more than does magnesium. The reason for this may well be that the electronegativity of aluminium (1.5) is closer to that of these minor elements than is that of magnesium (1.2).

TITANIUM AND VANADIUM

Titanium and vanadium are probably present as tetravalent ions because these valence states are most common in rock-forming minerals (Rankama and Sahema, 1949). These elements have a relatively high concentration in biotite, and a lesser one in hornblende and in this way are similar to cobalt, nickel, chromium, and iron. The difference, however, is that chlorite contains less of these elements than does hornblende. Normally one would expect these elements to behave in a fashion analogous to that of iron, because of their similar electronegativities—1.65 for iron and 1.6 for both $\mathrm{Ti}^{\cdot\cdot\cdot\cdot}$ and $\mathrm{V}^{\cdot\cdot\cdot\cdot}$. It may be that these two elements, both having a high charge, may be less readily taken up by chlorite because it already contains a rather high proportion of trivalent aluminium in six-coordinated positions and it is necessary for the net charge to remain neutral. This might be accomplished by substituting more trivalent aluminium for tetravalent silicon but, as has been pointed out above, this substitution is somewhat limited in chlorite.

MANGANESE, ZIRCONIUM AND SCANDIUM

The behavior of this group of elements is similar to that of magnesium. Manganese, zirconium, and scandium occur most abundantly in hornblende, less so in biotite, and least of all in chlorite. This is to be expected because the electronegativities of these ions is rather similar: $Mg^{\cdot\cdot}$1.2; $Mn^{\cdot\cdot}$1.4; $Zr^{\cdot\cdot\cdot\cdot}$1.4; and $Sc^{\cdot\cdot\cdot\cdot}$1.3.

Wager & Mitchell (1951) suggest that scandium and zirconium probably occupy calcium sites in minerals. This is rather difficult to evaluate in these analyses because hornblende contains the most calcium, as well as the most magnesium. It will be noted, however, that the manganese and zirconium contents are approximately a factor of two greater in hornblende than in the other two silicates. Scandium is up to ten times more abundant in hornblende than in chlorite and biotite, suggesting that scandium may replace calcium, whereas zirconium and manganese probably do not. This may be explained by the lower electronegativity of scandium, which is closer to that of calcium (1.0) than is zirconium.

CONCLUSIONS

It has been shown that the electronegativities of the elements can be used to predict their distribution among the minerals in which they occur.

The degree to which silicon is replaced by aluminium in the silicon-oxygen tetrahedra appears to exert an important influence on the other structural sites in the minerals. Biotite has the most aluminium in the silicon position, hornblende the least, the chlorite an intermediate amount. This is explained by the effective electronegativities of the oxygens surrounding the tetrahedral sites. The hornblende structure is the least polymerized of these minerals, so that these oxygens have the smallest relative electronegativities of the three minerals. Chlorite has less aluminium than biotite because of the effect of the hydroxyl units on the electronegativity of the bridging oxygens.

The major elements capable of filling the octahedral sites (Fe, Mg, Al) are preferentially taken up by the minerals according to their electronegativities and that of the oxygen atoms surrounding the sites. Thus hornblende, whose octahedral oxygens have the greatest electronegativity, contains more electropositive magnesium than the other minerals. Biotite, whose oxygens have the smallest electronegativity value, contains the most iron, which has a high electronegativity. Chlorite contains the most aluminium, which has an intermediate electronegativity value.

The minor elements fall into groups having similar electronegativities and these behave according to the major element they most resemble. Thus cobalt, nickel, and chromium, with electronegativities similar to that of iron, are most abundant in biotite, the mineral richest in iron.

The enrichment of these elements in chlorite relative to hornblende is probably due to the effect of octahedrally coordinated aluminium in chlorite.

Titanium and vanadium are also richer in biotite than in the other two minerals, but are higher in hornblende than in chlorite. It is suggested that the high charge of these cations is responsible for this.

The behavior of manganese, zirconium, and scandium parallels that of magnesium. These elements have similar electronegativities.

REFERENCES

BRAGG, W. L. (1937): *Atomic Structure of Minerals*, Ithaca.

FYFE, W. S. (1951): Isomorphism and bond type, *Am. Mineral.*, **36**, 538–542.

HONERJAEGER-SOHM, M. & KAISER, H. (1944): Beruecksichtigung des Untergrundes bei der Messung von Intensitaetsverhaeltnissen, *Spectrochim. Acta*, **2**, 396–416.

KAISER, H. (1944): Ueber die Verschiedenen Verfahren zur Auswertung der Spektren bei Quantitativen Spektrochemischen Analysen, *Spectrochim. Acta*, **2**, 1–17.

NICKEL, E. H. (1953): The distribution of major and minor elements among co-existing pyrite and ferromaganesian silicates, *Ph.D. Thesis*, *University of Chicago.*

——— (1954): The distribution of iron, manganese, nickel and cobalt between co-existing pyrite and biotite in wallrock alteration, *Am. Mineral.*, **39**, 494–503.

RAMBERG, H. (1952): Chemical bonds and distribution of cations in silicates, *Journ. Geol.*, **60**, 331–355.

RANKAMA, K. & SAHAMA, TH. G. (1949): *Geochemistry*, Chicago.

SHAW, D. M. (1953): The camouflage principle and trace-element distribution in magmatic Minerals, *Journ. Geol.*, **61**, 141–151.

WAGER, L. R. & MITCHELL, R. L. (1951): The distribution of trace elements during strong fractionation of basic magma, *Geochim. Cosmochim. Acta*, **1**, 129–208.

THE DISTRIBUTION OF IRON, MANGANESE, NICKEL, AND COBALT BETWEEN CO-EXISTING PYRITE AND BIOTITE IN WALLROCK ALTERATION[1]

E. H. Nickel,[2] *Mines Branch, Ottawa, Canada.*

Abstract

Pyrite and biotite samples from a schist body enclosing scheelite veins have been analyzed spectrographically. Cobalt and iron in the biotite show a distinct decrease in the areas where pyrite has been developed, indicating that the metallic constituents of the pyrite have probably been derived from the wallrock minerals.

The ratios of the cobalt, nickel, and manganese contents in pyrite to those in biotite can be considered to be a measure of the sulphophile characters of these elements. On this basis, cobalt is the most sulphophile, followed by nickel and manganese, in that order.

The writer recently had an opportunity to study a scheelite deposit in the Michipicoten district of Ontario. The deposit is in the form of irregular quartz-scheelite veins with some molybdenite and calcite. There is abundant pyrite in the wallrock near the mineralized veins and in zones parallel to the veins. Where the pyrite is developed the wallrock appears to be lighter in color than some distance away; this feature is particularly evident in remnants of schist in the quartz veins.

The quartz-scheelite veins lie conformably in the central portion of a narrow schist body. The schist consists largely of quartz, calcite, albitic plagioclase, biotite, hornblende, and chlorite, with minor epidote. There is a general correlation between the type of ferromagnesian mineral and the development of pyrite. Where there is pyrite, biotite is commonly the only ferromagnesian mineral present; where there is no pyrite, chlorite and hornblende are usually present, sometimes to the exclusion of biotite. Because of the close association between biotite and pyrite, the distribution of elements between these two minerals is considered to be of particular interest. The interrelations between the silicates is discussed in a separate paper (Nickel, 1954).

Analytical Methods

The biotite analyses were carried out spectrographically as outlined briefly in the paper preceding this (p. 486). The minor elements in pyrite were also determined spectrographically using a D.C. arc source. The arcing was preceded by pre-heating to drive off the sulphur. Iron was used as internal standard.

---

[1] Extracted from a thesis for the Ph.D. degree, University of Chicago.

[2] Mineragraphic Laboratory, Mines Branch, Department of Mines and Technical Surveys, Ottawa, Canada.

Thirty-four samples of biotite were analyzed, and sixteen of pyrite. The minor elements analyzed in pyrite are cobalt, nickel, and manganese; their values are listed in Table 1. Other elements, present as traces in some of the specimens but not determined quantitatively, include copper, titanium, and zinc.

TABLE 1. MANGANESE, NICKEL, AND COBALT IN PYRITE

Sample	Manganese Weight %	Nickel Weight %	Cobalt Weight %
S-133-30	0.0014	0.13	0.40
S-133-37	.0021	.140	.38
S-133-42	.0013	.125	.50
S-133-47	.0024	.085	.37
S-133-64	.0028	.097	.240
S-133-90	.0008	.113	.133
S-133-94	.0020	.095	.248
S-133-125	.0024	.084	.315
S-133-131	.0036	.144	.240
S-133-135	.0028	.12	.76
Tl-10E	.0011	.14	.265
T1-20E	.0036	.125	.217
T1-40E	.0025	.11	.16
T1-60E	.0009	.082	.32
T1-70E	.0016	.11	.230
T1-80E	.0007	.115	.265

In Table 2 are given the amounts of cobalt, nickel, manganese, and iron in the biotite samples analyzed. Other major and minor elements were determined as well, but since they were not detected in pyrite, these are not of much significance for the present study. The more complete biotite analyses are to be found in Nickel (1953).

VARIATIONS IN THE COMPOSITION OF BIOTITE AS RELATED TO THE DEVELOPMENT OF PYRITE

It is necessary to consider whether the pyrite, at the time of its formation, was in physico-chemical equilibrium with the wallrock minerals or, more specifically, with the biotite. If there is no genetic relationship between the two, then the major and minor elements in the two minerals should bear no consistent relationship to each other. If, however, there was an exchange of ions between these two phases, then the presence or absence of pyrite should, under certain circumstances, be reflected by appropriate changes of composition in the biotite.

The most obvious element to consider in this respect is iron, since it

Table 2. Iron, Manganese, Nickel, and Cobalt in Biotite

Sample	Iron Weight %	Manganese Weight %	Nickel Weight %	Cobalt Weight %
S-133-30	10.6	.118	.0873	.0052
S-133-42	11.2	.120	.0786	.0026
S-133-47	10.0	.118	.0660	.0016
S-133-64	9.7	.197	.0802	.0014
S-133-67	8.1	.142	.0841	.0032
S-133-79	5.3	.154	.0774	—
S-133-90	6.4	.137	.0653	—
S-133-94	9.5	.156	.0653	.0030
S-133-99	12.0	.130	.0825	.0066
S-133-102	12.5	.148	.0762	.0061
S-133-108	10.4	.128	.0896	.0090
S-133-113	10.2	.132	.119	.0111
S-133-121	9.7	.123	.0660	.0072
S-133-125	9.3	.118	.0720	.0006
S-133-131	9.0	.121	.0621	.0007
S-133-135	10.0	.118	.0790	.0025
S-133-142	9.3	.118	.0943	.0065
S-133-147	9.5	.128	.0692	.0053
T1-50W	11.5	.128	.0848	.0070
T1-40W	10.6	.115	.0865	.0069
T1-30W	9.9	.118	.0778	.0072
T1-20W	10.2	.126	.0660	.0070
T1-10W	12.1	.122	.0928	.0090
T1-0	10.7	.138	.0825	.0065
T1-10E	7.9	.157	.0510	—
T1-20E	5.7	.142	.0700	—
T1-30E	10.6	.127	.0865	.0075
T1-40E	8.1	.131	.0802	.0064
T1-50E	10.7	.131	.0849	.0077
T1-60E	7.9	.120	.0928	.0055
T1-70E	7.9	.131	.0542	—
T1-80E	7.7	.135	.0786	—
T1-90E	10.3	.132	.0943	.0097
T4-50W	10.4	.139	.0833	.0074

is a major constituent in both pyrite and biotite. Of the minor constituents, cobalt is probably the most suitable because of the high cobalt content of pyrite, and its relatively low concentration in biotite. This latter condition is necessary because the proportion of pyrite to biotite is rather small, and if a minor element is abundant in the silicate, then the amount taken into the few pyrite crystals formed would not significantly affect the content of this element in the biotite. For this reason nickel is less suitable than cobalt in determining whether an exchange between the sulphide and silicate has taken place.

Figures 1 and 2 show the variation of the iron and cobalt content in the biotite of samples from two sections taken at right angles to the strike of the foliation of the schist. The T-1 samples (Figure 1) were taken from a trench across schist and orebody made to expose bedrock. The S-133 samples (Figure 2) were taken from a diamond drill core dipping at forty-five degrees, also cutting schist and orebody.

These diagrams clearly show a decrease in the iron and cobalt content of the biotite in the neighborhood of pyrite. This suggests very strongly that there was some sort of cation transfer between the biotite and pyrite, and that the distribution of elements between these two minerals represents at least an approach to equilibrium at the time of formation of the pyrite.

SULPHOPHILE CHARACTER OF COBALT, NICKEL, AND MANGANESE

Assuming that a state of equilibrium exists, or existed, it is interesting to inquire into the distribution of elements between the pyrite and biotite. Cobalt, nickel, and manganese can be considered in this respect. Iron cannot properly be discussed in this way because it is a major constituent whose content, in the pyrite at least, is fixed.

TABLE 3. RATIO OF MINOR ELEMENT CONTENT IN PYRITE TO THAT IN BIOTITE

Sample	% Metal in Pyrite/% Metal in Biotite		
	Cobalt	Nickel	Manganese
S-133-30	78	1.49	.0119
S-133-42	194	1.59	.0108
S-133-47	236	1.28	.0203
S-133-64	169	1.21	.0142
S-133-90	>600	1.20	.0058
S-133-94	83	1.45	.0128
S-133-121	33	1.73	.0292
S-133-125	573	1.16	.0203
S-133-135	316	1.53	.0237
T1-10E	>600	2.75	.0070
T1-20E	>600	1.78	.0254
T1-40E	25	1.50	.0191
T1-60E	59	0.89	.0075
T1-70E	>600	2.04	.0122
T1-80E	>600	1.47	.0052

Table 3 shows the ratios of cobalt, nickel, and manganese in pyrite to that in biotite. It should be noted here that the cobalt ratios show considerable fluctuations. These are mainly due to variations in the biotite, and in general reflect the amount of pyrite developed, the highest ratios

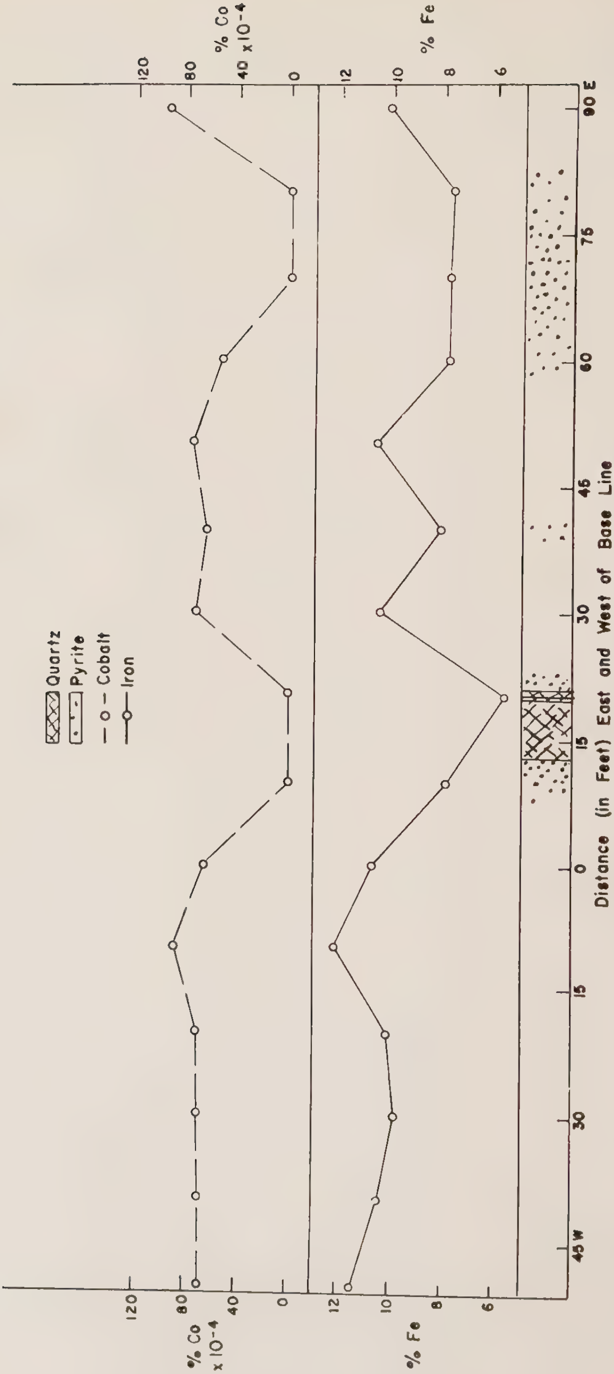

FIG. 1. Variations in the content of cobalt and iron in biotite from samples of trench 1 (T-1).

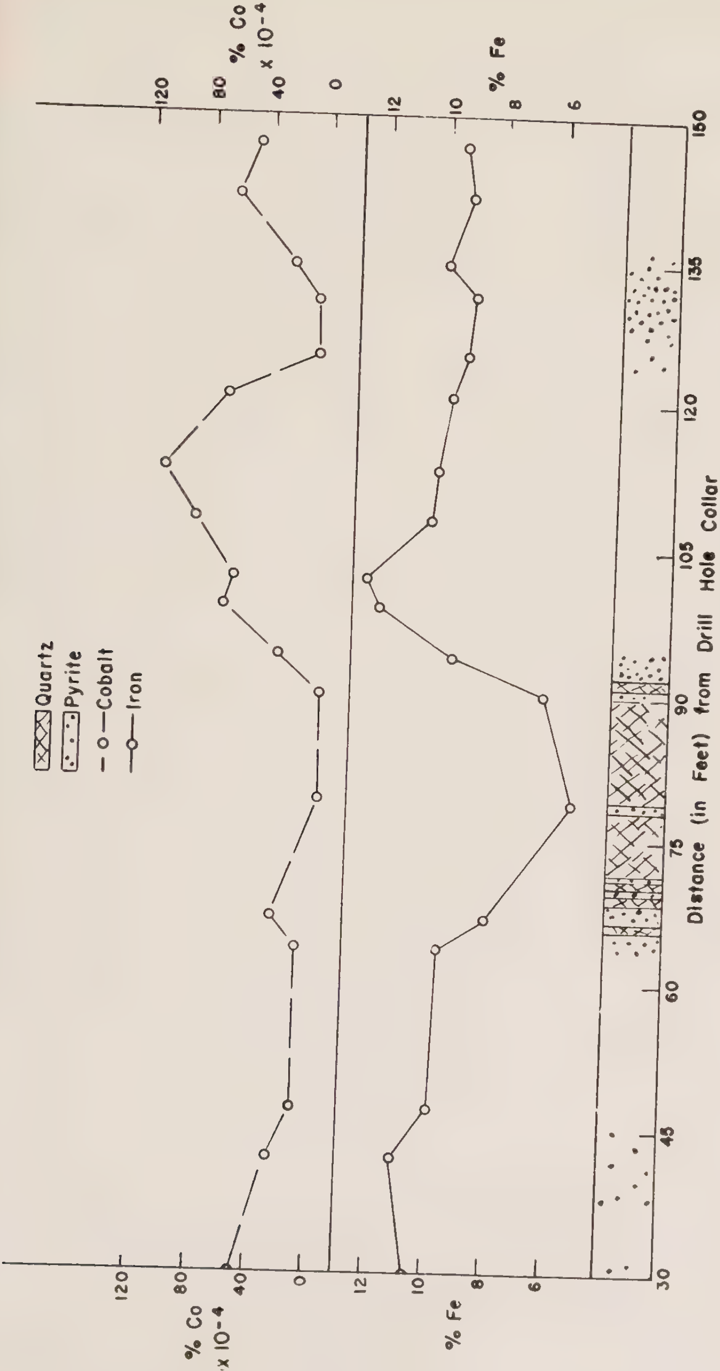

FIG. 2. Variations in the content of cobalt and iron in biotite from samples of diamond drill core no. S-133.

associated with the heaviest sulphide mineralization. This suggests that the highest ratios probably represent the closest approach to equilibrium distribution of the cobalt.

As can be seen, there is a large difference between the ratios of cobalt, nickel and manganese. This can be taken as a measure of the sulphophile nature of these elements or, in other words, the relative tendencies of these metals to form sulphides as opposed to silicates. This statement requires several qualifications. In the first place, any tendencies shown must be considered as applicable chiefly to the physico-chemical conditions existing in this instance, unless further evidence extends this observation over a wider range. Secondly, the only sulphide considered here is pyrite, so the tendencies exhibited must be restricted to only this sulphide until, again, further observations support a more general view.

With these qualifications in mind it can be stated, then, that of the three elements here considered, cobalt is the most sulphophile, nickel less so, and manganese is the least sulphophile of all. This same order of metal affinity for sulphur relative to silicate anions appears to be true for the monosulphides, as well, on the basis of thermochemical data (Ramberg, 1953).

It is probable that the polarizing power of the metals will influence their distribution between silicate and sulphide phases because of the difference in polarizability of sulphur and oxygen. Sulphur, more easily polarized than oxygen, should have the greatest attraction for the cation showing the greatest polarizing power. An idea of the degree of polarization can be obtained from the metal-sulphur distances in cobalt, nickel, and manganese disulphides having the pyrite structure. These are: CoS_2—2.33; NiS_2—2.42; and MnS_2—2.59 (Haraldsen, 1947, p. 6).

Cobalt, it will be noted, has the smallest metal-sulphur distance, although its normal ionic radius is greater than that of nickel. This suggests that the cobalt-sulphur bond is more covalent than the bonds in nickel and manganese disulphides, indicating a greater polarizing power for cobalt. Similarly, nickel and manganese have respectively decreasing polarizing powers. Thus the sulphophile natures of cobalt, nickel, and manganese can be explained on the basis of their relative polarizing abilities.

Significance of Pyrite-Silicate Relationships in Regard to Theories of Ore Genesis

The major and minor element relationships in biotite and pyrite discussed above make it evident that there is probably some genetic connection between these two phases. The conventional interpretation of wallrock alteration is that the "solutions" carrying the ore materials effect changes in the mineralogical and chemical composition of the host rock. To apply this reasoning here would require that those elements necessary for the formation of the sulphide minerals have been removed from the wallrock and carried away. Apart from the improbability of such a coincidence it can hardly be expected that the conditions favoring the deposition of certain elements would at the same time and at the same place cause the removal of these self-same elements. A more reasonable assumption, or so it appears to the author, is that *the metallic constituents of the pyrite have at least in part been derived from the wallrock silicates.*

Numerous examples of the "bleaching" of wallrock silicates close to hydrothermal deposits have been cited in geological literature. Perhaps the best known districts in which this has been noted include the Butte area (Sales, 1914) and the East Tintic District, Utah (Lovering, 1949). Sales suggests that the iron silicates were broken down to form the pyrite of the altered zones (p. 32). Lindgren (1933, p. 534) has invoked the same process to explain the development of pyrite in the alteration zones of mesothermal gold-quartz veins.

The close spatial relationship between biotite and pyrite has been mentioned earlier, as well as the general lack of chlorite and hornblende with pyrite. This association can be explained in one of several ways: The mineralogical differences may represent varying compositions of the original sediment and the introduced sulphur reacted only with the biotite to form pyrite; or the introduction of sulphur into certain positions in a compositionally homogeneous rock caused the mineral assemblage to break down into largely biotite and pyrite.

Considering the possibility that sulphur moved evenly through a rock complex of varying mineralogy, it is structurally improbable that volatiles would move more or less evenly through a rock of varying composition; it is much more reasonable that movement would take place along more or less well-defined low pressure areas. Also, it has been observed in many studies of wallrock alteration that minerals relatively high in Bowen's Reaction Series are transformed into minerals lower in the scale during ore deposition. A number of examples have been summarized by Butler (1932). One would assume, then, if sulphur had complete access to the hornblende in the schist, the hornblende would have been destroyed.

The other possibility—namely, that certain changing physico-chemical conditions, including the introduction of sulphur, have caused the change in the silicate mineral assemblage—will now be considered. This could be regarded as a more or less closed system except for the sulphur, and would require that the bulk chemical composition of the rock remain relatively uniform. Strict uniformity would, of course, be impossible because of material is obviously necessary to form even one pyrite crystal from neighboring constituents. Bulk chemical analyses have not been made in this study, so at this time no information is available on the quantitative distribution of the various elements through the rock as a whole. But speculation suggests that breakdown of a mineral assemblage into biotite, pyrite, and non-ferromagnesian minerals is possible.

To form an equivalent volume of biotite from hornblende with the approximate composition of the hornblende analyzed would involve a loss of calcium and silicon, and an increase in potassium, iron, aluminum, and water. The abundant calcite and quartz in the schist and in the orebody could account for the calcium and silicon freed. The potash required in biotite may have come from potash feldspars. In this connection, refractive index determinations of the schist feldspars indicate that all the feldspar associated with biotite, and most of that associated with chlorite and hornblende is a sodic plagioclase. In one specimen, however, only microcline was found. The sole ferromagnesian mineral in this specimen was chlorite; biotite was characteristically absent.

Is it not possible, then, that a mineral assemblage including potash feldspar and an iron-rich aluminous hornblende could have been altered by the action of sulphur, water, and probably heat to an assemblage consisting of biotite, talc, pyrite, quartz, and a hornblende of a different composition? A feature observed in thin-section from a specimen about 1200 feet from the orebody lends partial support to this theory. The hornblende there commonly contains a core of a much darker, highly altered hornblende which may represent the original mineral.

Whether the other ore minerals—scheelite and molybdenite—can be considered to have a similar origin to that suggested for the pyrite must remain, in this study at least, an unanswerable question. The close spatial relationship between ore and pyrite suggests a genetic relationship. Yet none of the analyses of the silicates show even a trace of tungsten or molybdenum. This could be explained in a number of ways. The scheelite and molybdenite may, indeed, have been introduced into their present positions from a considerable distance and from an unknown source. A second possibility is that the schist minerals contain tungsten and molybdenum but that they are present in amounts too small to be detected. This explanation might appear reasonable for tungsten since the spectrographic method used has rather a low sensitivity for tungsten; but molybdenum, if present in amounts greater than one part per million, should have been detected.

Still a third possibility, although one that has no direct supporting evidence, is that the original minerals in this sedimentary complex contained both tungsten and molybdenum but that these have been released by metamorphism and have migrated to the central ore zone, or out of the area of immediate observation. That they have completed their migration and that pyrite has not, could be due to the tungsten and molybdenum being released earlier than the iron. In this connection, paragenetic studies of numerous ores containing these elements have shown that in practically all cases tungsten and molybdenum minerals are deposited earlier than pyrite (Edwards, 1947, p. 114). If an origin by metamorphic differentiation (Ramberg, 1952, pp. 265, 266) can be ascribed to this deposit, the process could be considered as having been arrested at a stage where tungsten and molybdenum have completed their migration to a stable area, whereas pyrite is still more or less where is was formed.

CONCLUSIONS

Variations in the iron and cobalt content of biotite have been observed and can be correlated with the development of pyrite in the schist. This indicates that the metallic elements in the pyrite have likely been derived from the wallrock minerals—in this case biotite. No tungsten or molybdenum were detected in the wallrock silicates.

The distribution of cobalt, nickel, and manganese in co-existing biotite and pyrite indicate their relative sulphophile characters. Cobalt is the most sulphophile of these elements, followed by nickel and manganese, in that order.

REFERENCES

AHRENS, L. H. (1953): The use of ionization potentials, part 2. Anion affinity and geochemistry, *Geochim. Cosmochim. Acta*, **3,** 1–29.

BUTLER, B. S. (1932): Influence of the replaced rock on replacement minerals associated with ore deposits, *Econ. Geol.*, **27,** 1–24.

EDWARDS, A. B. (1947): *Textures of the Ore Minerals and their Significance*, Melbourne.

HARALDSEN, H. (1947): Interatomic distances and chemical bonds in compounds with pyrite and marcasite structure, *Norsk. Vid.-Akad. Mat.-Natur. Kl. Avh.*, **4.**

LINDGREN, W. (1933): *Mineral Deposits*, ed. 4, New York.

LOVERING, T. S. (1949): Rock alteration as a guide to ore—East Tintic District, Utah, *Econ. Geol. Monograph 1.*

NICKEL, E. H. (1953): The distribution of major and minor elements among co-existing pyrite and ferromagnesian silicates, *Ph.D. Thesis, University of Chicago.*

——— (1954): The distribution of major and minor elements among some co-existing ferromagnesium silicates, *Am. Mineral.*, **39,** 486–493.

RAMBERG, H. (1952): *The Origin of Metamorphic and Metasomatic Rocks*, Chicago.

——— (1953): Heats of reaction among solids as related to various ionic properties, and some geochemical implications, *Jour. Geol.*, **61,** 318–352.

SALES, R. (1914): Ore deposits at Butte, Mont., *Trans. Am. Inst. of Mining Engineers*, **44,** 3–106.

THE CRYSTAL STRUCTURE OF COVELLITE, CuSe AND KLOCKMANNITE, CuSe

L. G. Berry, *Queen's University, Kingston, Ontario, Canada*

Abstract

The crystal structure proposed by Oftedal (1932) for covellite, CuS, is confirmed and found to hold also for klockmannite, CuSe. They are hexagonal with space group D_{6h}^4-$P6_3/mmc$; covellite with $a=3.796$, $c=16.36$ Å and cell content 6[CuS]; klockmannite, with $a=3.938$, $c=17.25$ Å, and cell content 6[CuSe]. The atoms are in the following positions: 2Cu in (*d*) $\frac{1}{3}, \frac{2}{3}, \frac{3}{4}$; 2S or 2Se in (*c*) $\frac{1}{3}, \frac{2}{3}, \frac{1}{4}$; 4Cu in (*f*) $\frac{1}{3}, \frac{2}{3}, z$, with $z=0.107$ in CuS and $z=0.10_7$ in CuSe; 4S or 4Se in (*e*) $00z$, with $z_S=0.064$ and $z_{Se}=0.06_6$.

Covellite

Oftedal (1932) has described the crystal structure of covellite as

Hexagonal, D_{6h}^4—$P6_3/mmc$; $a = 3.80$, $c = 16.4$ kX
2Cu in (*d*) $\frac{1}{3}, \frac{2}{3}, \frac{3}{4}$; 4Cu in (*f*) $\frac{1}{3}, \frac{2}{3}, z$, with $z = 0.107$
2S in (c) $\frac{1}{3}, \frac{2}{3}, \frac{1}{4}$; 4S in (*e*) 0, 0, z, with $z = \frac{1}{16}$

The lattice dimensions were taken from the earlier work of Roberts & Ksanda (1929) and Gossner & Mussgnug (1927).

In order to check this structure in connection with the study of klockmannite, a small cleavage flake (0.05×0.5×2 mm.) from the Leonard mine, Butte, Montana was mounted for single crystal study. Unfortunately it was not possible to obtain an equidimensional fragment because of the perfect basal cleavage of covellite. Rotation and Weissenberg films with Cu*K* ($K\alpha = 1.5418$ Å) and Mo$K\alpha$ (0.7107 Å) radiation yielded the cell dimensions

$$a = 3.796, \qquad c = 16.36 \text{ Å}$$

Three sets of zero layer Weissenberg films, using three films in each set separated by brass foil, yielded intensity data for about ninety $h0\bar{h}l$ reflections with Mo$K\alpha$ radiation. The intensities, estimated by visual comparison with a standard series of graded exposures, were converted to $|F_o|$ values using the Lp factor and a scale factor (Table 1). The signs of the structure factors were calculated assuming Oftedal's structure for covellite, and a two dimensional Fourier series was summed in a plane perpendicular to an *a* axis, using Patterson-Tunell strips. The resulting Fourier map showed high peaks at $(\frac{2}{3}, -, \frac{1}{4})$ and $(\frac{1}{3}, -, \frac{6.5}{60})$ and moderate peaks at $(\frac{1}{3}, -, \frac{1}{4})$ and $(0, -, \frac{3.8}{60})$ The positions of these peaks correspond closely to the atomic positions given by Oftedal, the high peaks representing copper atoms and the moderate peaks sulphur atoms.

TABLE 1. COVELLITE: STRUCTURE FACTOR DATA FOR THE $h0\bar{h}l$ ZONE

$h0\cdot l$	$\lvert F_o \rvert$	F_c	$h0\cdot l$	$\lvert F_o \rvert$	F_c	$h0\cdot l$	$\lvert F_o \rvert$	F_c
00.0	270	270	10.26	0	0	30.26	0	−5
00.2	12	−19	10.27	7	4	30.28	11	11
00.4	15	−16	10.28	8	−7			
00.6	115	−148	10.29	8	−3	40.0	0	−9
00.8	49	63				40.1	12	−8
00.10	0	−10	20.0	33	−23	40.2	14	14
00.12	24	30	20.1	24	19	40.3	22	−23
00.14	55	−56	20.2	35	36	40.4	0	1
00.16	41	36	20.3	64	58	40.5	6	9
00.18	29	13	20.4	4	3	40.6	0	6
00.20	33	31	20.5	24	−22	40.7	16	14
00.22	43	−33	20.6	17	16	40.8	27	−24
00.24	24	−9	20.7	35	−33	40.9	0	7
00.26	10	−9	20.8	58	−57	40.10	15	−8
00.28	21	17	20.9	17	−18	40.11	16	−16
			20.10	25	−17	40.12	0	−3
10.0	31	−35	20.11	37	38	40.13	7	−5
10.1	28	−29	20.12	0	−8	40.14	20	19
10.2	46	54	20.13	18	12	40.15	7	4
10.3	103	−88	20.14	37	40	40.16	7	3
10.4	8	5	20.15	14	−9	40.17	7	11
10.5	31	32	20.16	13	−24			
10.6	24	23	20.17	14	−24	50.0	0	−5
10.7	46	44	20.18	0	5	50.1	0	4
10.8	69	−75	20.19	0	7	50.2	0	8
10.9	23	25	20.20	8	−14	50.3	15	13
10.10	27	−22	20.21	15	11	50.4	0	1
10.11	40	−49				50.5	0	−5
10.12	4	−10	30.0	94	89	50.6	0	4
10.13	18	−15	30.2	0	−6	50.7	10	−8
10.14	34	50	30.4	14	−6	50.8	16	−14
10.15	17	12	30.6	65	−62	50.9	0	−4
10.16	13	9	30.8	24	27	50.10	0	−4
10.17	26	29	30.10	0	−5	50.11	10	10
10.18	0	6	30.12	11	15	50.12	0	−2
10.19	6	−9	30.14	24	−30	50.13	0	3
10.20	18	−18	30.16	20	20	50.14	15	11
10.21	22	−13	30.18	15	7			
10.22	0	4	30.20	9	17	60.0	17	16
10.23	0	−6	30.22	14	−19	60.2	0	−1
10.24	7	−5	30.24	10	−5	60.4	0	−1
10.25	7	12				60.6	16	−12

Structure factors, calculated for $000l$ and $101l$ reflections over a small range of the z parameters (z_{Cu} 0.107 to 0.110 and z_{S} 0.0625 and 0.064), gave the best agreement with $|F_o|$ in terms of the reliability index, $R=\sum[|F_o|-|F_c|]/\sum|F_o|$, when

$$z_{Cu} = 0.107 \quad \text{and} \quad z_S = 0.064.$$

Structure factors for all $h0\bar{h}l$ reflections within the range of observation, calculated with these parameters, were then corrected by a temperature factor. The temperature factor ($B=1.84$) was found by plotting log $|\overline{F_c}|/|\overline{F_o}|$ as a function of $(\sin\theta/\lambda)^2$. The resulting F_c values are given in Table 1. The reliability index, $R=0.22$, indicates fairly satisfactory agreement between observed and calculated structure factors, considering the unsuitable shape of the cleavage fragment used for obtaining the intensity data. The data here confirm Oftedal's structure but indicate that a slight change in z_S parameter is desirable.

KLOCKMANNITE

The lattice dimensions and possible space group of artificial CuSe are given by Earley (1949)

$$\text{Hexagonal,} \quad D_{6h}^4\text{—}P6_3/mmc; \qquad a = 3.938, \quad c = 17.25 \text{ Å}$$

who also found that the x-ray powder patterns of klockmannite and artificial CuSe are identical. The natural material is unsuitable for single crystal study. The similarity of lattice dimensions and symmetry suggest that covellite and klockmannite are possibly isostructural. Earley's films show evidence of the existence of a superstructure in CuSe. A heavily exposed rotation film about the a axis shows weak diffuse rows requiring a twelve-fold a axis and the rotation about the c axis shows a few weak lines of nearly continuous diffraction parallel to the Bernal curves. No further information about the nature of the superstructure could be obtained.

In 1951 several students cooperated in calculating intensities for the $000l$ reflections of klockmannite, using Oftedal's atomic positions for covellite, over a range of values for the two variable z parameters. The observed intensities were estimated visually on Earley's original zero layer Weissenberg film, $h0\bar{h}l$ (using CuK radiation and a small thin hexagonal plate of CuSe). On a graph of z_{Cu} against z_{Se} areas were eliminated in which the relation between each pair of calculated intensities is opposed to the relation between the corresponding pair of observed intensities. This procedure leaves a small area in which the order of calculated intensities in decreasing magnitude is the same as the order of observed intensities, here the parameter values are $z_{Cu}=0.109$ and $z_{Se}=0.068$. The work was laid aside at that time when it was found that these parameters result in rather poor agreement between calculated and observed intensities for $10\bar{1}l$ reflections.

TABLE 2. KLOCKMANNITE: STRUCTURE FACTOR DATA FOR THE $h0\bar{h}l$ ZONE

$h0 \cdot l$	$\lvert F_o \rvert$	F_c	$h0 \cdot l$	$\lvert F_o \rvert$	F_c	$h0 \cdot l$	$\lvert F_o \rvert$	F_c
00.0	378	378	10.9	17	7	20.8	74	−103
00.2	11	−8	10.10	36	−31	20.9	20	−5
00.4	0	8	10.11	34	−37	20.10	33	−25
00.6	>67	−235	10.12	36	−6	20.11	21	29
00.8	40	40	10.13	37	−29	20.12	30	−5
00.10	46	−53	10.14	86	90	20.13	27	24
00.12	55	65	10.15	48	25	20.14	59	73
00.14	28	−47	10.16	35	26	20.15	32	−20
00.16	81	78	10.17	0	23	20.16	35	21
00.18	0	8	10.18	0	17			
00.20	20	33	10.19	0	−2	30.0	67	137
00.32	61	−64	10.20	50	−36	30.2	41	−3
			10.21	34	−22	30.4	42	4
10.0	46	12				30.6	56	−101
10.1	59	−56	20.0	46	9	30.8	21	19
10.2	>69	110	20.1	50	39			
10.3	44	−62	20.2	51	77	40.0	24	4
10.4	0	−17	20.3	29	42	40.1	0	−17
10.5	13	8	20.4	16	−12	40.2	23	33
10.6	39	−6	20.5	0	−6	40.3	19	−18
10.7	54	67	20.6	37	−5	40.4	0	−5
10.8	70	−135	20.7	56	−50	40.5	0	2
						40.6	13	−2

The crystalline CuSe, made by Earley in 1946, now consists of subparallel aggregates of tiny six-sided plates. It is not possible to segregate a single plate large enough to mount. In breaking up a group, the individuals inevitably split or bend. The crystal used by Earley, a clean hexagonal plate (0.1 mm. in width), has unfortunately been lost. The present appearance of the material suggests that the process of ordering which produced the superstructure indicated by Earley's films has now proceeded further.

The intensities, re-estimated from Earley's $h0\bar{h}l$ Weissenberg film (CuK radiation) by comparison with a series of graded exposures and converted to structure factors, $\lvert F_o \rvert$, are given in Table 2. Several apparently reasonable arrangements of copper and selenium were considered. One trial arrangement, with 2Cu in $(00\frac{1}{4})$, 4Cu in $(\frac{1}{3}, \frac{2}{3}, z)$, 2Se in $(\frac{1}{3}, \frac{2}{3}, \frac{3}{4})$ and 4Se in $(00z)$ which gives better agreement in the $hki0$ intensities, results in peaks on the $h0\bar{h}l$ Fourier map essentially similar in position to those found for CuS. A Fourier synthesis, using the observed structure factors with signs determined for the covellite arrangement, gives a map with major peaks at $(0, -, \frac{4}{60})$, $(\frac{1}{3}, -, \frac{7}{60})$, $(\frac{1}{3}, -, \frac{1}{4})$, $(\frac{2}{3}, -, \frac{1}{4})$ and some minor peaks. The first and third peaks are probably due to selenium and correspond closely in position to the sulphur peaks in the Fourier map of covellite, while the second and fourth are due to copper atoms. The minor peaks are probably ripples due to termination of the series at $\sin\theta/\lambda = 0.63$. The peak positions lead to the parameters $z_{Cu} = 0.114$ and $z_{Se} = 0.068$ agreeing closely with those found earlier and slightly larger than the values for covellite. Structure factors, calculated over a range of z values first for copper, then for selenium agree best with the observed values for

$$z_{Cu} = 0.10_7, \qquad z_{Se} = 0.06_6.$$

These values, however, can hardly be considered accurate beyond the second decimal place.

The calculated structure factors (F_c) corrected by a temperature factor ($B = 1.68$) obtained in the same way as for covellite are given in Table 2 The agreement, indicated by the reliability index ($R = 0.46$) is mucl poorer than for covellite. This is to be expected since data the were obtained from only one film and for a smaller range of reflections. The observed structure factors for some of the strongest reflections are mucl lower than the calculated values.

TABLE 3. INTERATOMIC DISTANCES IN COVELLITE AND KLOCKMANNITE

Covellite CuS		Klocknannite CuSe	
S_{II} —S_{II}	2.09, 3.80	Se_{II} —Se_{II}	2.28, 3.94
Cu_I —S_I	2.19	Cu_I —Se_I	2.27
Cu_{II}—S_{II}	2.30	Cu_{II}—Se_{II}	2.38
Cu_{II}—S_I	2.34	Cu_{II}—Se_I	2.46
Cu_I —Cu_{II}	3.21	Cu_I —Cu_{II}	3.35
S_I —S_{II}	3.75	Se_I —Se_{II}	3.90

The structural data here obtained result in the interatomic distances shown in Table 3. Cu_I has coordinated to it three S_I or Se_I in a plane parallel to 0001 and Cu_{II} is surrounded by three S_{II} or Se_{II} and one S_I or Se_I in nearly perfect tetrahedral coordination. S_I or Se_I is coordinated to three Cu_I in a plane perpendicular to c and two Cu_{II} on a line parallel to c in a trigonal bipyramid arrangement with the latter distance about 8% larger. S_{II} or Se_{II} is surrounded by three Cu_{II} and one S_{II} or Se_{II} in a nearly tetrahedral arrangement. The interatomic distances lead to the following atomic radii:

$$S = 1.05, \qquad Se = 1.14, \qquad Cu = 1.23 \text{ Å}.$$

The same average value for copper results from both CuS and CuSe structures using the above radii for S and Se. The S—S and Se—Se distances are in almost exact agreement with the values for the tetrahedral covalent radii given by Pauling (1948). This agreement confirms the values for the z_S and z_{Se} parameters established in this study.

The variation in the Cu—S and Cu—Se distances in the trigonal bipyramid is greater for Cu—Se, where the difference between Cu_I—Se_I and Cu_{II}—Se_{II} is 0.19. A larger value for the z_{Cu} parameter in klockmannite would reduce this difference slightly (to 0.14 with $z_{Cu}=0.11$, Cu_{II}—$Se_I=2.41$ and Cu_{II} –$Se_{II}=2.40$) McCullough (private communication) points out that this difference is comparable to that found in the di-*p*-tolylselenium dihalides (McCullough & Marsh, 1950) where the Se—X distance along the vertical axis of a nearly trigonal dipyramid yields a selenium radius of 1.40 Å while the Se—C distance yields a Se radius of 1.17 Å.

Acknowledgments

The writer wishes to thank Professors George Tunell and J. D. McCullough of the University of Cailfornia at Los Angeles for helpful advice during the course of this work, also to acknowledge the award of a Fellowship by the John Simon Guggenheim Memorial Foundation which made possible a period of study in California. Thanks are also due to the National Research Council of Canada for a grant in aid of research.

References

Earley, J. W. (1949): Studies of natural and artificial selenides: I-Klockmannite, CuSe, *Am. Mineral.*, **34,** 435–440.

Gossner, B. & Mussgnug, F. (1927): Über die Kristallstructur von Zinnober und Covellin, *Cbl. Min.*, Abt. A, 410–413.

McCullough, J. D. & Marsh, R. E. (1950): The crystal structure of di-*p*-tolylselenium dichloride and di-*p*-tolylselenium dibromide, *Acta Cryst.*, **3,** 41–45.

Oftedal, I. (1932): Die Kristallstruktur des Covellins (CuS), *Zeits Krist.*, **83,** 9.

Pauling, L. (1948): *The Nature of the Chemical Bond*, ed. 2, Ithaca.

Roberts, H. S. & Ksanda, C. J. (1929): The crystal structure of covellite, *Am. J. Sci.*, **17,** 489–503.

GERMANIUM AND OTHER TRACE ELEMENTS IN SOME WESTERN CANADIAN COALS

John A. C. Fortescue, *University of British Columbia, Vancouver, Canada.*

Abstract

This paper is a report on the results of spectrographic analyses of the ash of twenty-four coal samples from British Columbia, the Yukon and the Northwest Territories. The samples were selected from the collection of coals in the geology Department of the University of British Columbia.

Traces of germanium were found in six of the samples examined. A concentration of germanium greater than 0.1% was apparent in coals from Hornaday River N.W.T., and from Cape Caution B.C. The distribution of germanium in the samples examined was erratic; especially in the coal sample from Cape Caution.

Introduction

V. M. Goldschmidt (1930, 1937, 1944, 1954) was the first worker to use carbon arc spectroscopy for the analysis of coal ash. During these studies Goldschmidt discovered an unexpectedly high concentration of germanium and other trace elements in the ash of some European coal samples. Later work has shown that Goldschmidt's findings were not unique, and that coals from many parts of the world contain similar concentration of trace elements. A comprehensive bibliography of previous work in this field of research is given by Stadnichenko *et al.* (1953).

The Origin of Trace Elements in Coal

Goldschmidt (1930) suggested three ways in which elements might be concentrated in coal ash.

(1) Concentration by growing plants.
(2) Concentration by residual enrichment of soil after the more soluble elements have been leached away.
(3) Concentration in a coal seam after burial by selective reaction of the elements in groundwater with the carbonaceous material in the coal.

The Distribution of Trace Elements in Coal

Both Headlee (1953) and Goldschmidt (1944) have published figures for the concentration of elements in coal ash as shown in Table 1.

Headlee found that all the trace elements, with the exception of germanium, were evenly distributed across the coal seams which he examined, but germanium ions were concentrated in the top and bottom

TABLE I. THE CONCENTRATION OF ELEMENTS IN COAL ASH

Element	Maxinum Concentration Factor (Goldschmidt)	Concentration Factor (Headlee)	Average amount in grams per ton (Goldschmidt)	Average per cent of metallic oxides (Headlee)
Boron	1,000	10–185 times	3,000	—
Silicon	—	Less than average	—	SiO_2 = 44.8
Magnesium	—	Less than average	—	MgO = 0.99
Manganese	—	Less than average	—	MnO_2 = 0.046
Copper	5	1–10 times	500	CuO = 0.062
Cadmium	300	—	50	—
Calcium	—	Less than average	—	CaO = 2.7
Beryllium	200	1–10 times	1,000	BeO = 0.008
Zinc	300	1–185 times	20,000	ZnO = 0.051
Lead	100	1–185 times	1,000	PbO = 0.048
Molybdenum	—	1–10 times	—	MoO = 0.016
Vanadium	10	1–10 times	1,200	V_2O_5 = 0.050
Germanium	16,000	1–185 times	11,000	GeO_2 = 0.013
Nickel	100	1–10 times	8,000	NiO = 0.046
Tin	—	1–185 times	—	SnO_2 = 0.022

After Goldschmidt (1944) and Headlee (1953).

few inches of the seams which he examined, there being only a trace of germanium in the middle part of the seam. In a detailed study of the top three inches of a seam Headlee found that there was a gradation from 121 ppm. germanium in the quarter inch sample taken from the seam edge, to 2 ppm. in a sample three inches from the edge of the seam. A similar "contact enrichment" was found in the bottom four inches of another seam.

This experimental evidence appears to support Goldschmidt's third suggestion for the origin of trace elements in coal. Headlee's examination showed that all the germanium had been precipitated in the coal from the groundwater by the time such water had percolated more than a few inches into the coal seam. Rankama (1950, p. 736) in a discussion of the deposition of germanium in coal states "it (germanium) is precipitated as bivalent compounds because of the reducing action of the coal, and the enrichment is increased still more owing to the adsorbtive properties of the carbonaceous material." Thus the experimental findings of Headlee appear to support the theories of deposition of both Goldschmidt and Rankama.

McClelland (1953) in a discussion of the germanium content of Canadian coals states that "germanium is not uniformly distributed through a coal seam either vertically or horizontally." This is an important point because Headlee considered that the germanium content variation in a coal seam was only in the vertical direction.

To sum up, previous work has indicated that in general, trace elements, with the exception of germanium, occur uniformly throughout a coal seam. The germanium content of coal seams in at least one area has been shown to be concentrated at the edges of the seam, and in other areas the concentration varies laterally along the seam. In any systematic search for germanium in coal these factors should be considered.

PREVIOUS SPECTROGRAPHIC WORK ON COALS OF WESTERN CANADA

Newmarch (1953) describes spectrographic analyses of coal ash from the Michel area near Crowsnest Pass, British Columbia.

Newmarch was primarily interested in an analysis of coal seams for trace element content in order to discover if such data might be used for correlation of seams. He found the following germanium concentrations in the samples he analyzed.

TABLE 2. GERMANIUM CONTENT OF COAL FROM MICHEL B.C.

Seam	No. of Samples	Ash %	Germanium Content*
B	24	10.6	1.1
A		11.9	—
U_3?	12	9.8	—
U_3	9	7.5	.2
L_3	5	25.9	—

After Newmarch, 1953.

* Numbers plotted do not equal percentages of element present but are relative to one another for any one element and approximate to percentage figures.

Newmarch states that he ashed his coals at 750° C. This temperature would tend to volatilize any germanium present as the dioxide.*

It would be interesting to examine a sample of Michel coal ashed below 500° C., especially if the sample were taken from the top or bottom few inches of the seam. The average of 1.1 units of germanium in 24 samples of Seam B would appear to be a relatively high percentage of the metal.

PROCEDURE

(1) *Sampling*. Each specimen was examined, and a representative sample taken from it. The sample was then pulverized in an agate mortar. Approximately 3 grams of the resulting powder was transferred to a a wide mouthed crucible.

---

* Germanium oxides and sulphides are volatile above 700° C. (Powell *et al.*, 1951).

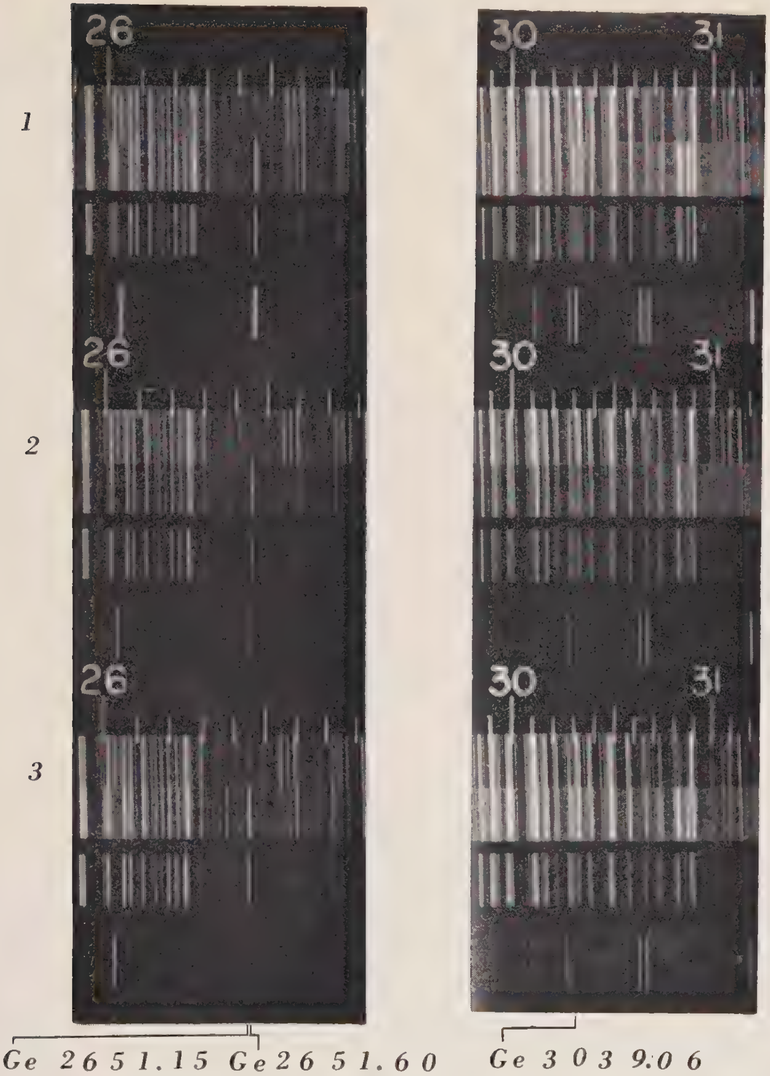

FIG. 1. 1, 2, 3 are photographs of the spectra of the Cape Caution coal ash sample. The individual spectra bands in each sample reading from top to bottom are: Iron Spectrum, Cape Caution Coal Ash 20 secs, Cape Caution Coal Ash 10 secs and Germanium Standard 10 secs. The germanium content of the standard samples is 1%, 0.1% and 0.01% in samples 1, 2, and 3 respectively.

(2) *Ashing.* a) The first two coal samples were ashed in crucibles without lids over a bunsen burner. Spectrographic analysis of such ash showed few trace elements present and as a result of this observation all later

TABLE 3. SPECTROGRAPHIC LINES USED IN THE IDENTIFICATION OF TRACE ELEMENTS IN COAL ASH

Element	Wave Length of Line in Armstrong Units	Intensity
Boron	2496.78	(9)
	2497.73	(10)
Manganese	2576.10	(3)
Germanium	2651.15	(10)
	2651.60	(10)
	3039.06	(10)
Magnesium	2782.99	(6)
Lead	2833.07	(6)
Tin	2863.32	(8)
Silicon	2881.59	(10)
Beryllium	3130.72	(10)
	3131.06	(10)
Molybdenum	3132.60	(10)
Nickel	3134.10	(10)
Calcium	3158.87	(8)
Vanadium	3184.00	(5)
	3185.40	(5)
Cadmium	3261.05	(10)
Copper	3273.96	(10)
Zinc	3345.00	(10)

From Brode (1946).

ashing was carried out in a muffle furnace.

b) All the preliminary coal samples were ashed in a muffle furnace in which the temperature was not allowed to exceed 430° C. This temperature was considered low enough to minimize the danger of volatilization of trace elements (Powell, *et al.* 1951, p. 542).

c) After all the preliminary ashing had been completed and the spectrographic plates of the ash had been made, I received a copy of the report by Stadnichenko, *et al.* (1953). For all re-run samples the ashing method which they suggest was adopted, as follows.

(i) 3 gms of coal dust placed in a shallow porcelain dish.
(ii) The dishes were placed in a cold muffle furnace in which the following conditions were maintained.
  200° C. ± for 20–30 minutes with furnace door open.
  220° C. ± for 6 hours or until sample was ashed.
  410° C. for 30 minutes to drive off last trace of carbon.

During the ashing procedure each sample was raked over several times with a glass rod.

TABLE 4. DESCRIPTION OF SAMPLES ASHED

No.	Locality	Description	Ash Colour	Remarks
1	Cape Caution B.C.	Bituminous?	Orange brown	—
2	Flint Vermillion Bluffs, Princeton, B.C.	Bituminous?	Orange brown	—
3	Camp Robertson	Bituminous?	Light Grey	—
4	Near Port Haney C.P.R., B.C.	Lignite	Whitish Grey	—
5	Rashings, No. 4 Shaft Extension	Bituminous	Grey	—
6	Peel River, Y.T.	Albertite? Dyke	Greenish Brown	Very little ash about 10% by volume of sample
7	Sable Arm Baynes Coal Co.	Bituminous	White to Rose Pink	—
8	Princeton	Bituminous	Yellowish Brown	—
9	Coalmont	Bituminous	White	Resinous high gas content
10	Collings Gulch Nr Tulameen River B.C.	Sub Bituminous	Orange Brown	
11	Chua Chua N. Thompson, B.C.	Cannel Coal	Dark Grey	
12	Coal from Iron River	Bituminous	Grey	
13	6 Miles North Alexander ferry W. Bank of Fraser River B.C.	Lignite	Brownish Dark Grey	
14	Hamilton Lake	Fossil Wood	Dark Red	Probably incombustible
15	No. 4 Shaft Union Mine Comox	Sub Bituminous?	Light Brown	
16	Quatsino	Sub Bituminous?	Light Brownish Yellow	
17	Rocky Mt. Canyon Peace River	Bituminous	White	
18	Cape Caution B.C.	Lignite	Brownish Orange	
19	Glacier Gaulch B.C.	Sub Bituminous?	Medium Grey	Metamorphosed
20	"2" Hornaday River area N.W.T.	Lignite	Dark Grey	
21	"3" Hornaday River area N.W.T.	Fossil Wood	Orange	
22	"6" Hornaday River area N.W.T.	Fossil Wood	Orange grey	
23	"4" Hornaday River area N.W.T.	Lignite	Dark grey	
24	Cornwallis Island	Lignite	Yellowish Brown	

(3) *Spectrographic Method.* The ash samples were spectrographed with a Hilger Medium Quartz Spectrograph. Each sample was arced between National Special Graphite Eelctrodes at a current of 4.5 amp at 110 volts D.C. The spectra were recorded on Kodak 2×10 Spectrographic glass plates (Type 11-F (3)) which were developed for 5 minutes in D19 developer and fixed for at least five minutes in F5 fixing solution at room temperature (68° F.); then they were washed for one hour and air dried.

Four ash samples were exposed on each plate. Each sample was ashed for two periods of time; 10 seconds and 20 seconds. Two standard spectra were used for each *plate* sample, an iron spectrum above, and an R.U.* spectra below. These two spectra were used to locate the exact position of the characteristic lines used to identify each element.

* A standard prepared by Hilger Ltd. consisting of small quantities of 50 elements incorporated in a base of zinc, calcium and magnesium oxides. The quantity of each element is adjusted so that the "persistent lines" (Raies Ultimes) and the most sensitive lines appear for each element in the powder.

Table 5. Elements Detected in Coal Ash Samples

Sample	Boron	Manganese	Germanium 26 (lines)	Magnesium	Lead	Tin	Silicon	Germanium 3039.06	Beryllium	Molybdenum	Nickel	Calcium	Vanadium	Cadmium	Copper	Zinc
1	2	2	—	1	—	—	2	—	—	—	—	—	—	—	—	—
2	3	—	—	3	—	—	1	—	3	—	—	2	—	—	3	—
3	2	3	—	2	—	—	1	—	—	—	—	3	—	—	3	—
4	1	3	—	2	3	—	1	—	3	—	—	2	—	—	3	—
5	3	3	—	3	—	—	1	—	3	—	3	—	3	—	3	3
6	1	2	—	1	2	2	1	—	1	—	1	2	1	—	1	—
7	2	3	—	2	—	—	1	—	3	—	—	2	3	—	2	—
8	1	3	—	2	—	—	1	—	—	—	—	1	—	—	2	4
9	1	2	—	3	3	—	1	—	3	—	—	3	3	—	2	4
10	1	3	—	2	3	—	1	—	3	3	4	3	—	—	2	—
11	1	—	4	1	2	—	1	4	3	—	—	3	3	—	3	3
2	1	2	—	—	2	—	1	—	3	3	—	3	3	—	3	3
1	1	1	—	2	2	—	1	—	2	4	—	1	—	—	1	3
12	1	3	—	3	—	3	1	—	3	—	—	2	—	—	3	—
13	1	3	?	1	3	—	1	4	2	3	—	3	3	—	2	—
14	2	2	—	3	—	—	2	—	—	—	—	—	—	—	3	4
15	2	3	—	1	2	—	1	—	4	—	—	1	—	—	2	3
16	1	3	—	1	4	—	1	—	3	—	—	2	—	—	3	3
17	1	3	—	1	4	—	1	—	2	3	—	2	—	—	2	3
18A	2	3	3	1	3	—	1	3	2	2	2	1	—	—	3	3
19	2	3	—	1	3	—	1	—	3	—	—	3	—	—	2	3
20	1	1	—	1	3	—	1	—	3	—	—	1	—	—	2	3
21	1	3	2	1	3	—	2	1	3	—	—	1	—	—	2	—
22	1	2	2	1	—	—	2	1	3	—	—	1	—	—	—	—
23	1	2	—	1	?	—	1	—	—	—	—	1	—	—	2	4
24	1	1	4	1	1	4	1	3	2	3	4	1	3	—	2	3

Key to Intensity of lines: (1) Strong; (2) Medium; (3) Weak; (4) Pressure not detected.

Note: (1) The absence of a line or a very weak line may not mean that an element is absent. For example the manganese line used had an intensity of (3) and would appear as a weak line in all but the most strongly manganous samples. Hence the intensity of a line noted above may be taken as relative only.

(2) The absence of lines of common elements may be due to interference.

(4) *Reading of the Spectrographic Plates.* The spectra exposed on each plate were thrown onto a screen. The image of the iron spectrum above each sample was then compared with the standard iron spectrum in Brode (1946) and the presence or absence of the following elements in

Table 6. Results of Repeat Analysis of Germanium Positive Samples

	No	Ge 26	Ge 30	Ge Standard	Remarks	Ash Number
First Re-runs	11	3	3	.01	Trace only	2
	13	3	3	.01	Tarce only	2
	22	2	2	.01	Re-ash	2
	24	4	3	R.U.	Trace only	1
	22	—	4	.01	Suggest Re-ash	3
	21	3	3	.01	Trace only	2
	18A	1	1	.01	Re-ash	2
	6	—	—	.01	No Germanium present	2
Second Re-runs	18B	2	2	.01		2
	18B	1	1	1.0	Standard > Sample	3
	18B	1	1	0.1	Standard ≃ Sample	3
	18B	1	1	.01	Standard < Sample	3
	22	1	1	.01	Standard < Sample	2
	22	1	1	1.0	Standard > Sample	4
	22	1	1	0.1	Standard ≃ Sample	4
	22	1	1	.01	Standard < Sample	4

the sample was recorded. An estimate of the intensity of the lines present was made by eye; no densitometer was used.

Discussion of Results

(1) *Detection of Elements Other Than Germanium.* Fewer elements were detected in samples ashed in a bunsen flame (No. 1 and No. 2) than in ash of the same coal samples ashed in muffle furnace.

The fact that zinc was undetected in several of the samples may be due to the fact that the zinc spectra are usually more sensitive to interference than the spectra of other elements, especially if only small amounts of zinc are present.

(2) *Germanium.* Six of the ashed coal samples showed detectable amounts of germanium. These samples were re-ashed and spectrographed again with a germanium (.01%) standard* used in place of the R.U. powder.

Two of these re-run samples showed relatively large concentrations of germanium and four showed only a trace of the metal.

---

* Ratio quantitative powder with either (.01%) or (0.1%) or (1%) of each of the following Be, Co, Ca, Ge, In, Rb, Se, Tl, Y, in a zinc base prepared and standardized for use in qualitative spectroscopy by Dr. S. J. Lewis for Adam Hilger Ltd.

The samples from Cape Caution and Hornaday River N.W.T. which were twice positive were re-ashed and spectrographed a third time against .01%, 0.1% and 1% germanium standards. A photograph of the third plate of the sample from Cape Caution appears as Plate I. It will be noted that this plate shows an apparent concentration of germanium of approximately .1% in the sample. No germanium was detected in three other samples of Cape Caution coal. The re-analysis of the original sample checked with the first result.

CONCLUSIONS

Many elements present in small amount in coal can be detected spectrochemically.

The finding of germanium in 6 out of 24 samples can be considered high because the coal seams were not selectively sampled for germanium analysis.

In any future work of this nature a satisfactory method of ashing should be evolved for each type of coal examined. In spite of the low oven temperature at which these coals were ashed there is still a possibility that germanium was lost due to local burning of the coal. This ashing problem is stressed by Stadnichenko *et al.* (1953, p. 3).

The results of the analysis of Cape Caution coal underline the importance of accurate and systematic sampling of coal seams if their true germanium content is to be discovered.

If systematic sampling and analysis were carried out on the coal seams from which the six germanium positive coals were taken, higher concentrations of germanium might be found in selected parts of the seams.

ACKNOWLEDGMENTS

The author would like to express his thanks to Dr. H. V. Warren, Dr. R. E. Delavault, and Dr. R. M. Thompson for their help and encouragement with the project; and to thank other members of the University staff and senior students for their constructive criticism of the work as it progressed. Finally, the author wishes to thank the Britannia Mining and Smelting Company, Limited, whose scholarship facilitated this study.

REFERENCES

AUBREY, K. U. (1953): Germanium resources of the British Commonwealth, British Commonwealth of Nations, *Scientific Liaison Officer, London.*

BRODE, W. R. (1946): *Chemical spectroscopy*, New York.

GOLDSCHMIDT, V. M. (1930): *Nachr. Ges. Wiss. Göttingen, Math. phys. Kl.* 398.

——— (1937): The Principles of Distribution of Chemical Elements in Minerals and Rocks, *Jour. Chem. Soc.*, 655–673.

——— (1944): Occurrence of rare elements in coal ashes, in Bangham *Progress in Coal Science*, Butterworth, London (1950), p. 238.

——— (1954): *Geochemistry*, Oxford.

Hames, F. A. (1950): Gallium and germanium survey in the Carrall Street gas works British Columbia Electric Railway Co. Ltd., Vancouver, B. C. *University of British Columbia, Dept. of Mining and Metallurgy* (unpublished).

Headlee, A. J. W. (1953): Germanium and other elements in coal and the possibility of their recovery, *Min. Eng.* (Oct. 1953), 1011.

——— & Hunter, R. G. (1953): Elements in Coal Ash and their Industrial Significance, *Ind. and Eng. Chem.*, **45**, 548–551.

McClelland, W. R. (1953): Germanium resources of the British Commonwealth of Nations, *Scientific Liaison Officer, London.*

Newmarch, C. B. (1953): Geology of the Crowsnest coal basin with special reference to the Fernie Area, *B.C. Dept. of Mines*, **33**.

Nichols (1953): Progress report issued on germanium content of American coals, *U. S. Dept. of Int.* letter, Sept. 14th (1953).

Powell, A. B., Lever, F. M. & Walpole, R. D. (1951): The extracting and refining of germanium and gallium, *Jour. App. Chem.*, **1**, 541–552.

Rankama, K. & Sahama, T. G. (1950): *Geochemistry*, Chicago.

Stadnichenko, T., Murata, K. J., Zubovic, P. & Hufschmidt, E. L. (1953): Concentration of germanium in the ash of American coals, a progress report. *U. S. Geol. Survey* Cir. 272.

Thompson, A. P. & Musgrave, J. R. (1953): Germanium—Byproduct of Primary Importance, *Min. Eng.* Jan. 1953. Sec. 1.

Vaes, J. F. (1948): Reniérite, a germaniferous sulfide from the Prince Leopold mine, Kipushi, Belgium Congo. *Ann. Soc. Belge. Géol.* Bull. 72, 19–32.

NOTES AND NEWS

BRANNERITE FROM ONTARIO, CANADA

E. W. Nuffield, *University of Toronto, Toronto, Canada*

The Blind River area, situated on the north shore of Lake Huron about 80 miles east of Sault Ste. Marie, was last year the scene of a modern staking rush following the discovery of economically-significant amounts of uranium in Long township. The original find was at one time prospected for gold. It was re-staked in 1948 as a radioactive discovery but the claims were allowed to lapse. Finally it was again staked in 1951 and in 1953, a new company, Pronto Uranium Mines, was formed to take over and explore the property.

The rocks in the area are all Precambrian in age. Unconformably overlying the Basement Group, is the sedimentary group of the Huronian Series of which a quartz-pebble conglomerate at or near the base, contains the interesting radioactive minerals. This conglomerate outcrops intermittently in the form of an inverted S, measuring about 20 miles from north to south and 30 miles from east to west. The rocks on the lower limb dip toward Lake Huron which is about a mile to the south, while those on the middle and upper limbs dip toward each other. Thus the sediments are regionally folded about an east-west axis and plunge to the west.

Most of the prospecting and diamond drilling in the area has up to the present been concentrated in Long township on the lower limb (Pronto Uranium Mines) and west of Quirke Lake in township 150 on the upper limb (Algom Uranium Mines). The two regions have furnished the majority of specimens for mineralogical studies.

The conglomerate bed varies in thickness, but on the Pronto property averages 8½ feet. It has been traced for 4000 feet along strike and an average of 1400 feet down the dip by diamond drilling. It grades locally into an arkosic sandstone or quartzite and into an arkose. The typical conglomerate consists of well-rounded quartz pebbles, up to 2 inches in diameter, in a pyrite-sericite matrix. The pyrite occurs as crystals and in massive form. It is randomly distributed throughout the matrix but also occurs concentrated in zones, sometimes around quartz pebbles. Rarely it fills tiny fractures in the pebbles. The sericite is generally too fine grained for satisfactory optical study. Occasional clusters of muscovite have been developed throughout it.

Studies of the radioactivity by means of autoradiographs of polished rock slabs and thin and polished sections indicate that in the typical conglomerate it is generally confined to individual grains randomly distributed throughout the matrix or as concentrations of grains, rather than as veins. The presence of radioactivity is dependent upon the presence of pyrite although the intensity of radioactivity is not related to the amount of pyrite. Some sections suggest a segregation of radioactivity to the sides of pyrite zones.

The deposits are so extensive that it will be some time before a detailed description of the mineralogy can be given. However it appears certain at this time that brannerite is responsible for much if not most of the radioactivity. It is interesting to note that this mineral, which until recently was known only from Idaho, has been discovered in at least five other widely separated areas in the world (Pabst, 1954). In the Blind River area it occurs as reddish-brown grains of near-microscopic size, more or less altered to a dense white to yellowish white radioactive product. The mineral is metamict and before ignition often gives the x-ray powder pattern of either rutile or anatase. After a momentary ignition at red heat, a pattern identical with the pattern of ignited brannerite from Idaho is obtained.

A semi-quantitative spectrographic analysis performed by the Ontario Department of Mines gave the following results from a specimen of typical matrix material: Y 0.1 to 1.0%, Ce 0.05 to 0.5, Yb trace, La trace, U 0.1 to 1.0, Th trace, Ti 1.0 to 10, Cb trace, Ta none. It may be concluded from this that the metamict minerals common to Ontario which contain appreciable amounts of Cb and/or Ta, are not important here.

Two sections of diamond drill core from different holes showed tiny veinlets of a black mineral. Uncrushed fragments of this material gave the typical UO_2 pattern with smooth arcs. This may therefore be described as pitchblende. Veined pitchblende may be quite rare in the conglomerate. Individual grains which had not been crushed, also gave the pitchblende pattern with smooth arcs. Recently R. J. Traill[1] of the Geological Survey of Canada, identified as uraninite, crystals in conglomerate from the area, which gave a UO_2 powder pattern but with interrupted arcs. It appears therefore that both finely-crystalline and coarsely-crystalline UO_2 is present.

Several specimens of a lustrous black radioactive substance without crystal form were obtained at or near the surface. One specimen consists of irregular masses intimately associated with pyrite, covering almost a square inch of surface. This burns to a white ash in an open crucible over a Bunsen burner. It is identical with the material which has been described as thucholite but which has been shown by Davidson & Bowie (1951) to be a mixture of hydrocarbons enclosing pitchblende or uraninite.

---

[1] Oral communication at the Prospectors and Developers meeting in March, 1954 at Toronto.

In addition to these minerals, monazite, zircon, galena and chalcopyrite have been identified.

Acknowledgments

Mr. Franc Joubin, President of Algom Uranium Mines, kindly made available the material for this study. I am also indebted to the Research Council of Ontario for a grant in aid of research.

References

Davidson, C. F. & Bowie, S. U. (1951): On thucholite and related hydrocarbon-uraninite complexes, *Geol. Surv. Great Britain*, No. 3, 1.

Pabst, A. (1954): Brannerite from California, *Am. Mineral.*, **39**, 109.

A MAGNESIUM BORATE FROM ISÈRE, FRANCE, AND SWIFT RIVER, YUKON TERRITORY, WITH *X*-RAY POWDER DATA FOR SOME ANHYDROUS BORATES

R. M. Thompson and J. A. Gower, *University of British Columbia, Vancouver, Canada.*

During a study of the minor element content of sphalerite (Warren & Thompson, *Ec. Geol.*, **40,** 318, 1945) the relatively high (0.15 per cent) tin content of marmatite from the St. Christoph Mine, Isère, France, was noted, This sample is a compact crystalline aggregate showing an adamantine lustre and an almost jet black color. On a sawn surface, the sphalerite groundmass shows many small ill-defined greenish-white prismatic crystals of diopside, and small (2 mm.) irregular areas of an unknown, fairly hard, black, finely fibrous mineral.

In polished section, the sphalerite shows exsolved chalcopyrite and a lesser amount of stannite in the form of minute dots and blebs. The unknown fibrous mineral is distinctly pleochroic in dull gray to light blue gray, and highly anisotropic in light orange, blue, and fiery red. In places it is intergrown with diopside. The hardness was estimated as E and the mineral is negative to all etch-reactions.

Thin sections show coarse masses of sphalerite intergrown with diopside, chlorite, and small areas of the black fibrous opaque mineral. The fibrous mineral also occurs as capillary divergent bursts, or as unoriented needles in diopside or chlorite.

In 1945 an *x*-ray powder photograph was taken at the University of Toronto, but as the mineral could not be identified, no further work

TABLE 1. *X*-RAY POWDER DATA FOR SOME ANHYDROUS BORATES
Iron radiation (λ = 1.937 Å), manganese oxide filter

Ludwigite, Phillipsburg, Montana		Paigeite, Crestmore, California		Pinakiolite, Langban, Sweden		Warwickite, Edenville, New York		Hulsite, Brooks Mtn., Alaska		St. Christoph, Isére, France		Swift River, Yukon Territory	
I	*d*	*I*	*d*	*I*	*d*	*I*	*d*	*I*	*d*	*I*	*d*	*I*	*d*
2	7.37	4	7.42	1	5.81	4	6.55	5	5.37	1	5.90	5	7.32
2	6.16	2	6.16	8	5.42	4	4.20	1	4.99	9	5.34	1	5.87
1	5.69	1	5.63	1	4.97	2	3.73	4	4.49	1	4.88	8	5.31
7	5.12	7	5.12	1	4.70	3	2.97	5	3.87	2	4.19	2	4.92
3	3.00	1	4.70	1	3.64	½	2.84	½	3.09	2	3.56	3	3.61
½	2.92	1	3.74	3	2.99	5	2.75	4	2.96	2	3.08	½	3.09
2	2.81	4	3.04	½	2.88	10	2.57	½	2.75	3	2.95	1	2.96
2	2.74	1	2.92	9	2.70	1	2.48	5	2.67	10	2.67	10	2.66
10	2.56	5	2.83	10	2.51	1	2.24	2	2.59	4	2.60	2	2.60
1	2.52	3	2.75	½	2.40	½	2.20	10	2.53	½	2.54	2	2.50
½	2.34	10	2.56	3	2.30	1	2.13	½	2.49	½	2.48	1	2.43
½	2.31	5	2.36	½	2.24	2	2.08	1	2.35	½	2.35	1	2.36
5	2.17	½	2.33	4	2.16	3	1.979	½	2.24	½	2.25	½	2.28
1	2.12	½	2.27	½	2.07	1	1.867	½	2.18	5	2.13	½	2.25
4	2.03	6	2.17	6	1.986	½	1.838	½	2.13	7	2.03	½	2.18
3	2.00	4	2.14	½	1.917	½	1.813	½	2.09	2	1.776	5	2.13
½	1.955	7	2.05	2	1.836	1	1.791	4	2.04	1	1.753	7	2.04
2	1.917	2	1.998	½	1.805	3	1.721	½	1.973	½	1.721	2	1.779
1	1.873	½	1.961	4	1.623	1	1.632	½	1.937	½	1.699	3	1.568
3	1.767	7	1.926	2	1.548	2	1.595	½	1.859	3	1.558	5	1.541
½	1.728	1	1.878	5	1.518	1	1.553	½	1.779	7	1.541	½	1.509
½	1.706	½	1.857	4	1.496	3	1.501	1	1.732	½	1.524	1	1.487
2	1.668	4	1.776	½	1.430	1	1.471	½	1.702	½	1.484	1	1.441
½	1.595	1	1.670	½	1.416	2	1.380	½	1.640	½	1.388	½	1.398
4	1.577	5	1.586	½	1.386	1	1.338	1	1.610	½	1.366	3	1.362
3	1.539	1	1.538	½	1.352	1	1.327	1	1.580	2	1.355	3	1.332
½	1.529	6	1.528	½	1.328	½	1.284	½	1.559	4	1.332	½	1.300
3	1.513	5	1.505	2	1.307	1	1.272	½	1.546	½	1.288	½	1.246
4	1.501	4	1.487	1	1.283	½	1.243	½	1.507	½	1.249	½	1.227
4	1.477	½	1.466	½	1.227	½	1.226	4	1.479	½	1.239	½	1.198
5	1.380	5	1.388	1	1.150	1	1.184	1	1.434	1	1.220	2	1.180
½	1.358	½	1.366	½	1.121	2	1.152	½	1.353	1	1.176	½	1.116
½	1.316	½	1.352	4	1.080			½	1.333	4	1.067	2	1.067
2	1.301	½	1.339	1	1.032			1	1.314	1	1.049	1	1.050
1	1.293	6	1.315	2	1.015			½	1.291	3	1.017	3	1.019
2	1.282	½	1.300	2	1.002					4	1.008	2	1.008
1	1.252	3	1.283										
1	1.205	2	1.251										
½	1.190	2	1.217										
1	1.181	1	1.200										
4	1.158	2	1.183										
1	1.142	3	1.166										
4	1.087	½	1.144										
½	1.080	½	1.131										
½	1.070	½	1.105										
½	1.061	4	1.087										
2	1.043	1	1.068										
2	1.024	½	1.052										
5	1.020	2	1.044										
1	1.002	6	1.028										
5	0.998	3	1.003										
		3	0.997										
		1	0.992										
		4	0.983										

was attempted as more pressing problems were at hand, The problem was tackled later at the University of British Columbia and a qualitative spectrographic analysis showed essential amounts of magnesium and boron, minor amounts of iron and tin, and traces of silicon, manganese and copper.

X-ray powder photographs of ludwigite, paigeite, pinakiolite, hulsite, warwickite, sussexite, and camsellite were taken but these photographs showed little resemblance to that of the unknown. The anhydrous borates, jeremejevite and nordenskiöldine, were not available, but seem to be ruled out on the basis of the spectrographic analysis. No agreement was found between the observed spacings given by Takeuchi (*Acta Cryst.*, **5**, 580, 1952) for a possible new borate from the Suan Mine, North Korea, and those of the unknown.

At this time, J. A. Gower was engaged in a study of the Seagull Creek batholith and its metamorphic aureole (unpublished M.A.Sc. thesis, *University of British Columbia*, 1952). This area lies in the southeastern Yukon Territory between latitudes 60° and 60° 15′ N, and longitudes 131° and 131° 30′ W. Swift River control station at mile post 733 on the Alaska Highway is the only settlement in the area.

A magnetite-pyrrhotite deposit in limestone and dolomite outcrops on the east bank of the south fork of Swift River, one mile north of two small lakes that mark its source. In samples of diamond drill core that were left at the outcrop, several sulphides including small amounts of stannite were noted in a gangue of serpentine, diopside, calcite, dolomite, chlorite, and clinohumite. Ludwigite needles about 0.1 by 0.5 mm. occur in intimate association with magnetite. This mineral was identified by its powder photograph.

Present in very small amounts is a black fibrous mineral resembling ludwigite, and intimately intergrown with magnetite, some of which may be pseudomorphous after it. This mineral has a submetallic lustre, is black in color and streak, has hardness 5, specific gravity 3.45 ± 0.02, opaque except on thinnest edges, and cleavage was not detected. In polished section, the mineral is similar to ludwigite and the Isère unknown.

A qualitative spectrographic analysis showed essential magnesium, iron, and boron, minor amounts of tin, manganese, and silicon. An *x*-ray powder photograph shows strong similarities to the unknown from Isère, France. Dr. Clifford Frondel kindly compared the powder photographs of rhodizite and kotoite with that of the Swift River mineral, but reports no similarity.

Until further material is available to permit a complete description, it would be premature to claim either unknown as a new mineral species.

NAUMANNITE FROM REPUBLIC, WASHINGTON

R. M. Thompson, *University of British Columbia, Vancouver, Canada.*

In 1949, while cataloguing some specimens which had been previously donated to the University, I noticed a specimen showing several thin black metallic bands in milky crustified quartz, and labelled "petzite, Republic, Washington." A preliminary investigation of the microscopic properties suggested that one of the minerals comprising the black bands was naumannite (Ag_2Se) and later confirmation was obtained by microchemical tests and an *x*-ray powder photograph.

The hand specimen shows three concentric black metallic bands about 4 mm. in thickness alternating with bands of crustified quartz. A polished surface shows that each black band consists of a groundmass of argentian tetrahedrite in which small particles of gold, electrum, pyrite, chalcopyrite and naumannite are embedded. In places the assemblage approaches an emulsion texture.

The identification of naumannite from Republic is of interest because it has been known for many years that the element selenium occurs in the ore from this district. M. H. Joseph, (*Eng. and Mining Jour.*, Nov. 25, 1899) lists selenite of silver amongst several ore minerals of the Republic camp but gives no details. Later, Umpleby (*Wash. Geol. Survey* Bull. No. 1 p. 39, 1910) suggests that silver is partly in the form of silver selenide and partly as gray copper. Palmer (Lindgren & Bancroft, *U.S.G.S.* Bull. 550, 148, 1924) suggests the possible presence of gold selenide (Au_2Se_3) in the ore, because after the removal of free gold with an alkaline sulphide solution the ratio of gold to selenium was approximately constant and equal to 2:3. The synthesis of gold selenide has been reported and this compound may occur in Republic ores but in view of the occurrence of naumannite it appears the latter is responsible in part, if not entirely, for the selenium content. A complete modern mineralographic study of this striking and unusual ore would be of interest.

I would like to express my thanks to Dr. James W. Earley who compared the *x*-ray powder pattern with patterns of naumannite from type localities.

MINERAL OCCURRENCES IN WESTERN CANADA

R. M. Thompson, *University of British Columbia, Vancouver, Canada.*

These notes continue the reporting of some of the rarer ore minerals found in British Columbia. Most of the minerals described below are believed to be first occurrences in British Columbia.

Kobellite. $6PbS \cdot FeS \cdot 2Bi_2S_3 \cdot Sb_2S_3$. Dodger Tungsten Mine, near Salmo, Nelson M.D., B.C. Mr. C. C. Rennie, geologist at the Dodger Tungsten Mine for Canadian Exploration, Limited, submitted a small hand specimen of milky quartz with lead gray capillary crystals protruding from a vug and embedded in the quartz at one end of the specimen. Mr. Rennie describes the occurrence as follows: "the specimen is from a quartz mass containing coarse crystals of scheelite, abundant sericite mica, some molybdenite and minor pyrite, about three feet above a flat lying granite contact. The same mineral has been noted in a specimen from a quartz-calcite vein at the granite contact.

The country rock of the ore zone consists of altered limestones and skarn, containing abundant pyrrhotite, in contact with granite. The ore zone is considerably veined and partially replaced by quartz."

An x-ray powder photograph was taken and identified as kobellite by direct comparison with the pattern of kobellite from Hvena, Sweden (Nuffield, *Univ. Toronto Studies, Geol. Ser.* **52,** 86–89, 1948). Mr. Rennie kindly made further samples available but the lead-gray minerals contained in the quartz or dolomitic gangue proved to be bismuthinite or boulangerite. It is hoped that additional material will be found in order that a necessary new analysis of this rare mineral may be made.

Sperrylite, $PtAs_2$ and *thorianite,* ThO_2. Mr. Ernie Howard of Minto, B.C. submitted a sample of black sand from the Fraser River near Lytton for identification of the radioactive minerals. The sample is composed of the following minerals listed in order of their abundance: magnetite (67 per cent by weight), garnet, ilmenite, zircon, rutile, olivine, platinum, gold, quartz, epidote, thorianite, chromite, feldspar, cinnabar, muscovite, calcite, scheelite, and sperrylite.

Thorianite is present in all screen sizes below 60 mesh and an assay of 5 per cent U_3O_8 equivalent was obtained on the minus 200 mesh size using a scaling type geiger counter. The mineral occurs in blackish grains from 50 to 150 microns in diameter. Many grains are rounded and others are almost perfect cubes. An x-ray powder photograph is in exact agreement with thorianite ($a = 5.58$ Å) from Balangoda, Ceylon. The mineral is probably the uranoan variety because the grains gave a positive uranium bead test. The resulting radiation tracks on nuclear track plates proved useful in distinguishing irregular thorianite grains from other black minerals. This occurrence makes interesting speculation as there are no known radioactive lode deposits in the vicinity.

One highly modified cubic crystal and several hard tin-white rounded grains were observed in the $-80+100$ fraction. The x-ray powder pattern of these grains is in good agreement with the pattern of sperrylite from the Vermilion mine, near Sudbury, Ontario. Although platinum is of fairly frequent occurrence in this section of the Fraser River, the writer believes that this is the first recorded identification of sperrylite.

Empressite, $Ag_{2-x}Te$, *Rickardite,* $Cu_{2-x}Te$, and *Native tellurium.* Grotto Group (Kindle, *Geol. Surv. Canada,* Memoir 212, 1936) near Pitman, Skeena M.D., B.C. This property is situated on Hardscrabble creek about one mile west of the Canadian National railway and about 1½ miles from Pitman flag station. A quartz vein containing values in gold, silver, and copper, occurs along the contact of a 12 foot andesine diorite prophyry dike intrusive into andesite.

Dr. Joseph T. Mandy supplied the writer with several samples of ore in which he suspected telluride mineralization. The vein quartz is white to gray-black in colour and contains many thin (2 mm.) fractures which are partially filled with quartz crystals. Some surfaces are drusy and others show small flat vugs. Pyrite, chalcopyrite and specularite occur massive or disseminated throughout the quartz.

Native tellurium is present in the form of conspicuous tin-white prismatic crystals up to 3 mm. in length. It is less commonly found as small cleavage masses and as a paper-thin encrustation on drusy quartz.

Empressite occurs sparingly as small velvety-black masses embedded in quartz and showing a distinct conchoidal fracture. A mineral closely resembling empressite but with a superficial brown tarnish gave the same *x*-ray powder pattern as that of empressite? (material 4) described by Thompson, Peacock, Rowland & Berry (*Am. Mineral.* **36,** 467, 1951). At present there is not sufficient of this mineral for a chemical analysis.

Rickardite is present in traces and is best developed as a thin coating on a small cleavage mass of tellurium adjacent to an area of chalcopyrite. The rickardite may be of secondary origin. On account of the vuggy nature of the telluride rich portions of the ore, polished section relationships are difficult to obtain, but it is obvious that the tellurides are late in the paragenetic sequence.

Gold is present but the nature of its occurrence is unknown. The ratio of silver to gold varies but is in the order of 20:1.

Alabandite, MnS, *dyscrasite,* Ag_3Sb, and *native antimony.* Contact Group, McDame Creek, Liard M.D., B.C. These claims are located between the head waters of McDame and Cottonwood Creek's at an elevation of 6000 feet. The main showing consists of a vein cutting dolomitized limestone and is composed chiefly of galena, sphalerite, and magnetite. The writer is indebted to Mr. J. McDougall who collected specimens for study during the summer of 1951 while with the Geological Survey of Canada as a student assistant, and to Mr. E. H. Kohse and Mr. P. R. Wilson who assisted in the study of polished sections.

The vein material consists of fine grained masses of sphalerite, galena, and magnetite with practically no gangue minerals. A thin black coating of manganese oxide is present on most of the weathered surfaces. Magnetite occurs as subhedral to anhedral grains from 0.1 to 0.6 mm. in diameter and occasionally shows core replacement by galena, sphalerite or gangue. Pyrite is of similar occurrence in grains about 0.5 mm. in size. Pyrrhotite occurs as small irregular grains scattered through the matrix of galena and sphalerite and also as minute exsolution bodies in alabandite and sphalerite, Excellent examples of replacement of pyrrhotite by colloform marcasite are found. Sphalerite is associated with chalcopyrite and galena as irregular grains up to 1 cm. in size and is replaced by galena to some extent. It is intimately associated with and contains inclusions of alabandite and pyrrhotite. Arsenopyrite occurs in euhedral to subhedral crystals 0.1 mm. in length in the galena-sphalerite matrix. The crystals are partially replaced by galena, sphalerite, and pyrargyrite.

The presence of a primary manganese mineral was suspected when the black coating on the weathered surfaces was observed. The mineral proved to be alabandite. It was recognized by its violent reaction to HCl and was confirmed by an x-ray powder photograph. It occurs in what appear to be long narrow exsolution laths in sphalerite and as irregular grains up to 4 mm. in size.

Galena occurs as irregular veinlets ramifying through the sphalerite and forming a matrix enclosing many minerals. Widely scattered grains of a white, weakly anisotropic mineral ranging up to 1 mm. in size were identified as native antimony. Dyscrasite also occurs in the galena as pale yellowish grains up to 0.25 mm. in size. The mineral often shows rhombic outlines and tarnishes rapidly. It is rarely seen in contact with native antimony. In addition to the above, the galena contains minute inclusions of two unknown soft isotropic minerals and brilliant white distinctly anisotropic rhombs, prisms, and cubes of a third unknown up to 20 microns in size.

This deposit is unusual in that it shows minerals which are considered typical of both hypothermal and epithermal type mineralization. There is a possibility of more than one period of mineralization or that the assemblage represents a telescoped deposit. Further work is necessary to give a clearer picture of the paragenesis.

NATIVE TIN ASSOCIATED WITH PITCHBLENDE AT NESBITT LABINE URANIUM MINES, BEAVERLODGE, SASKATCHEWAN

JACK F. B. SILMAN, *Queen's University, Kingston, Ontario, Canada.*

Pitchblende at Nesbitt LaBine Uranium Mines occurs in fractures cross-cutting a slatey formation. Certain parts of the fractures are heavily mineralized with calcite, hematite and pitchblende. Associated with the pitchblende is pyrite, chalcopyrite, bornite, chalcocite, covellite, sphalerite, galena and native tin. Samples from three separate veins on the first level and from one vein on the second level of the mine are unique in containing native tin.

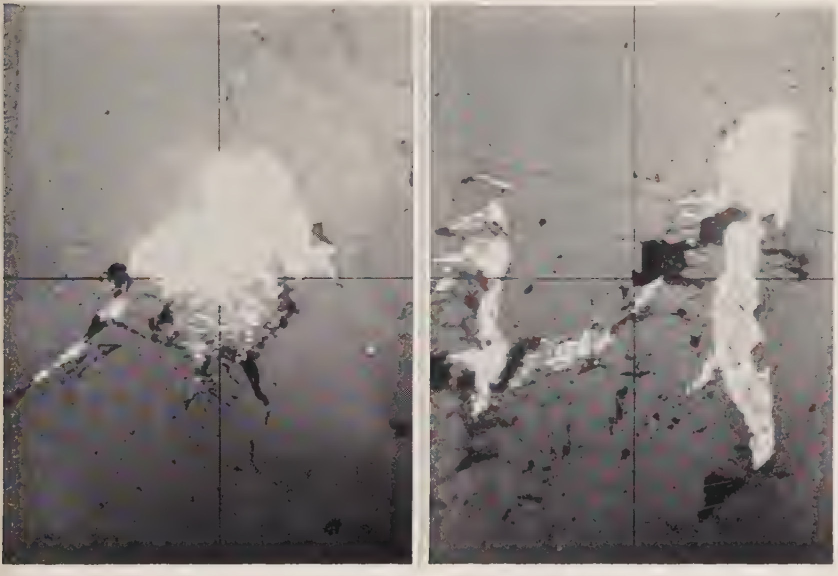

FIGS. 1 and 2. Photographs of native tin in polished section (×102). Native tin (white) in calcite (grey).

The native tin was first found in polished sections prepared on lead laps using tin oxide abrasive. Later sections containing the mineral were polished on linen with chromium oxide to preclude any possible contamination. In polished sections the tin is creamy white in colour, ductile, very soft (approximating the hardness of argentite) and occurs in discrete grains up to 1.5 mm. in diameter. Feathery tongues from the main masses penetrate the host calcite (Figs. 1 and 2). Under crossed nicols the mineral is weakly anisotropic with polarization colours yellowish grey to bluish grey.

Each reaction with the standard reagents on the grains and on a standard are as follows:

Reagent	Sample	Standard of Refined Tin
HNO_3	Fumes stain irridescent	Fumes stain irridescent, white deposit noticed on larger sample.
	Liquid causes effervescence and etching, stains brownish black	Liquid causes effervescence and etching stains brownish black, leaves white deposit
HCl	Fumes tarnish light brown, eventually irridescent	Fumes tarnish light brown, eventually irridescent
	Liquid slowly stains dark brown to black	Liquid slowly stains differentially light brown to dark brown to black
KCN	Fumes negative	Fumes negative
	Liquid negative	Liquid very slowly stains light brown
$FeCl_3$	Fumes negative	Fumes negative
	Liquid quickly stains light brown to dark brown to black	Liquid quickly stains light brown to dark brown to black, leaves white deposit
KOH	Fumes negative	Fumes negative
	Liquid negative	Liquid slowly stains light brown
$HgCl_2$	Fumes negative	Fumes negative
	Liquid quickly stains dark brown to black	Liquid quickly stains dark brown to black
Aqua Regia	Fumes stain light brown to irridescent	Fumes stain light brown to irridescent
	Liquid quickly stains dark brown to black	Liquid quickly stains dark brown to black

Confirmation of Native Tin

The identity of the mineral has been confirmed both by *x*-ray and spectrographic means. *X*-ray photographs of three samples were taken; two from one polished section and one from another from a different vein. The three photographs are identical with a master photograph prepared from refined tin. One of the samples studied with *x*-rays was analyzed spectrographically by conventional D.C. arc methods and proved to contain only tin with traces of copper and silver. Approximately fifty grams of vein material were pulverized, leached with HCl and evaporated to dryness. A spectrographic analysis of the residue again confirmed the presence of tin.

Native tin associated with cassiterite has been found in gravel deposits from several localities. To the writer's knowledge native tin *in situ* has not been reported. Its presence indicates a reducing environment, free from iron, sulphur etc. at the time of formation otherwise cassiterite or some other compound of tin would have been formed. The sequence of deposition of the vein minerals appears to be as follows: minor calcite and quartz; hematite, pitchblende and pyrite; late calcite and hematite;

chalcopyrite, bornite, chalcocite, covellite, sphalerite and galena; native tin. The actual age relation of the tin to other metallics is indeterminate as it occurs in and completely surrounded by late calcite. Study of this peculiar occurrence is continuing.

ON THE OCCURRENCE AND ORIGIN OF XONOTLITE[1]

Charles H. Smith,[2] *Geological Survey of Canada, Ottawa, Canada.*

The recently reported occurrence of xonotlite ($5CaO \cdot 5SiO_2 \cdot H_2O$) in Puerto Rico by Kaye (1953, p. 860) resembles similar occurrences associated with the ultrabasic rocks of the Bay of Islands Igneous Complex, western Newfoundland. The latter are believed to be the first reported Canadian occurrences. The mineral has similar optical properties to those described by Larsen (1923) and others, and gives an *x*-ray pattern similar to xonotlite from Isle Royale, Michigan (McMurdie & Flint, 1943) but variations in the modes of occurrence have a bearing on the origins of xonotlite suggested by Kaye. The specimens studied are now deposited in the Brush Mineral collection at Yale University (Specimen Nos. 6776 and 6777).

The Puerto Rican occurrence is located at the fault contact of serpentinite and a metavolcanic rock. Kaye concludes that conditions at the contact were critical to its formation, and suggests that either heat generated during shearing caused a calcite vein to alter to xonotlite in the presence of siliceous emanations from the serpentinite, or that the xonotlite formed prior to movement but later movements caused recrystallization of the "massive" xonotlite into "parallel-fibrous" xonotlite.

Both massive, i.e. unoriented xonotlite aggregates, and fibrous forms of xonotlite are found in the Bay of Islands area. Fibrous xonotlite occurs in veins up to 3 inches in width and several feet long, cutting altered sedimentary rocks near faulted contacts with serpentinite at Winter House Brook and Shoal Brook, Bonne Bay, and near First Trout River Pond. Fibrous and massive xonotlite are found with other lime-bearing minerals filling joints in serpentinite near the basal contact of the North Arm Mountain pluton. Four separate bodies, composed of prehnite, pectolite, phlogophite and xonotlite, are exposed in the valley walls of a stream draining into North Arm, Bay of Islands. The largest body is 55 feet long and 10 feet wide. Xonotlite also occurs as a secondary alteration mineral formed from the metamorphic minerals related to the ultrabasic contacts. In one place, a calcic hornfels was altered to a mass of prehnite, xonotlite, calcite and clinozoisite, with only ragged relicts of the original diopsite remaining. About thirty miles further south, in the Lewis Hills intrusion, fragments of xonotlite were found in the alluvium, suggesting that xonotlite has formed in other parts of the ultrabasic masses as well.

---

[1] Published by permission of the Deputy Minister, Department of Mines and Technical Surveys, Ottawa, Canada.

[2] Geologist, Geological Survey of Canada.

The xonotlite occurs as a vein-forming mineral, formed after the solidification, serpentinization and faulting of the ultrabasic plutons. It is found in joints near the faulted contacts of the ultrabasic rocks, and may occur in either the ultrabasic or metamorphic rocks. Bleaching along the vein margins suggests the solutions were fairly hot. Xonotlite is found in limestone near igneous contacts at Tetela de Xonotla, Mexico (Winchell & Winchell, 1951) and at Goose Creek, Virginia (Shannon, 1925). No source of lime exists in the ultrabasic rocks now exposed at the contacts in the Bay of Islands area, and it is believed that the lime to form xonotlite was derived from the calcium-rich rocks of the contact metamorphic aureole, by heated solutions circulating along the fault contacts. Whether the solutions represent very late emanations from the serpentine, or hydrothermal solutions related to some later igenous activity, is not known. However, there is no evidence to support the suggestions of Kaye that the xonotlite formed by the alteration of vein calcite or that the action of stress was necessary to cause its crystallization in well-developed fibers.

REFERENCES

KAYE, C. A. (1953): A xonotlite occurrence in Puerto Rico: *Am. Mineral.*, **38,** 860–862.

LARSEN, E. S. (1923): The identity of eakleite and xonotlite: *Am. Mineral.*, **8,** 181–182.

McMURDIE, H. F., & FLINT, E. P. (1943): *X*-ray patterns of hydrated calcium silicates, *J. Research, N.B.S.*, **31,** 225–228, R.P. 1560.

SHANNON, E. V. (1925): Mineralogy and petrography of Triassic limestone conglomerate metamorphosed by intrusive diabase at Leesburg, Virginia: *Proc. U. S. Nat. Mus.*, **66,** art. 28.

SMITH, C. H. (1952): The Bay of Islands Igneous Complex, Newfoundland—northern half: unpublished Ph.D. dissertation, Yale University.

WINCHELL, A. N. & WINCHELL, H. (1951): *Elements of Optical Mineralogy*, **2,** 4th ed., New York.

WALKER MINERALOGICAL CLUB*

OFFICERS 1953

Honorary President, A. L. Parsons; *President*, C. C. Stevenson; *Past President*, J. A. MacDonald; *Secretary*, Mrs. W. H. Bush; *Treasurer*, Mrs. M. H. Frohberg, *Editor*, L. G. Berry; *Councillors*, F. Ebbutt, R. Ford, D. Hogarth, V. B. Meen.

ABSTRACT OF PROCEEDINGS, 1953

January 22, 1953. Dr. V. B. Meen, Director of the Royal Ontario Museum of Geology and Mineralogy, addressed the Club on Mineral Collecting in the United States, 1952. Dr. Meen illustrated his talk with color slides and showed mineral specimens. Refreshments were served.

February 19, 1953. Mr. C. V. G. Phipps, instructor in the Department of Geological Sciences at the University of Toronto, spoke on An Excursion Around Australia. Mr. Phipps also showed color slides and exhibited specimens of Australian minerals.

March 19, 1953. A letter from Colonel J. J. Livingston inviting the Club to join the Mineralogical Society of the District of Columbia in a collecting trip at some future date, was read. An auction, sale of minerals, lucky draws and "indoor" collecting were held in the basement workrooms of the Royal Ontario Museum of Geology and Mineralogy. Refreshments were served.

April 16, 1953. The President announced that 11 members would be driving to Washington in May to join the Mineralogical Society in a collecting trip. Mr. D. Hogarth, graduate student of University of Toronto, spoke on Mineralogy of a Vein at the Nicholson Uranium Mines, Lake Athabaska. Mr. D. H. Gorman, lecturer in the Department of Geological Sciences, University of Toronto, spoke on twinned crystals. Dr. E. W. Nuffield, assistant professor in the Department of Geological Sciences, University of Toronto, addressed the Club on Recent Research on the Torbernite Minerals.

May 23, 1953. The annual Spring Field Trip took place at the quarries of the Canada Crushed Stone Company near Dundas where blue celestite was collected. A picnic lunch was held at Webster's Falls.

October 2–4, 1953. The Club met at Drag Lake Lodge, Haliburton for the Autumn Field Trip. Members were divided into 3 groups for collecting. One group led by Mr. G. Steel collected tremolite, scapolite, sunstone, etc. A second group under Mr. R. Ford visited the Cardiff Mines, Hill Top Mine and Fission Mine and gathered uraninite, fluorite, apatite, magnetite, scapolite. Dr. V. B. Meen led a third group to Fish Tail Lake where garnets and iolite were gathered. Friday evening color slides of previous collecting trips as well as individual trips by the members, were shown. On Saturday evening, Dr. V. B. Meen spoke to the Club briefly on his recent discovery of a second meteoritic crater lake in northern Quebec and illustrated his talk with color slides. Color slides of Glacier National Park were shown by Mr. and Mrs. F. La Rheir, American visitors from Detroit. Fluorescent minerals donated to the Club by Mr. E. J. Tolamini of New Jersey, were then distributed to members.

---

* Founded in 1938 and named in honor of the late Professor T. L. Walker (1867–1942), then Professor Emeritus of Mineralogy and Petrography in the University of Toronto and Director of the Royal Ontario Museum of Mineralogy. The by-laws of the Club were published in *Am. Mineral.*, **34,** 469, 1949.

October 30, 1953. A joint meeting of the Metal Arts Guild and Walker Mineralogical Club was held. Miss Nancy Meek, Miss Margaret Goodfellow and Mr. J. Sullivan of the Metal Arts Guild spoke on their preference in cut stones and exhibited samples of their jewellery. Mr. G. Waite listed 40 varieties of Canadian gemstones and gave their sources. Mr. G. Steel showed slides of lapidary equipment used by various members, while Mr. J. N. A. Pelletier showed a motion picture of a lapidary at work. Mr. A. Fussel spoke briefly on the making of silver spoons, then passed around samples of his work.

November 19, 1953. Mr. F. Ebbutt announced that recent donations to the Peacock Memorial Prize Fund by mining firms totalled $1,733.36. Mr. D. H. Gorman briefly summarized one of the papers entered for the Peacock Memorial Prize—The Coalescence of Hexagonal and Cubic Polymorphs in Tetrahedral Structures as Illustrated by some Wurtzite-Sphalerite Crystal Groups by R. S. Mitchell and Alice S. Corey. Dr. Ernest H. Nickel was announced as the winner of the 1953 Peacock Memorial Prize and was presented with a check for $100. Mr. Nickel then gave his prize winning paper entitled (in two parts) Part 1. The distribution of major and minor elements among some co-existing ferromagnesium silicates. Part 2. The distribution of iron, manganese, nickel and cobalt between co-existing pyrite and biotite in wallrock alteration. The prize-winning paper appears in this number of the *American Mineralogist*, **39**, 486–503.

Dr. V. B. Meen commented briefly on a field trip he had conducted to Haliburton and Renfrew County for members of the Geological Society of America which had met in Toronto the previous week.

December 10, 1953. Mr. M. G. Savauge, gemmologist and diamond buyer for T. Eaton C. Ltd., spoke on Precious Stones and exhibited a collection of cut stones.

The Council of the Walker Mineralogical Club wishes to acknowledge the courtesy of the Council of the Mineralogical Society of America in again making possible the publication of a Canadian number of *The American Mineralogist.*

MRS. HELEN BUSH, *Secretary*

Peacock Memorial Prize. A prize of $100 is again offered by the Walker Mineralogical Club for the best paper on pure or applied mineralogy (including petrology) submitted by a graduate student of any university or similar institution. Closing date June 30, 1954. For further conditions write Secretary, Walker Mineralogical Club. 100 Queen's Park, Toronto.

CLAY MINERAL TECHNOLOGY

is the theme of the Third National Clay Minerals Conference to be held at the Rice Institute, Houston, Texas, October 27–28–29, 1954. The Conference is sponsored by the Clay Minerals Committee of the National Research Council. A special part of the program will be devoted to fundamental or applied papers. Anyone interested in presenting papers in *any* of these or *other* fields pertaining to clays or related minerals is invited to announce their intentions to A. F. Frederickson, Washington University, St. Louis 5, Missouri, on or before July 15, 1954.

A detailed program, including field-trip information, will be available on request in August, 1954. *Everyone* interested in any aspect of clay mineralogy, technology or related fields is cordially invited to attend the Conference.

ANNUAL MEETING

The thirty-fifth annual meeting of the Mineralogical Society of America will be held in Los Angeles, California, Monday through Wednesday, November 1–3, 1954. A series of field trips is being planned, some to precede and some to follow the meeting.

Abstracts of papers to be presented at the annual meeting must be received by the Secretary on or before *July 15, 1954*. Abstract blanks may be obtained from the Secretary.

NOMINATIONS OF OFFICERS FOR 1955

President: Harry H. Hess, Princeton University. Princeton, Massachusetts

Vice-President: Clifford Frondel, Harvard University, Cambridge, Massachusetts

Secretary: C. S. Hurlbut, Jr., Harvard University, Cambridge, Massachusetts.

Treasurer: Earl Ingerson, U. S. Geological Survey, Washington, D. C.

Editor: Walter F. Hunt, University of Michigan, Ann Arbor, Michigan

Councilor (1955–58): Leonard G. Berry, Queen's University, Kingston, Ontario, Canada

The above Fellows have been nominated by the Council as officers of the Mineralogical Society of America for 1955. They will be voted on at the election in October 1954.

C. S. Hurlbut, Jr., *Secretary*

1954 Pacific Coast Regional Conference on Clays and Clay Technology

The 1954 Pacific Coast Regional Conference on Clays and Clay Technology is to be held on the Berkeley campus of the University of California on June 25 and 26. The subject of the Conference will be the clay-water system.

Papers related to permeability of liquids through formations, swelling of clays, viscosity and plasticity will be presented by workers in the fields of petroleum, soil science, soil mechanics, geophysics, and ceramics. The same arrangement that was so successful during the First National Conference at Berkeley is to be followed with papers in the mornings and discussions in the afternoons. Thus, an excellent opportunity is provided for an exchange of information and ideas between the representatives of the above fields.

The General Electric X-Ray Diffraction School will also be held on the Berkeley campus and will precede the Conference, June 21 to 25.

INTERNATIONAL UNION OF CRYSTALLOGRAPHY

Third General Assembly and International Congress

Paris, 21–28 July 1954

Secretary of the Local Committee: A.-J. Rose, 1, rue Victor-Cousin, Paris 5e

Accommodation: American Express

Provisional Programme

Wednesday 21st July

10:00 a.m. *Opening Meeting*
2:30 p.m. Inauguration of the Exhibition
3:30 p.m. Congress Communications

Thursday 22nd July

9:30 a.m. General Lectures (Crystal Growth)
2:30 p.m. Congress Communications

Friday 23rd July

9:30 a.m. General Lectures (Low Temperature structure determinations, and Clathrate compounds
2:30 p.m. Congress Communications

Saturday 24th July

9:30 a.m. Congress Communications
Free Afternoon
12:45 p.m. Departure for the "Châteaux de la Loire"; tour excursion A (return on Sunday evening)

Sunday 25th July. Free

Afternoon Tour of Paris and surroundings (excursion B)

Monday 26th July

9:30 a.m. General Lectures (Neutro Diffraction)
2:30 p.m. Congress Communications
9:00 p.m. General Lecture

Tuesday 27th July

9:30 a.m. Preparatory Lectures for Sy posium on "The Mechanis of Phase Transition in Cr tals"
2:30 p.m. Congress Communications

Wednesday 28th July

9:30 a.m. Preparatory Lectures for Sy posium on "The Locatio and Function of Hydrogen
2:30 p.m. *Closing Meeting*

Thursday 29th July

9:30 a.m. & 2:30 p.m. Symposium: T Mechanism of Phase Trans tions in Crystals

Friday 30th July

9:30 a.m. & 2:30 p.m. Symposium: The Lo cation and Function of Hy drogen

By request of many colleagues, the Organizing Committee has decided to include th following sections:

16.—Electron Diffraction 17.—Clay minerals

Sessions on "The Teaching of Crystallography" and "Crystallographic data" will b held in the course of the Congress.

Receptions and Visits

A programme of receptions and visits will be organized for Crystallographers and Men bers accompanying them; this will be handed to them with invitations on their arrival i Paris.